UNIVERSITY OF LATVIA

FACULTY OF MEDICINE

Jolanta Upīte

ANTI-AMYLOID-β TREATMENT AND IMPROVED METHODOLOGY FOR INTRACEREBRAL DRUG DELIVERY COMBINED WITH QUANTITATIVE HISTOPATHOLOGICAL ANALYSIS IN ALZHEIMER'S DISEASE MOUSE MODELS

DOCTORAL THESIS

Submitted for the degree of Doctor Degree in Basic Medical Science including Pharmacy

Subfield of Pharmaceutical Pharmacology

Riga, 2022

The doctoral thesis study was carried out at the University of Latvia, Faculty of Medicine, Department of Pharmacology (Riga, Latvia), at the University of Oslo at Translational Neurodegeneration and Neuropathology Laboratory (Oslo, Norway) and at the University of Alabama at Birmingham, Cell Developmental and Integrative Biology (Birmingham, U.S.) from 2015 – 2021.

The thesis consists of the 7 chapters, reference list and contains supplementary information section.

Form of the thesis: dissertation in Basic Medical Science including Pharmacology, subfield of Pharmaceutical Pharmacology

Supervisor: *Dr. habil. Med.,* Prof. **Baiba Jansone**

Co-advisor: *Dr. med.*, Prof. **Jens Pahnke**

Reviewers:

1) *Dr. habil. Biol.*, Prof. **Ruta Muceniece**, University of Latvia

2) *Dr. med.*, **Līga Zvejniece**, Latvian Institute of Organic Synthesis

3) *MD, PhD,* Prof. **Mojca Kržan**, University of Ljubljana

The thesis will be defended at the public session of the Doctoral Committee of Medicine, Pharmacy and Biology Sciences, University of Latvia, at 15:00 on November 25th, 2022 at the University of Latvia House of Science, 3 Jelgavas Street, room 401.

The thesis is available at the Library of the University of Latvia, Raiņa blvd. 19, Riga.

Chairman of the Doctoral Committee _____/

Dr. med., Professor **Valdis Pīrāgs**

Secretary of the Doctoral Committee _____/

Dr. biol., Associated Professor **Līga Plakane**

SUMMARY

Alzheimer's disease (AD) is a progressive and irreversible neurodegenerative disease. Multiple morphological changes, such as amyloid-β (Aβ) and hyperphosphorylated tau protein accumulation, as well as neuroinflammation, cause synaptic dysfunction and irreversible cognitive impairment. Currently, available symptomatic drug therapies do not cope with the progression of the disease, indicating the need for new drug therapies and enhancing studies of drug repurposing. The delivery of the tested compounds to the brain may be challenging due to the selective permeability of the blood brain barrier (BBB). The development of new drugs delivered into the brain is an important strategy for studying the mechanisms underlying brain diseases. In preclinical studies, mini-osmotic pumps represent a suitable delivery system for enhancing drug delivery across the BBB and studying the effects of long-term treatment using this intracerebral infusion technique. However, when selecting this drug delivery system, it is crucial to perform the accurately brain cannulation and followed by precise histological quantification of the Aβ pathology in the brain.

The goal of this thesis was to evaluate the effects of an anti-inflammatory drug as well as to improve methodology for intracerebral drug delivery and quantitative analysis of Aβ plaques in the brain of the AD mouse model.

The findings of this thesis indicated that the subchronical administration of the anti-inflammatory drug auranofin at low doses significantly reduces Aβ pathology in the transgenic AD mouse model, had no effect on spatial memory processes, and did not induce changes in the expression of the studied inflammatory and synaptic plasticity proteins.

Subsequently, two novel experimental methods have been developed to perform stereotactic brain infusion experiments by using an easy-to-produce, skull-shaped silicone fixation adapter and an analytic toolbox for Aβ pathology characterization in relation to the distribution of experimental compounds. Both optimized and generated methods improved the performance of the brain cannulation and histopathological evaluation of Aβ plaques after continuous long-term intracerebral injection *in vivo*.

To summarize, the data obtained on the effects of the anti-inflammatory drug and the new developed methods enhance preclinical research in the AD field, and further studies would expand their usage and potential impact.

Keywords: Alzheimer's disease; transgenic mouse model; amyloid-β; auranofin; intracerebral infusion; mini-osmotic pump; cannula fixation; histopathological quantification

KOPSAVILKUMS

Alcheimera slimība (AD) ir progresējoša un neatgriezeniska neirodeģeneratīva slimība. Dažādas morfoloģiskas izmaiņas, piemēram, amiloīda-β (Aβ) un hiperfosforilēta tau proteīna uzkrāšanās, kā arī neiroiekaisums, var izraisīt sinaptisko disfunkciju un neatgriezeniskus kognitīvos traucējumus. Pašreiz pieejamās medikamentozās terapijas ir simptomātiskas un īslaicīgi efektīvas. Tās nespēj novērst slimības progresēšanu, kas norāda uz nepieciešamību pēc jaunu un esošo medikamentozo terapiju turpmāku izpēti. Jaunu, uz smadzenēm mērķētu zāļu terapijas izstrāde ir svarīga stratēģija, lai pētītu smadzeņu slimību ārstēšanas iespējas un to patofizioloģiskos mehānismus. Tomēr zāļu nokļūšana smadzenēs noteiktiem savienojumiem var tikt apgrūtināta hematoencefāliskās barjeras (BBB) selektīvās caurlaidības dēļ. Piemērota vielu ievades sistēma, kas spētu nodrošināt dažādu savienojumu BBB šķērsošanu, un to efektivitātes pētīšanu ilgtermiņā, ir mini-osmotiskie sūkņi. Pirmsklīniskajos pētījumos, izmantojot šāda veida ievades sistēmas, ir svarīgi precīzi veikt smadzeņu kanulāciju un histoloģiski kvantificēt infuzēto eksperimentālo vielu izplatību smadzenēs.

Promocijas darba mērķis bija novērtēt pretiekaisuma zāļu vielas iedarbību uz dažādiem AD patofizioloģiskiem mehānismiem, kā arī pilnveidot metodoloģiju intracerebrālai zāļu ievadei un Aβ plāksnīšu kvantitatīvai analīzei smadzenēs AD peļu modelī.

Tika novērots, ka pretiekaisuma viela auranofīns mazās devās (1 mg/kg un 5 mg/kg) ievērojami samazināja Aβ patoloģiju, bet neietekmēja telpisko atmiņu un iekaisuma, kā arī sinaptiskās plasticitātes procesos iesaistīto biomarķieru proteīnu ekspresiju transgēno AD modeļdzīvnieku smadzenēs.

Sekojoši, tika optimizētas un iestrādātas jaunas pieejas divām zinātniskām metodēm, lai uzlabotu eksperimentālo vielu ilgstošu un nepārtrauktu intracerebrālu ievadi, izmantojot mini-osmotiskos sūkņus. Pirmā metode, nodrošināja precīzu un noturīgu intracerebrālās kanulas fiksāciju, izmantojot optimizētu silikona adapteri. Otra metode, veicināja pielāgotu Aβ patoloģijas kvantifikācijas analīzi, attiecībā pret intracerebrālo ievades punktu. Attīstītās un optimizētās metodes uzlaboja intracerebrālās kanulācijas un histopatoloģiskās kvantificēšanas procesu AD *in vivo* eksperimentālajos moduļos.

Kopumā iegūtie dati par pretiekaisuma vielu auranofīnu un jaunu metožu attīstīšanu un pilnveidošana sniedz nozīmīgu pienesumu pirmsklīniskos pētījumos AD jomā.

Atslēgas vārdi: Alcheimera slimība; transgēnās peles modulis; β-amiloīdu patoloģija; auranofīns; intracerebrālā ievade; mini-osmotiskais sūknis; kanulas fiksācija; histopatoloģiskā kvantifikācija

Table of Contents

ABBREVIATIONS

3×Tg –	triple-transgenic
3D –	three-dimensional
5-hmC –	5-hydroxymethylcytosine
5-mC –	5-methylcytosine
ACh –	acetylcholine
AChE –	acetylcholinesterase
aCSF –	artificial cerebrospinal fluid
AD –	Alzheimer's disease
AMPA –	α-amino-3-hydroxy-5-methyl-4-isoxazolepropionic acid
ANOVA –	analysis of variance
APOE –	apolipoprotein E
APOE e2 –	apolipoprotein E epsilon 2
APP –	amyloid precursor protein
Aβ –	β-amyloid
Aβ40 –	amyloid beta peptide 1-40
Aβ42 –	amyloid beta peptide 1-42
BACE1 –	β-site APP-cleaving enzyme 1
BBB –	blood-brain barrier
BChE –	butyrylcholinesterase
CA –	cornus ammonis
CAA –	cerebral amyloid angiopathy
cAMP –	cyclic adenosine monophosphate
CD –	cluster of differentiation
CDK5 –	cyclin-dependent kinase 5
CNS –	central nervous system
CPu –	striatum
CR –	Congo red
CSF –	cerebrospinal fluid
DA –	dopamine
DG –	dentate gyrus

DMSO – dimethyl sulfoxide

DNA – deoxyribonucleic acid

EOAD – early-onset Alzheimer's disease

ERK1/2 – extracellular signal-regulated kinase 1/2

FAD – flavin adenine dinucleotide

GABA – γ-aminobutyric acid

GAD67 – glutamic acid decarboxylase 67

GFAP – glial fibrillary acidic protein

GLUTs – glucose transporters

GSK-3 – glycogen synthase kinase 3

GWAS – genome-wide association studies

hAPP – human amyloid precursor protein

HDAC – histone deacetyltransferase

Homer-1 – Homer protein humolog-1

Iba-1 – ionized calcium binding adaptor molecule 1

IL – interleukin

ip – intraperitoneal

KCC2 – K+-Cl- cotransporter 2

LOAD – late-onset Alzheimer's disease

LTP – long-term potentiation

MAPK – mitogen-activated protein kinase

MAPT – microtubule associated protein tau

mEOAD – mendelian EOAD

miRNAs – micro ribonucleic acids

mT21 – trisomy 21 mosaicism

ncRNAs – non-coding RNAs

NE – norepinephrine

NFTs – neurofibrially tangles

NF-κB – nuclear factor kappa-light-chain-enhancer of activated B cells

NKCC1 – Na+-K+-2Cl- cotransporter 1

NMDA – N-methyl d-aspartate

nmEOAD – nonmendelian EOAD

NO – nitric oxide

NSAIDs – nonsteroidal anti-inflammatory drugs

OXPHOS – oxidative phosphorylation

PBS – phosphate-buffered saline

PFA – paraformaldehyde

PKC – protein kinase C

PSEN1 – presenilin-1

PSEN2 – presenilin-2

ROI – region of interest

ROS – reactive oxygen species

SRB-1 – scavenger receptors type B-1

TBI – traumatic brain injury

Tg – transgenic

TLR – Toll-like receptors

TREM-2 – myeloid cell 2

Wnt – wingless-int

τP – tau protein

Goals and objectives of the thesis

The goal of the thesis:

To evaluate the effects of an anti-inflammatory drug as well as to improve methodology for intracerebral drug delivery and quantitative analysis of Aβ plaques in the brain of the AD mouse model.

Objectives of the thesis:

1. To determine the effects of the subchronic intraperitonially administered anti-neuroinflammatory drug auranofin in the 14-month-old transgenic $APP^{NL\text{-}G\text{-}F/NL\text{-}G\text{-}F}$ mouse model:
    1.1. on spatial learning/memory and anxiolytic behaviour;
    1.2. on the cortical and hippocampal density of proteins involved in:
        1.2.1. β-amyloid (Aβ) pathology ((anti-Aβ antibody (W0-2) and Congo Red (CR));
        1.2.2. microgliosis (glial fibrillary acidic proteins, GFAP) and astrogliosis (ionized calcium-binding adaptor molecule-1, Iba-1);
        1.2.3. synaptic plasticity (glutamic acid decarboxylase 67 (GAD67) and homer protein homologue-1 (Homer-1)).
2. to improve the method for cannula fixation for the long-term intracerebral infusion by using an optimized fixation adapter.
3. to develop a new toolbox for the histopathological analysis of long-term intracerebrally injected anti-Aβ compounds.

Thesis for defence:

1. Subchronic administration of auranofin may have a positive impact on behaviour and reduce Aβ pathology and influence neuroinflammatory process in the brain of transgenic mouse model of AD.
2. Optimisation of the fixation method for the brain cannula and adapter promotes to perform stereotactic brain infusion experiments in secure and high-quality reproducible manner.
3. A new analytic toolbox can serve as an alternative approach to perform an extensive analysis of histological images and quantification of Aβ pathology parameters after long-term intracerebral injection in transgenic AD mice.

Publications

This thesis is based on the following papers, which are referred to in the text by their Roman numerals

Paper I **J. Upīte**, I. Kadish, T. van Groen, B. Jansone. Subchronic administration of auranofin reduced amyloid-β plaque pathology in a transgenic $APP^{NL\text{-}G\text{-}F/NL\text{-}G\text{-}F}$ mouse model. Brain Research, 2020; 1746: 147022. https://doi.org/10.1016/j.brainres.2020.147022.

Paper II Á.Sike, J. Wengenroth, **J. Upīte**, T. Brüning, I. E. Delgado, P. Sántha, H. Biverstål, B.Jansone, H. Jostein, M. Krohn, J. Pahnke. Improved method for cannula fixation for long-term intracerebral brain infusion. Journal of Neuroscience Methods, 2017; 290: p. 145-150. https://doi.org/10.1016/j.jneumeth.2017.07.026.

Paper III **J. Upīte**, T. Brüning, L. Möhle, M. Brackhan, P. Bascuñana, B. Jansone, J. Pahnke. A new tool for the analysis of the effect of intracerebrally injected anti-amyloid-β compounds. Journal of Alzheimer's disease, 2021; Online ahead of print. https://doi.org/10.3233/JAD-215180.

Conference thesis

1. **J. Upīte**, T. Brüning, L. Möhle, M. Brackhan, P. Bascuñana, B. Jansone, J. Pahnke. A new tool to access the effect of intracerebrally administred anti-amyloid compounds. 15th International Conference on Alzheimer's & Parkinsons's Diseases, March 15-20, 2022, Barcelona, Spain: Scientific Programm Barcelona, 2022, P327, p.[660].
2. **J. Upīte**, I. Kadish, T. van Groen, B. Jansone. Auranofin reduced the amyloid – β pathology in a transgenic APPNL-G-F/NL-G-F mouse model. 8th European Congress of Pharmacology, December 6-8, 2021.
3. **J. Upīte**, T. Brüning, B. Jansone, J. Pahnke. New quantification method for amyloid-β plaques in relation to intracerebral injection channels. TransportDEMENTIA4 (TD4), May 20th, 2021: General Information, P.14.
4. **J. Upīte**, T. Brüning, B. Jansone, J. Pahnke. A novel approach for the quantification of amyloid-β plaques. Baltic Winter School 2 (BWS2): Focus on Neurodegenerative Diseases, April 9th, 2021: General Information, P. 11.
5. **J. Upīte**, T. Brüning, B. Jansone, J. Pahnke. A novel approach for quantification of amyloid-β plaques after long-term intracerebral brain infusion using Alzet microosmotic pumps. 78th International Scientific Conference of the University of Latvia. Book of Abstracts 2020, P.11.
6. **J. Upīte**, B. Jansone. Systemic Long-Term drug administration in different AD mice. FEBS3+ conference of Latvian, Lithuanian and Estonian Biochemical Societies, June 17-19, 2019, Book of Abstracts Riga 2019, P.31.
7. **J. Upīte**, I. Kadish, T. van Groen, B. Jansone. The behaviour effects of Auronofin in Transgenic APP NL-G-F/NL-G-F mice. 14th International Conference on Alzheimer's & Parkinsons's Diseases, March 26-31, 2019, Lisbon, Portugal: Scientific Programme Lisbon, 2019, P.1.
8. **J. Upīte**, I. Kadish, T. van Groen, B. Jansone. Auranofin decrease progression of neurodegeneration by reducing Aβ peptide deposition in APPNL-G-F/NL-G-F mice. BaltPharm Forum 2019, Book of Abstracts 2019, p.256-257.
9. **J. Upīte**, I. Kadish, T. van Groen, B. Jansone. Auranofin reduces brain amyloid-β (Aβ) load in Alzheimer disease APPNL-G-F/NL-G-F mice model. 77th International Scientific Conference of the University of Latvia. Book of Abstracts 2019, P.7.

10. **J. Upīte**, A. Sike, V. Piļipenko, U. Beitnere, M. Krohn, H. Biverstal, V. Z. Kluša, J. Pahnke, B. Jansone. An improved methodology for long-therm continuous intracerebral infusion of experimental substances by Alzet microosmotic pumps. 75th International Scientific Conference on Medicine of the University of Latvia. Book of Abstracts 2017, P.97.

1. LITERATURE OVERVIEW

1.1. Alzheimer's disease

Alzheimer's disease (AD) is the commonest cause of dementia with an estimated more than 50 million sufferers worldwide. Statistics indicate as there's currently no cure available the number of AD patients could double every decade and may even grow up to 152 million in 2050. In addition, data represents enormous strain on the health care system, which has been valued at nearly $244 billion with tendency to growth, us mental and physical stability has been skewed to family caregivers and therefore creating a negative influence on the overall economy (Alzheimer's Association and Association, 2020; Janoutová et al., 2020).

AD is a neurological and irreversible disease of central nervous system (CNS), that it becomes worse with time. There are several forms of dementia (manifests as the loss of cognitive functioning - thinking, remembering, and reasoning) and AD is the most common type. The onset of psychological changes is usually so insidious the neither the family not the patient can date the time of its beginning and most patients come attention months or years after decline begun. It has been thought that AD begun 20 years or even earlier symptoms get noticeable. Brain disease such us AD cause non-reversable damage by destroying nerve cells in areas of the brain involved in memory, thinking, speaking or learning processes (Junakovic and Telarovic, 2021). Symptoms of AD can differ from mild to moderate or to severe stages. Generally, behavioural and cognitive impairments mirror the affected brain regions in AD. The length of each stage of AD has been influenced by age, genetics, gender and other risks factors. In the mild stage, the patients are able to perform daily tasks without an assistance, but small day-to-day happenings could not be remembered, or appointments are forgotten, and possessions misplaced. Once the memory disorder has become pronounced, other failures become increasingly apparent, therefore at the moderate and severe stage patients should have continuous day-care, as individuals may have difficulties communicating or performing regular multiple tasks (moderate stage) or being bedfast (severe stage) (Alzheimer's Association and Association, 2020; Apátiga-Pérez *et al.*, 2021). Although AD has been described at every period of adult life, the majority of patients are in their 60s or older, a relatively small number have been in their late 50s or younger. The incidence rate of clinically diagnosed AD patients is similar throughout the world, and it increases comparably with age. Prevalence rates, which depend also on overall mortality, are 3 times higher in women. The prevailing reason that has been stated is that there exist differences in lifespan between males and females, by pointing

out that women live longer than man (Weller and Budson, 2018; Devkota, Williams and Wolfe, 2021; Schwartzentruber et al., 2021).

Researchers have found that there are multiple risk factors which could may affect the development and progression of AD. Well-established pathological hallmarks of AD are β-amyloid (Aβ) and neurofibrially tangles (NFTs) containing hyperphosphorylated tau protein (τP) accumulation which may contribute to the damage and death of neurons by interfering with neuron-to-neuron communication at synapses and causing subsequent cognitive decline. Other brain changes associates with inflammation and atrophy or even well-being of cardiovascular system. AD represents an increasing challenge to public health and the health care system countries. Deposition of toxic proteins in the brain leads to dementia, motor dysfunction, and psychiatric disorders. Despite enormous efforts, so far, the pathological mechanism of of AD has not been revealed and treatment in not available. There is only three classes of drugs approved for use in AD, including disease-modifying drug amyloid antibody aducanumab, inhibitors to cholinesterase enzyme (naturally derived, synthetic and hybrid analogues) and antagonists to N-methyl d-aspartate (NMDA). There is an urgent need for medical breakthroughs to combat this debilitating disease (Junakovic and Telarovic, 2021).

1.1.1. Types and risk factors of AD

AD is divided into 2 subtypes - early-onset AD (EOAD) and late-onset AD (LOAD). EOAD is the rare form and accounts for approximately 1–6% of all cases. EOAD is defined as familial AD and characterized by having more than one member in more than one generation with AD, and ranges from 30–60 or 65 years. The second type is LOAD, which is more common with age of onset from 60 - 65 years or above. Both subtypes may occur in individuals with a positive family history of AD. Almost 60% of EOAD cases have several cases of AD within their families and 13% of these cases are inherited in an autosomal dominant manner (Fig.1) (Vally and Kathrada, 2019; Olsen and Singhrao, 2020).

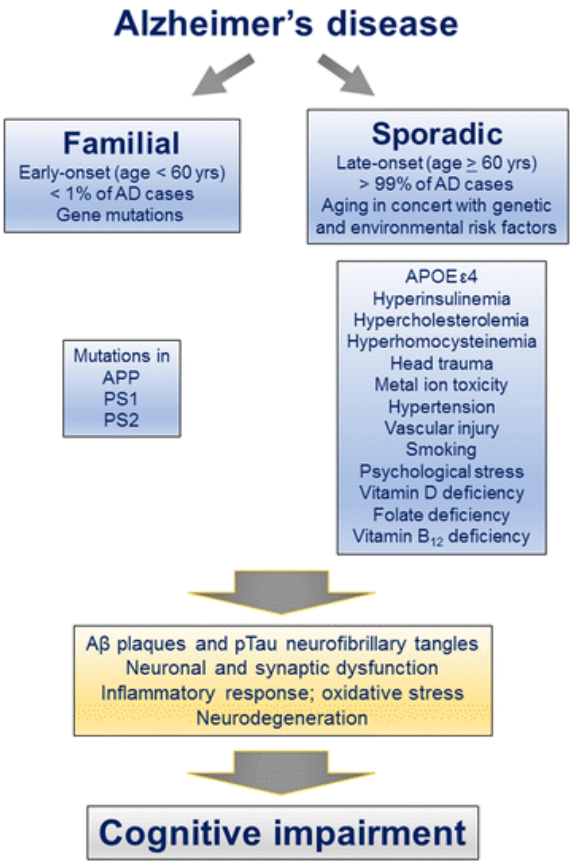

Fig.1. **Multifactorial nature of AD and involvement of several different etiopathogenic mechanisms. Adapted from** (Kazim and Iqbal, 2016)

1.1.1.1. Early-onset AD

The focus of research over the past years has been on LOAD, but patients, like Auguste Dieter, make the EOAD subclass impactful as prevalence rates of EOAD have been grown logarithmically in human population with age. EOAD has more aggressive clinical course with high rate of mortality than LOAD. Moreover, EOAD is typically diagnosed with average delay of 1.6 years. Numerous studies represent the differences between EOAD and LOAD, for instance EOAD has significant direct autosomal dominant transmission inheritance of a gene. Patients with EOAD autosomal dominant familial form not only have greater chance to develop AD within family members, but may also have different atypical clinical features, including seizures, headaches, walk impairment or hyperreflexia. Overall, patients with EOAD, compared to comparably impaired LOAD patients, not only have better memory recognition scores and semantic memory, but also a tendency to have worse focusability, executive functions and visuospatial skills (Mendez, 2017, 2019; Tublin *et al.*, 2019).

Several studies indicate, that EOAD divides in 2 forms by observing inheritance patterns. The first form, mendelian EOAD (mEOAD), accounts only 10% of all EOAD cases and are most often caused by mutations in amyloid precursor protein (APP), presenilin-1 (PSEN1), and presenilin-2 (PSEN2) genes. Other form, nonmendelian (nmEOAD), is generally considered to be multifactorial and not obviously autosomal dominant and has been thought to be simply an extreme phenotype of LOAD, interacting with it environmental and genetical factors ((Tellechea *et al.*, 2018; Mendez, 2019; Nuebling *et al.*, 2021). Furthermore, a new study indicates that low-degree trisomy 21 mosaicism (mT21) promotes EOAD. The patients who carry mT21 gene are mostly diagnosed with Down Syndrome because of triplication of the APP gene and its localization on chromosome 21 (Nuebling *et al.*, 2021).

In general, neuropathological distinctions between EOAD and LOAD remains unclear. In some EOAD and few LOAD cases neuropathology has been characterized by diffuses cotton wool Aβ plaques without neuritic pathology or neuroinflammation, but as disease progresses the structure of Aβ plaques could change and set another course on the development of AD. There is urgent need to better define the pathological differences between both types of AD (Reitz, Rogaeva and Beecham, 2020; Duarte-Abritta *et al*., 2021).

1.1.1.2. Late-onset AD

The LOAD may be genetic, but it is more likely a result of brain changes caused by lifestyle and environmental impacts. These brain changes involve several different etiopathogenic mechanisms in concern with aging, such as metabolic imbalances, head trauma, metal ion toxicity, hypertension, vascular injury, psychological stress, and vitamin deficiencies. Environmental risk factors including air pollution, diet, infections, and many others may induce oxidative stress and inflammation and increase the risk for developing AD (Hughes and Hajjar, 2021; Knopman *et al*., 2021).

Two main and best-known genetic risk factors linked to LOAD are apolipoprotein E (APOE) and myeloid cell 2 (TREM-2) proteins. The APOE gene can be found on chromosome 19 and comes in multiple forms, but most commonly occurs: APOE epsilon 2 (APOE e2), APOE e3 and APOE e4. Multiple large-scale genome-wide association studies (GWAS) have identified over 30 genome-wide significant common variant signals in addition to APOE that influence risk for LOAD. Moreover, a systematic neuropathological studies of large autopsy cohorts have been suggested that APOE genetic forms correlates with the presence and severity of different protheopathies, such us, the lesions of Aβ plaques and NFTs containing hyperphosphorylated tau. The greatest genetic risk for LOAD in the human population are

having e4 form. Unlike, other genetical forms of APOE, the e4 is less effective to remove Aβ plaques from the brain by promoting its aggregation and deposition in insoluble fibrillar structure. Additionally, several studies have reported that APOE influences microglial cells. The gene who codes a protein in the brain that is expressed on microglial cells and also involved in removing degenerated tissue, including remnants from neuroinflammation is TREM-2. Data reveal that the deficiency of TREM-2 protein has been inhibiting Aβ aggregation in primary microglial culture and in a mouse brain model. Furthermore, the TREM-2 protein may accelerate aging processes, neuronal cell loss and reduce microglial activity, which could trigger neuroinflammation. This diversity of genes mostly points to specific pathways, e.g., lipid metabolism, endocytosis/intracellular trafficking, inflammation, immune response, synaptic function, and transcription, indicating a major role for these pathways in the development of LOAD (Kleinberger *et al.*, 2017; Schwartzentruber *et al.*, 2021).

Overall, the pathogenesis of LOAD remains to be clarified. However, several studies consistently reported that there are middle-life risk factors which may affect the selectivity and progressivity of neuropathological hallmarks of LOAD and could be modifiable during lifestyle changes. One of the potential modifiable risk factors are linked with vascular and metabolic system, e.g., hypercholesterolemia, diabetes mellitus, hypertension and atherosclerosis. These conditions are associated with impaired functionality of the cerebrovascular system, particularly the blood-brain barrier (BBB). BBB is a barrier who consists of a continuous layer of endothelial cells and regulates the transport of several environmental stressors, such us, toxins or pathogens. However, inflammation and immune responses can disrupt the integrity of the BBB, allowing normally impermeant substances to enter the brain. For example, vascular insufficiency can cause decrease of cerebral blood flow and thus activate Aβ cleavage and accumulation and initiate neurodegeneration in the brain. Longitudinal population studies have reported that midlife and later-life hypertension have harmful effects on brain health by disturbing haemostatic balance of the BBB. The unregulated high blood pressure may increase brain Aβ protein accumulation and affect cognitive abilities in older adults. Hypertension is a treatable risk factor of LOAD. Some studies have been stating that antihypertensive treatment could be only known preventive action for dementia. However, it is still inconclusive, if lowering blood pressure could reduce Aβ plaques and cognitive decline. Additionally, BBB is responsible for the transport of sufficient amount of glucose to astrocytes and neurons (Banks *et al.*, 2021; Gindorf *et al.*, 2021).

The pathophysiologic background for the role of chronic hyperglycaemia in the development of LOAD includes reduced GLUTs (glucose transporters), glycation end product

accumulation, impaired insulin receptor activation and direct glucose neurotoxicity. Several studies have investigated the effectiveness of antidiabetic drugs to improve cognitive decline. Despite this fact, an intensive diabetic and insulin therapy could not be used as preventive treatment to delay LOAD progression possibly because of the increased risk of hypoglycaemia. In addition, some studies have shown that nutrient deficiency plays a significant role in glucose metabolism dysfunction in LOAD. Deficiency of thiamine, folate and vitamin B12 are important contributors to the induction of incorrect glucose transport and neuronal metabolism. General, the haemostasis between protein aggregation and clearance, as well as oxidative stress and reduction capacity, also tend to be interrupted and thus further leads to proteopathy progression of pathological aggregates: plaques of Aβ and NFTs of tau and of cell death in neurons. The various nutrients and food items (ω3, vitamins and antioxidants) have been studied for their potential as preventive treatment of LOAD, nonetheless, diet intervention studies are still limited and needed (Baumel *et al.*, 2021; Chauhan and Yadav, 2021).

Similarly, to hypertension and hyperglycaemia, other epidemiological studies have confirmed that midlife overweight, prevalence of body mass index, is one of the risk factors for developing LOAD. Data revealed that overweight was corelating to greater cortical atrophy in patients diagnosed with LOAD. Even more, there was measured 0.5% decrease in brain tissue volume for every unit increase in body mass index. Unfortunately, no studies are available by indicating that weight loss before the age of 65 years could be a complementary approach to the prevention strategy against dementia (Rabinovici, 2019; Knopman *et al.*, 2021).

According to the numerous studies, the risks of LOAD increases with the number of traumatic brain injuries (TBI). According to the Centres of Disease Control and Prevention a numerous TBI- related emergencies and hospitalizations occurs each year. A recent study found that greater the severity of the TBI (also know us concussion) the higher the risk of developing LOAD. Several study designs consisting of cohort studies, longitudinal studies and systematic reviews have shown that 4 weeks after TBI the neurofibrillary proteins, APP, PS1with Aβ protein were detected. The various prevention strategies have been offered, requiring use of seat belts, helmets and improving protocols for various sports injuries (Janoutová *et al.*, 2020; Litke *et al.*, 2021).

Overall, other environmental stressors such us psychological stress, air pollution, metals and smoking have an impact on the cerebrovascular system, Aβ deposition and microglial function. These environmental stimuli can cause not only Aβ toxicity, metal toxicity but also

oxidative stress, inflammation, apoptosis, excitotoxicity which could result in neuronal/ synaptic loss and cognitive complications (Knopman *et al.*, 2021; Litke *et al.*, 2021).

1.2. Pathophysiology of AD

Currently, there is a major lack of understanding of the complete disease mechanism in AD. Pathologically, the most prominent and early hallmark of AD (both EOAD and LOAD) is extracellular deposited Aβ protein forming senile plaques and later contributing to intracellular NFTs in hippocampus and the cerebral cortex. Misfolded and aggregated proteins in association with neuroinflammation, mitochondrial bioenergetic deficits, brain hypometabolism, impairment of BBB, angiopathy cause the death of neurons and the development of cognitive and memory impairment. The deposition of proteins in the form of amyloid fibrils and larger aggregates is the characteristic feature of more than 20 degenerative conditions affecting either the CNS or a variety of peripheral tissues. These conditions include not only Alzheimer's but also Parkinson's, and Huntington's disease or peripheral diseases like type-II diabetes, and Transthyretin amyloidosis. Aggregates of Aβ plaques are found in a time dependent, region-specific manner, starting in the hippocampus, particularly the *cornus ammonis* (CA) 1 and 2 zones followed by temporal lobe, frontal lobe, and finally occipital lobe involvements. These parts have abundant connections with other parts of the temporal lobe cortex and dentate gyrus (DG) of the hippocampus undoubtedly account for the amnesic component of the dementia (Ju and Tam, 2022; Rey *et al.*, 2022).

1.2.1. Amyloid pathogenesis

Amyloid pathogenesis starts with APP, which is normally bound to neuronal membranes. APP is a normal transmembrane glycoprotein and belongs to a family of associated proteins that includes mammalian amyloid precursor like proteins in *Drosophilia*. The function of APP is uncertain, but suggestions include roles in cell-cell and cell-matrix interactions. The predicted structure of APP consists of three domains: a) a small cytosolic, b) a transmembrane and c) a large extracellular, and compromises 770 amino acids, of which Aβ, a small residue peptides (amyloid beta peptide 1-40 (Aβ40) and 1-42 (Aβ42), in plaques are a derived from APP (Fig.2) (Lee, Jeong and Jang, 2021; Yang, Perrett and Wu, 2021).

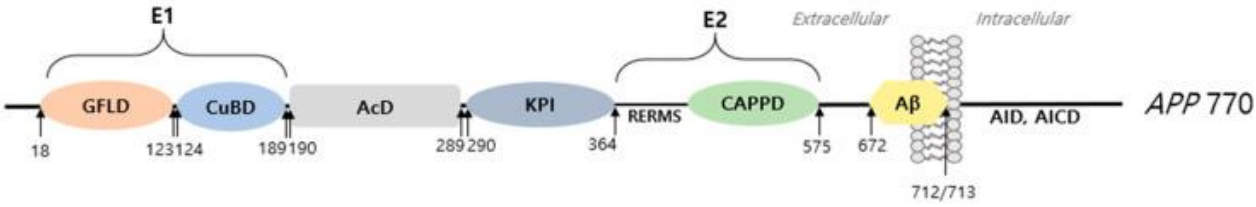

Fig. 2. **Schematic illustration of APP 770 isoform domain. APP consists of three domains: a large extracellular (E1), a transmembrane (E2) and a short cytoplasmic (intracellular) terminus. Adapted from** (Lee, Jeong and Jang, 2021)

In AD, APP generates amyloidogenic fragments by the action of proteases termed α, β, y secretase. The protein is proteolytically processed by different secretases via amyloidogenic (diseased) and non- amyloidogenic (non-diseased) proceeding pathways which either releases the Aβ peptide (cleaved by β- and γ-secretase) or precludes Aβ formation (cleaved by α-secretase) (Fig.3). The majority of APP is processed via the non-amyloidogenic pathway at the plasma membrane. In the non-amyloidogenic pathway, APP is cleaved by α-secretase near the middle of the Aβ region between Lys16 and Leu17, producing a soluble N-terminal fragment (APPs α) and a membrane-bound C-terminal fragment (C83), which can be further cleaved by the y-secretase isoform (Darling and Shorter, 2020; Finch, Bagit and Marko, 2020; Hsien *et al.*, 2020; Yu and Wu, 2021). The sequential cleavage by α and then y produces tiny fragments that are not toxic to neurons. These Aβ40 and Aβ42 peptides can be found in the cerebrospinal fluid (CSF) of normal patients, indicating that α- and y-secretase cleavages, small hydrophobic fragment p3, of APP are normal events. Production of p3 monomer is soluble and has a role in normal synaptic signalling, but there is still uncertainty regarding its exact functions. Several studies hypothesizing, that the α-secretase processing releases APPα, large soluble ectodomain, which provides neuroprotection and its occurrence associates with normal synaptic signalling, synaptic plasticity and neuronal survival (Tiwari *et al.*, 2019; Kuhn *et al.*, 2020). In the disease state, APP is cleaved differently. Cleavage by β- and y-secretase results in a 40 or 42 amino-acid forms (Aβ40 and Aβ42). β-site APP-cleaving enzyme 1 (BACE1) generates the amino terminus of Aβ and a γ-secretase multi-protein complex determines its length, with Aβ40 being more common and Aβ42 being the peptide that aggregates more rapidly and forms oligomeric aggregates at an earlier time point. These two secretases are aspartyl proteases, including a membrane-spanning (BACE1) and intramembrane that is made up of four proteins: PSEN, nicastrin, anterior pharynx-defective 1 and PSEN2 complex together (y-secretase). This complex regulates the activity of y-secretase and its approach to producing insoluble and toxic Aβ aggregates. Aβ42 aggregates rapidly into neurotoxic oligomers, leading to fibrils and

plaques. Atypical process of APP by β- and γ-secretase may result in imbalance between production and clearance of Aβ peptides (Strodel, 2021; Yang, Perrett and Wu, 2021).

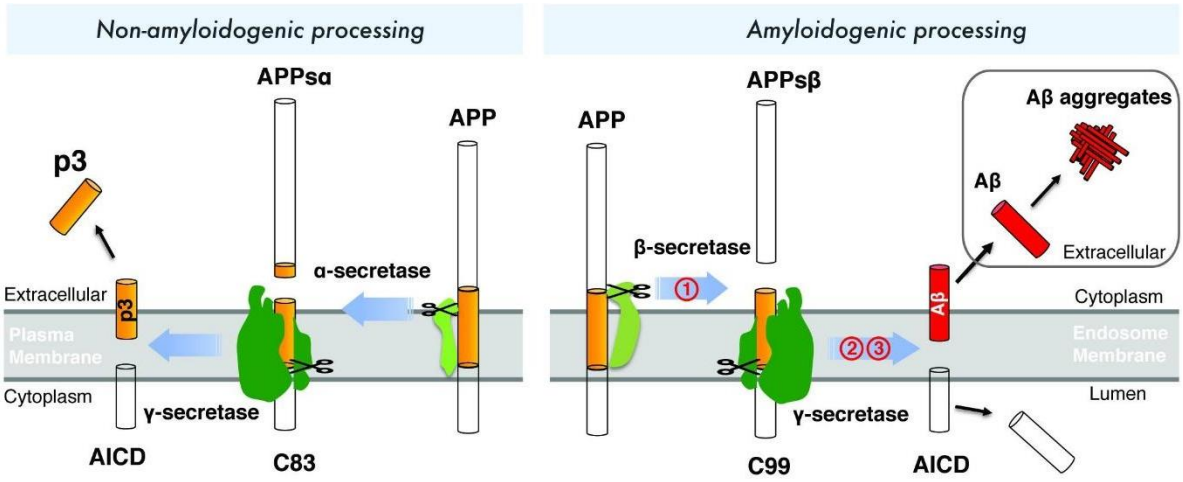

Fig. 3. **Schematic illustration of amyloidogenic and non-amyloidogenic processing of APP. Adapted from** (Zhao *et al.*, 2020)

A strong support for the importance of Aβ aggregation and oligomerization in the pathogenesis of AD comes from the observation that inherited, EOAD-causing mutations, enhance the production of Aβ42 resulting in increased intracerebral levels of Aβ42, or at least increased ratios of Aβ42/Aβ40, or an increased stability of prefibrillar aggregates. Another suggestive connection states that there are genetic deficits in the genes encoding APP and in a pair of endosomal proteins termed PSEN1 and PSEN2 in some early-onset forms of AD. The PSEN interact with, or may be a component of, γ- secretase, the enzyme which produces the Aβ42 fragment. Mutations of PSEN1 and PSEN2 also increase the relative levels of Aβ42. There is also a remarkable relationship in AD between certain circulating proteins, particularly Aβ and selected isoforms of APOE lipoproteins (Tsatsanis *et al.*, 2021; Yasuno *et al.*, 2021).

Several studies hold an opinion, that vascular changes have an important or direct role in the pathogenesis of AD. It has been pointed that probably the deposition of Aβ residues in the walls of cerebral vessels and a reduction of small blood vessels and associates with cerebral infarction. Deposition of Aβ may cause two types of diseases, cerebral amyloid angiopathy (CAA) and AD, were pathogenic mechanisms differs. Nonetheless, the two different pathways could interact during crosstalk between neurodegenerative process and the blood vessels. Evidence indicates as CAA affects perivascular drainage and Aβ aggregates clearance from the brain. Several pathological studies investigating post-mortem brain tissue from patients with

AD have indicated that Aβ aggregates can been found around arteries five times more that around veins. These studies support the idea that Aβ deposits exits in the brain and reduce perivascular clearance in CAA and AD patients. These promising findings indicates that there is a great need to recognize interactions between these two processes in disease pathogenesis (Grangeon *et al.*, 2021; Kalaria and Sepulveda-Falla, 2021).

Amyloid plaques are extracellular proteinaceous aggregates made of Aβ peptide, either as amyloid filaments or in non-filamentous form. There are four main types of plaques: a) diffuse, b) primitive, c) classic (mature) and d) burn-out (end-stage). Diffuse plaques are ill-defined focal aggregates of amyloid and pre-amyloid material and are about 60-300mm in diameter and do not contain τP. Primitive plaques are similar to diffuse plaques, however they are almost spherical and can be determined in smaller diameter (60-120μm). Classic (mature) or neuritic plaques, 60-120μm in diameter, that are often separated into dense core and could contain τP. Classic plaques have been characterized with eosinophilic plaque core, were microglial or astrocytic cells are migrating around the plaque periphery. These eosinophilic dense core aggregates have been labelled as cotton wool plaques and have been noted in EOAD. Burn out (end-stage) plaques are extracellular compact cores (Boon, 2020; Willumsen *et al.*, 2021). It is believed that there is a gradual movement towards from diffuse, through primitive to mature and finally end-stage plaques. Plaques are widely distributed in the brain of patients with AD and may be not only neocortex and hippocampus but also in the basal ganglia, hypothalamus, the tegmentum of the midbrain and pons, the cerebellum and the subcortical cerebral with matter. Moreover, it appears that deposition of the peptides $A\beta_{40/42}$ results in increased mitochondrial oxidative stress, in blocked ion channels, neuroinflammation, disturbed calcium homeostatic balance and weakened energy metabolism and glucose regulation, which contributes to neurotic dystrophy (Kurokin *et al.*, 2021; Y. Sato *et al.*, 2021).

1.2.1. Neurofibrillary tangles and hyperphosphorylation of tau protein

The importance of NFTs has also been examined, and the way aggregation of Aβ plaque relates to tangle formation is unclear. On the other hand, several studies demonstrate that there could be protein-protein interaction in neurodegenerative diseases. These tangles are neuronal inclusion, formatted mainly of filamentous aggregates of hyperphosphorylated microtubule-associated τP that are variably ubiquitinated and glycated. Normal τP are predominantly axonal and by interaction with α- and β-globulin. It stabilizes the microtubules within the neuronal

cytoskeleton. Microtubules provides the crucial processes in neurons, such us, maintenance of neuronal structure, axonal transport and synaptic plasticity. The tau gene, microtubule associated protein tau (MAPT), is located on chromosome 17 and splicing of its transcripts leads to the synthesis of six main isoforms of tau, which serves as microtubule-binding sites. These isoforms have different N-terminal inserts and microtubule-binding domains, e.g., τP has 0,1 or 2 N-terminal inserts and 3 or 4 microtubule-binding domains, with are resulting from the splicing in or out of exons 2, 3 or 10 (Tarutani *et al.*, 2021). There are several kinases, activated by Aβ aggregates, which regulates phosphorylation of τP, including glycogen synthase kinase 3 (GSK3) and cyclin-dependent kinase 5 (CDK5). Hyperphosphorylation of τP, leads to its progressive oligomerization and induce structural changes of microtubule, thus persuades production of τP as soluble free paired helical filaments in higher levels. Deposition of these type oligomerized proteins disturbs stabilisation of tubule subunits. After structural collapse of microtubule, a large filament of τP aggregates as NFTs. Aggregation of NFTs could further initiate loss of communication between neurons, signal processing and neural apoptosis (Fig.4). Nonetheless, is still a matter of discussion and more evidence are needed, to prove which τP isoforms are responsible for neurotoxicity. Transmission processes of τP occurs commonly at synapses, where it's been released to the extracellular space by synaptic vesicles or direct translocation. Further, τP has been internalized through receptor or heparan sulphate proteoglycan, clathrin- and dynamin-mediated endocytosis and phagocytosis. Additionally, τP could be spread by extracellular vesicles that fuse to the membrane of the recipient cell (Pérez, Avila and Hernández, 2019; Perea, Bolós and Avila, 2020).

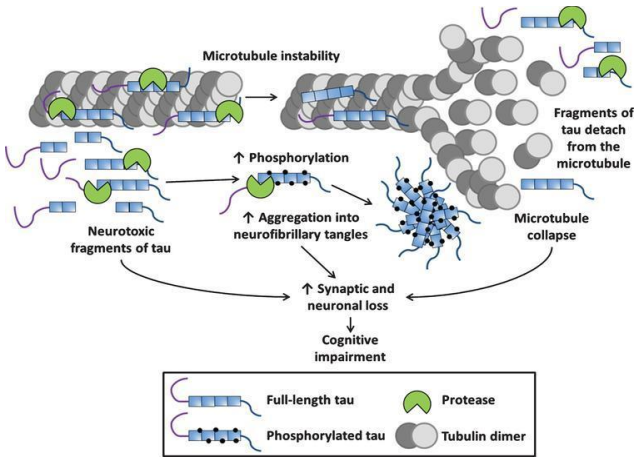

Fig. 4. **Schematic presentation of tau proteolysis and its affect to tauopathy pathogenesis. Adapted from** (Quinn *et al.*, 2018)

Remarkably, τP phosphorylation in AD can be viewed as a hierarchical process, meaning that some sites are phosphorylated earlier in the disease course. Several possible mechanisms may be involved. Studies demonstrates, that the τP isoforms associated with AD are 3- and 4-repeat tauopathies. Even more, there are about 45 potential phosphorylation sites in τP which have been differentially phosphorylated in AD patients. *In vitro* and *in vivo* experimental studies have confirmed that Aβ may induce pathological changes in neuronal τP. Experiments with transgenic (Tg) animals have shown that aggregation of Aβ are associated with increased levels of soluble τP and CSF τP levels. Other *in vivo* studies also showed that development of Aβ aggregates is linked to increased levels of CSF- τP. A few, post-mortem studies showed that density of NFTs was correlated with cognitive impairments in AD patients. The triple transgenic (3×Tg) mouse model of AD, which develops both Aβ and tau pathology, plaques developed before NFTs, and antibodies directed against Aβ reduced early-disease but not late-disease tau alterations. Several APP models exhibit some degree of Aβ-induced τP hyperphosphorylation, especially in dystrophic neurites near Aβ plaques, and increased CSF-tau levels. Additionally, β-secretase inhibition prevented the age-related increase of CSF-tau of APP mice (Busche and Hyman, 2020; Park *et al.,* 2020).

Recent imaging studies replicate the spreading of pathologic τP along the disease and observed a positive association between aggregated τP and cognitive decline, suggesting a toxic function of insoluble τP. Unfortunately, there are limited data from humans about relationships between formation of Aβ plaques and altered release, phosphorylation and aggregation of τP. There are data that reveals CSF levels of τP, especially P-tau217 and P-tau181, are increased in response to Aβ deposition in humans in early stages of AD. These all findings demonstrate that pathological process of Aβ can be activated by significant changes in metabolism of soluble τP. Moreover, it extends the amyloid cascade hypothesis of AD and suggests that there is strong correlation between Aβ pathology and τP aggregation. Research indicates that the role of Aβ is more complex, such that its presence enhances tau phenotypes throughout the disease course (Mattsson-Carlgren *et al.,* 2020).

1.2.2. Neuroinflammation

Apart from the Aβ and NFTs, neuroinflammation has been demonstrated as an important key role in the pathogenesis of AD. In AD neurons are injured and die throughout the brain by triggering a neurotoxicity. Undoubtedly, the fundamental task of neuron is to receive, conduct and transmit signals. To provide such a control of the chemical and electrical environment,

they are outnumbered by supporting cast of glial cells. Astrocytes and microglial cells are two main types of glial cells which are tangled in the inflammatory response in CNS. Both cell types work closely together and mediates some of the toxic effects in disease stats (Cuervo-Zanatta *et al.*, 2021; Du *et al.*, 2021). Neuroinflammation can be caused by various pathological conditions, e.g., trauma, infections or accumulation and deposition of various toxins, e.g., Aβ peptide. This interface with Aβ can evoke an inflammatory response that leads to irreversible synaptic and neuronal dysfunction. This complicated process involves several types of immune cells, lymphocytes, monocytes, macrophages and microglial cells of the CNS, which secretes numerous proinflammatory (prostaglandin E2, reactive oxygen species (ROS), nitric oxide (NO) etc.) and anti-inflammatory cytokines (interleukin (IL) 4, 6, 8, 10 and 13). Unbalanced secretion process, between both types of inflammatory mediators, can develop misleading reaction on current inflammatory process, which has been also implicated in the pathophysiology of AD (Lin, Zheng and Zhang, 2018; Lautrup *et al.*, 2019).

Astrocytes are the most plentiful and diverse of the glial cells and they play important part in guiding the construction of the nervous system. They also extend processes that form similar end feet on blood vessels, where they induce the endothelial cells to become sealed together by unusually well-developed tight junctions to form the BBB. This barrier prevents water-soluble molecules from passing in brain tissue from the blood. Additionally, astrocytes form unique glymphatic system, which eliminates different neurotoxic waste products, such us, Aβ and τP species. Theses glial cells can be found in different states of activation by responding to cytokines and chemokines. They even reduce or promote inflammation process. Astroglia, have been reported, as mediator, in regulatory control of Aβ clearance and degradation. Recently, reactive astrocytes (activated astrocytes that upregulates hypertrophic processes of glial fibrillary acidic protein (GFAP)) are showed as an early feature of AD. They are mainly triggered trough nuclear factor kappa-light-chain-enhancer of activated B cells (NF-κB) pathway, which causes a microglial activation by C3 receptors and develops a neuronal dysfunction. Furthermore, this activation state increases the levels of APP, β – and ɣ- secretases in the brain and produces accumulation of putative toxic Aβ oligomers. This phenomenon also occurs in several *in vivo* AD mice models, which contains three of five different mutations associated with an EOAD. Research data exposes that inhibiting astrogliosis in AD mouse brains results in Aβ accumulation with increased histology. Additionally, other *in vivo* experimental studies demonstrated that reactive astrocytes were found to release of excessive γ-aminobutyric acid (GABA) and glutamate levels causing incorrect homeostasis signalling

and creates imbalance between synthesis and clearance of Aβ peptides (Taşkiran-Sağ and Yemişçi, 2020).

Macrophages contain various actin-binding proteins, e.g., Ionized calcium binding adaptor molecule 1 (Iba1). Expression of Iba1 is upregulated in the activated microglia for several diseases, such us, AD. This microglia/macrophage-specific protein binds to fibrin and enhances its actin-bundling activity. It has been reported that Iba1 is a key molecule in membrane ruffing and phagocytosis. Moreover, this unique protein is involved in signalling pathways of calcium and the Ras homologous family of GTPases, which are important in multiple signal transduction pathways. Iba-1 is the essential molecule which regulate and enhances the actin reorganization in membrane ruffing and Rac activation. Previous studies identified increases in Iba1 cell counts, staining intensity or expression in AD compared with control samples in at least one brain region (Kenkhuis *et al.*, 2021).

Microglial cells are related to macrophages and involved in reactions to tissue damage and infection. These glial cells comprise 10 - 15% of the total cells in the CNS and can be found in all regions of the brain and spinal cord. As un innate immune player, throughout phagocytic and cytotoxic mechanisms, they destroy and clear unknown substances. There are three forms of microglia: a) ameboid, b) ramified and c) activated. The inflammatory phenotype manifests itself through activated microglia, and its neurotoxicity can initiate the inflammatory signalling cascade, including cytokines (TNF-α and IL-1β), free radicals, superoxide, fatty acid metabolites and ROS (Onyango *et al.*, 2021). It has been found that this microglia-mediated neurotoxicity, can induce the loss of the brain homeostasis, neuronal injury and increase mortality rate in AD. There are a number of molecular pathways that has been activated by specific receptors which determines how microglia will recognize Aβ species. Converging evidence implicate that microglia-mediated clearance of Aβ occurs by activating scavenger receptors. Stimulus of these receptors causes endocytosis of lipoproteins and adhesion to glucose-modified extracellular matrix proteins. Both types of proteins have been related with Aβ clearance across BBB. It has been also reported that scavenger receptors type B-1 (SRB-1) could promote cerebrovascular oxidative stress, neuronal dysfunction and CAA by binding Aβ fibrils (Koronyo-Hamaoui *et al.*, 2020). Additional *in vivo* studies have demonstrated a significant role of cathepsin B and D, a lysosomal cysteine proteases, which are involved in the basic processing of APP. Data reveals, that reducing endogenous inhibitor of cathepsin B and D, decreases accumulation of Aβ in lysosomes, revealing that Aβ is normally trafficked to lysosomes in substantial quantities (Sung *et al.*, 2020). Other receptors by which microglia recognize Aβ aggregates are cluster of differentiation (CD) 14, 36, 47, 67

and Toll-like receptors (TLR), e.g., TLR1, TLR2, TLR4, TLR6. These receptors activate signalling pathways that may induce phenotypic changes of microglia. For example, the activation of TLR2 promotes expression of IL-8 and TNF, initiation of scavenger receptors by occurrence of Aβ upregulates IL-1β and NO, and stimulation of the CD36-CD47 complex triggers phagocytic changes in microglia (Uddin *et al.*, 2020). Similarly, microglia-associated cognitive deficits have been linked with IL-33 by stating that it can increase microglial phagocytic activity and thus decreasing the plaque size of neurotoxic Aβ proteins (F. *et al.*, 2019; Hazen *et al.*, 2020). Moreover, activation of microglia can be provoked with the downregulation and upregulation of genes associated with AD. Transcriptomic studies *in vivo* mouse models of AD demonstrated that genes, such us, APOE and TREM2 might regulate autophagy of microglia and distribution of Aβ peptides through BBB. The reduction of the TREM gene workability might develop Aβ plaque formation and neuronal loss progression and disease pathology. Significantly, TREM2 also regulates microglial dysfunction in AD by disrupting its metabolism and altering microglia barrier functions (Agrawal and Jha, 2020).

1.2.3. Mitochondrial dysfunction and oxidative stress

The development of AD has been associated to mitochondrial dysfunction in the brain. Impaired oxidative phosphorylation (OXPHOS), decreased production of ATP, increase in oxidative stress and glycoses have been linked with mitochondrial dysfunction and well-documented in AD. Increasing evidence suggests that, the disturbances in mitochondrial dynamics and transport induced by APP and Aβ peptide might lead to neurodegeneration by preventing neurons to functionate normally (Leng and Edison, 2021).

Mitochondrial dysfunction may induce decrease of OXPHOS in AD microglia. OXPHOS is the last step in catabolism and the point at which the major portion of metabolic energy is released. In this process, molecules of nicotinamide adenine dinucleotide and flavin adenine dinucleotide (FAD) transfer the electrons that they have gained from oxidation of food molecules to molecular oxygen. Disturbed operating functions in OXPHOS increases oxidative stress which results as increase in Aβ and phosphorylated τP (Pan *et al.*, 2020). Accumulation of Aβ peptide and τP might activate a pro-inflammatory signalling molecule that are affecting metabolic functions of OXPHOS and glycoses. Several studies demonstrate that bioenergic failure of both processes could occur of the prolonged inflammatory process and increase of pro-inflammatory cytokine production (Onyango *et al.*, 2021). Moreover, *in vivo* studies with different AD mice models proves linking of various gene deficiency to mitochondrial

dysfunction. For instance, TREM2 plays a crucial role in supporting metabolic fitness of microglia in 5×FAD mouse model of AD, elevating those microglia from 5×FAD mice which have TREM2 deficiency have high lapidated microtubule-associated protein 1 light chain 3 and increased number of autophagic vesicles. It was observed that TREM2 deficiency may cause decreased phosphorylation of mammalian target of rapamycin marked pathway effector molecules which regulates cell growth, differentiation, hormone responses and autophagy. Some experimental treatment studies describe that reduced OXPHOS may decrease phagocytosis of Aβ (Pan *et al.*, 2020). Thus, emphasize TREM2 and ATP as important factors for the phagocytosis of Aβ by microglia. It has been observed that restoring mitochondrial function and mitophagy in microglia might reduce expression of cluster of differentiation 68 (CD68), increase in phagocytosis of Aβ and pro-inflammatory cytokine molecules, such us. IL-6 and TNF-α. Even more, evidence shows that increasing the capacity of ATP improves and regulates microglial bioenergic metabolism, autophagy, the way deposits of Aβ are recognized and reduction of Aβ pathology (Leyns *et al.*, 2019)

Significant decrease of ROS leads to mitochondrial dysfunction and have an important role to control immune response, regulates synaptic plasticity of neurons, inflammation and memory processes. When ROS have been produced in extra, those bits can trigger oxidative stress, damage mitochondrial structure and produce toxicity in the neuronal cells. Formation of such a process can result in the pathogenesis of many neurodegenerative diseases, such us AD. ROS levels can be dependent of various additional processes, e.g., metabolisms of immune activation, xanthine oxidase or arachidonic acids, ATP generation rate and reduction of glucose oxidation. As ROS levels are elevating it can damage mitochondrial deoxyribonucleic acid (DNA), there could be accumulation of age disturbed methandriol DNA mutations and lead to excessive ROS production, which highlight the emergence of the new DNA mutations. Since mitochondrial DNA has been localized close to free radical production sites, it can exhibit oxidative damages. When imbalance between free radical develops and detoxification arises, ROS production may crush antioxidant defences, leading to impairments of mitochondria. Though, the link between mitochondrial generated ROS and AD needs further exploration. However, increasing number of studies, demonstrates that mitochondrial dysfunction in microglia promotes pathogenesis and progression of AD. Further studies are needed to more precise describe mitochondrial dysfunction relativity with AD which may lead to new therapeutic strategies to delay progression of EOAD and LOAD (Li, Knight and Xu, 2022).

1.2.4. Neurotransmitter imbalance

The progressive deposition of Aβ exerts a neuromodulatory effects on synaptic activity and neurotransmitter release from presynaptic neuron terminals. In addition, anatomical studies in AD patients showed that such effects occur depending on different isoforms, accumulation status and concentration of the Aβ peptide. Various *in vitro* and *in vivo* studies have demonstrated that higher concentration of toxic Aβ peptides isoforms might induce complications on neurotransmitter release, the inaccuracy in regulating the neuronal long-term potentiation (LTP) or paired-pulse facilitation, impairments in synaptic plasticity and memory. Thought amyloid hypothesis, it has been proposed that imbalance in Aβ production and clearance can persuade deficiency in neurotransmission of various signalling molecules, including acetylcholine (ACh), glutamate, aspartate, dopamine (DA), norepinephrine (NE), histamine, 5-hydroxytryptamine (5-HT) and GABA. Notably, early detected and disturbed activity on different neurotransmitter systems has been associated with frequently observed behavioural symptoms – anxiety, depression or apathy, in the prodromal stage of AD (Ror Maratha, Falls and Vashist, 2019; Khan *et al.*, 2020).

1.2.4.1. Cholinergic system

The cholinergic system is involved in storing long-term memory, regulating cortical structure, cerebral blood dynamics and the wake-sleep cycle. Cholinergic hypothesis states that AD develops because of a deficit in the cholinergic transmission, and an eventual decrease in ACh synthesis and uptake by ACh receptors. ACh is an extensively distributed neurotransmitter in dentate nuclei with projections that entirely cover the CNS. Disruption of the cholinergic inputs to the cortex and hippocampus can influence all aspects of cognition, behaviour and decision-making processes (Jacinta, Ishola and Adeyemi, 2019; Binert-Kusztal, Starek and Dabrowska, 2021).

Collected data over the past decades suggests that both families of receptors (nicotinic acetylcholine receptors (nAChRs) and muscarinic acetylcholine receptors (mAChRs) not only regulate cognitive and memory processes but also influences the development of AD if their reduction are observed(van Erum, van Dam and de Deyn, 2019; Shekari and Fahnestock, 2021). The most evidence demonstrates nAChRs involvement in AD. In the peripheral nervous system, activation of nAChRs leads to rapid synaptic transmission, but in the CNS, these receptors regulates the release of neurotransmitters which provoke a reaction of presynaptic Ca^{2+} level increase and thus can facilitate the release of other neurotransmitters, such us, DA,

GABA, glutamate, 5-HT, NE and also ACh (Yiannopoulou and Papageorgiou, 2020). There are five different subunits which regulates and generates a variety of nAChRs in the CNS. The most recognised subunits which shows interaction with Aβ are α7 and β2. Each subunit and even their formed combinations may have a distinct properties and functions. The most widely expressed nicotinic subunit in the CNS is α7. This nAChRs subtype in presynaptic terminals mediates release of other neurotransmitters, elicits important changes in intracellular Ca^{2+} concentration, facilitates neuronal survival or gene expression. Moreover, α7 nAChRs are important fragments for developing of the glutamatergic synapses. Such an interaction among with neurotransmitter systems highlights that memory making processes might also began with regulation of glutamatergic neurotransmission. Studies have been expressed that Aβ42 is able reduce postsynaptic currents of α7 or non- α7 nAChRs, which demonstrates a clear interaction in between these two factors. However, the most sensitive component to Aβ induced toxicity, is α7 and β2 co-created subunit. The importance of this subunit type remains poorly understood, but some findings reveal a unique role for α7β2-nAChRs signalling during early, AD-related pathologic events. Under experimental conditions, it was discovered that Aβ42 interacts with α7β2- nAChRs, by producing a degeneration of basal forebrain cholinergic neurons - mainly involved in cognitive processes (Hampel *et al.*, 2019; George *et al.*, 2021). Some studies are presenting conflicting results about functional consequences of Aβ binding on nAChRs. It has been elicited that Aβ under different conditions- type and concentration, could act like an agonist and antagonist of theses receptors. Activation of nAChRs, e.g., with nicotine, could defence against Aβ caused neurotoxicity by disposing aggregated peptides. On the other hand, an inhibition of nAChRs, doses such us 0.1 and 10 μM of Aβ42, might result us increase of Aβ concentration and decrease of choline acetyltransferase, important enzyme which generates choline and acetate ions, accelerated loss of cholinergic fibres in the entorhinal cortex, inferior temporal gyrus and basal forebrain atrophy (Hahm *et al.*, 2018).

In the pathophysiology of AD, a mAChRs have also been involved. In AD, stimulation of mAChR M1 by agonists has been found to enhance APP generation and reduce Aβ production. Trough M1 mAChR stimulation it is well-known that protein kinase C (PKC) can be activated. PKC may stimulate the activity of α-secretase and the trafficking of APP to the cell surface. Several studies point to those cascades that might have triggered us well, such us, extracellular signal-regulated kinase 1/2 (ERK1/2) and Wnt (wingless-int), which can regulate α-secretase activity and APP processing. The loss of M1 mAChR increases amyloidogenic APP processing and promotes brain Aβ plaque pathology in AD (Shekari and Fahnestock, 2021). Experimental *in vivo* studies with 3×Tg mice model of AD, it was founded that M1 mAChR also affects

BACE1, by using selective M1 mAChR agonist AF267B and the level of BACE1 decreases, accompanied by a decreased Aβ level. Though, another study found that stimulation of M1 mAChR can upregulate BACE1 levels in human derived cell line via the signalling pathways, PKC and ERK1/2. In addition, activation of M1 mAChR neutralizes Aβ-induced neurotoxicity through the Wnt signalling pathway, as Aβ impairs the Wnt pathway and M1 mAChR stimulation, it further inactivates GSK-3β via PKC and induces the expression of Wnt-targeting genes for neuron survival. It was manifested that tau pathology interacts with M1 mAChR in AD. It was showed by *in vitro* study that activation of M1 mAChR by two agonists, carbachol and AF102B, significantly decreases tau phosphorylation. Different findings detected that the M1 mAChR increased the astrocytic and microglial response associated with Aβ. These obtained results suggest the importance of M1 mAChR in worsening AD related cognitive impairments. Other mAChR subtype, such as M4 has been suggested to play a role in psychosis. In addition to cognitive impairments, psychiatric symptoms are frequently observed in AD patients. AD-related psychiatric symptoms might be result of imbalance between cholinergic and dopaminergic systems. Corroborating cholinergic hypothesis, it has been demonstrated that DA efflux is increased in the nucleus accumbens of M4 knockout mice. Mice lacking M4 mAChR show increased locomotor activity and enhanced DA receptor D1-mediated effects. Thus, highlights that cholinergic transmission can regulate DA release trough M4 receptors. Indeed, it was discovered that the mixed M1/M4 mAChR agonist, xanomeline, has antipsychotic effects. Another *in vivo* experimental approach demonstrated that M4 mAChR-knockout mice display increased sensitivity to the disturbed effects of phencyclidine (Nam, Nam and Lim, 2020; Binert-Kusztal, Starek and Dabrowska, 2021).

At cholinergic synapses, the released of ACh is inactivated very rapidly in the synaptic clef by acetylcholinesterase (AChE), whitch is redused considerably in AD. ACh is degraded in the brain by two cholinesterases, AChE and butyrylcholinesterase (BChE). Studies have shown that AChE may interact with Aβ and further initiate the progression of the AD. It has been shown that AChE activity is reduced by 67% compared to the normal levels in the temporal lobe and hippocampus during the progression of AD. In AD patients, AChE is more abundant than BuChE, which contributes to the degradation of ACh in the hippocampus and cerebral cortex. Therefore, development of AChE and BChE inhibitors prevent the degradation of the neurotransmitter by increasing the levels of brain ACh and enhancing the brain cholinergic neurotransmission. In terms of the efficacy, these treatments have been shown to be most effective in increasing cholinergic neurotransmission and reducing Aβ protein aggregates (Moreta *et al.*, 2021).

1.2.4.2. Glutamatergic system

Glutamate is the excitatory neurotransmitter involved in the learning and memory process in the cortex and hippocampus. This neurotransmitter regulates a strong synaptic connection between pre- and post-synaptic neurons. Glutamate into the synaptic cleft activates NMDA and α-amino-3-hydroxy-5-methyl-4-isoxazolepropionic acid (AMPA) receptors. In AD, a tonic activation of NMDA has been associated with an increase of presynaptic release or re-uptake regulation of glutamate. Moreover, as Aβ induces oxidative stress and loss of insulin signalling thus in turn can cause glutamate excitotoxicity by deregulating the glutamatergic neurotransmission. As Aβ toxic insults are causing errors in the regulation of the neurotransmission that's creates the failure of glutamate role in memory, learning and cognition in AD patients (Abg Abd Wahab *et al.*, 2019; Findley *et al.*, 2019).

NMDA receptor activity has been synchronized with AMPA receptors. Co-activation of both receptors cause depolarization of postsynaptic membrane and increase of the Ca^{2+} ions. When AD progresses the cycle of glutamate production and regulation by NMDA receptors gets disturbed. Experimental results revealed that excess in glutamate can be induce by Aβ accumulation and, *vice versa,* that over expressed activation of NMDA receptors can enhance the production of Aβ. Chronically elevated glutamate levels inhibits axonal transport and triggers neurodegeneration trough Aβ deposition, which decreases potentiality of membrane and releases the Mg^{2+} ions from NMDA receptors. The increased flow of Mg^{2+} ions further leads to defective low of Ca^{2+} ions. The Ca^{2+} entry into the cell regulates extrasynaptic NMDA receptors. Ryanodine receptor 2 moderates the increased dendritic calcium and discharges intracellular Ca^{2+} concentration. Patients with mild-cognitive impairment show increased expression of ryanodine receptor 2, which overtime can eventually result in toxic Ca^{2+} concentrations and develop mitochondrial dysfunction, free radical production and neurodegeneration. Furthermore, Aβ can activate nicotinamide adenine dinucleotide phosphate oxidase trough NMDA receptors. Activation of this oxidase can induce unwarranted production of ROS and arachidonic acid. Also, NDMA receptor activation increases production of NO in Ca^{2+} and postsynaptic density-95 dependent manner. *In vivo* study with Tg AD mice model shows significant increase in NMDA, which induces higher NO concentration in the (CA1) region of hippocampus at earlier AD stages. Besides, parallel with the active extrasynaptic NMDA receptors mediated Ca^{2+} ion inflow, it also could activate the regulating responsive element binding protein of cyclic adenosine monophosphate (cAMP) and p53,

which contributes to promotion of cell survival and providing long-term memory (Findley *et al.*, 2019; Dejakaisaya, Kwan and Jones, 2021).

In addition, it has been reported that a widely studied member of the Homer protein family – Homer-1 is involved in the targeting of metabotropic glutamate receptors 1 and 5 by regulating their postsynaptic localization and intracellular signalling. *In vivo* study, using a Homer-1a-specific knockout mice model, demonstrated that metabotropic glutamate receptor 1 and 5 molecules were significantly decreased on the neuronal surfaces of a virus which harbours the Homer-1a gene. This study indicated that Homer-1a plays a important role by trafficking of metabotropic glutamate receptors 1 and 5. Other isoforms of Homer-1 protein, such us, b and c, declustering has been contributed to the Aβ-triggered loss of surface metabotropic glutamate receptors. It has been reported that synaptic surface clustering of metabotropic glutamate receptors are tightly coupled to Homer-1b/c and Aβ induced Homer-1b/c declustering necessitates activity of NMDA receptors, voltage-dependent calcium channels and the phosphoinositide 3-kinase pathway and calcineurin phosphatase. Moreover, it has been emphasised that this process might play a key role in Aβ induced demise of synaptic physiology (Clifton *et al.*, 2019)

The impact of Aβ aggregation reduces the amplitude and frequency in CA1 pyramidal neurons. Experiments with 3xTg AD mice models showed that increased Aβ concentrations declined expression of the glutamate receptor 1 AMPA subunit. Additionally, it was demonstrated that subunits, such us, glutamate receptor 2, 3 and 4 expression were downregulated in LOAD, along with decreased AMPA biding with CA1. *In vitro* studies, glutamate receptor 1 activity was upregulated in cortical and hippocampal neurons of APP knockout model, revealing that Aβ might directly impact the expression levels of AMPA various subunits. Notably, it was reported that glutamate receptor 2 can be upregulated in AD patients, supporting that activation of AMPA receptors might depend from progression of AD. This upregulation is likely a response to increased glutamate in presynaptic neurons, but chronic disproportionate stimulation could induce desensitization and internalization of the AMPA receptors (Babaei, 2021; Cascella and Cecchi, 2021).

It has been well-established in the literature that application of nicotine elicits glutamate release. Soluble Aβ40 and Aβ42 interact with α7 nAChRs and stimulated glutamate release from neurons and astrocytes can result in rising extracellular glutamate levels and excitotoxicity. The stimulated production of glutamate from Aβ activation causes rapid desensitization of α7 nAChRs, which leads to cell lysis and plaque deposition induce neurotoxicity. Desensitization of α7 nAChRs might increase the NMDA receptor expression,

and thus suggests a complex compensatory response to deposition of Aβ (Koola, 2020; Babaei, 2021).

1.2.4.3. GABAergic system

GABA are present in high concentrations in the CNS and are extremely potent modifiers of neuronal excitability. GABA is the primary neurotransmitter mediating inhibitory postsynaptic potentials in neurons in the brain. The role of this neuroinhibitory neutransmitter in AD is not well understood. Additionally, GABA interacts with glutamatergic and cholinergic neurotransmitter systems in the hippocampus and neocortex, the brain regions that are important to construct learning and memory processes. Immunohistochemical studies indicate that a large majority of the local circuit neuron localized in the dorsal horn of the spinal cord also synthesizes GABA. These neurons from axoaxonic synapses with primary sensory nerve terminals and are responsible for presynaptic inhibition. In GABAergic system the neurotransmission has been mediated by $GABA_A$ and $GABA_B$ receptors. $GABA_A$ receptor activation opens ligand-gated Cl^- channels. Meanwhile, $GABA_B$ receptors are metabotropic and either open K^+ or close Ca^{2+} channels. It has been demonstrated that the both receptors have been altered in aging and AD (Zhang *et al.*, 2021; Jiang *et al.*, 2022).

There are available reports that APP regulates neurotransmission of GABA. In the study using APP knockout mouse model it was showed that impairments in synaptic plasticity and deficiency in LTP have been associated with a reduction in GABA-elicited inhibitory. APP is one of the highly expressed proteins in the GABAergic neurons in the neurogenic DG. Notably, that the excitatory activity of GABA is very critical factor for synapse formation and dendritic development on new-born neurons. Thus, emphasises that APP play important role to regulate GABA neurotransmission in the neurons at different stages of life. The interaction with APP also appears with the L-type calcium channels by downstreaming depolarization of GABA in neurons (Tang, 2019; Govindpani *et al.*, 2020).

There are two major cotransporter systems which are operating influx- (Na^+-K^+-$2Cl^-$ cotransporter 1 (NKCC1)) and efflux-mediated (K^+-Cl^- cotransporter 2 (KCC2)) process of Cl^- ions. Changes in NKCC1 and KCC2 expression and activity may underline neuropathological conditions associated with detected failure in signalling procedure of GABA. Recent reviews have been indicating that APP may modulate GABA neurotransmission through KCC2. This change has been corresponded with downregulation of KCC2. During downregulation, APP elicits a depolarization of GABA, which has been indicated by an increase in intracellular Ca^{2+}

due to signalling downstream from $GABA_A$ receptor. APP over-expressed activity is self-regulated and unaffected of the APP intracellular or extracellular domains. Evidence reporting that APP over-expression is linked with a decrease in upstream stimulating factor, important regulator of the KCC2-encoding protein gene (solute carrier family 12 member 5) and it may maintain KCC2 levels in adult brain neurons. On the other hand, APP could regulate GABA reversal potential by modulating KCC2 levels in various ways. First, it could be regulated by influencing the latter's transcript level trough major transcription factor. Second, KCC2 plasma membrane stability could be troubled by limiting its modifications in the form of tyrosine phosphorylation and ubiquitination (Tang, 2019; Jiang *et al.*, 2022).

$GABA_B$ receptors are capable to form subtypes:1a and 1b. Subunit 1a is targeted dendritically and mediate postsynaptic inhibition, however 1b of $GABA_B$ receptor is axonal and inhibit glutamate release from presynaptic neuronal membrane. $GABA_B$ receptor 1a has two N-terminal sushi domain repeats, complement control proteins, which recognize binding sites in neuronal membranes. The large-scale study of proteins identified some potential interaction between sushi domain and membrane proteins, such us, APP. Rice et al. has reported that soluble APP extension domain can bind to the sushi domain of $GABA_B$ receptor 1a and reduce of synaptic vesicles and neurotransmission. This interaction between $GABA_B$ receptor 1a and APP is mainly engaged to axonal trafficking kinesin -1 and the motor adaptors c-Jun-amino-terminal kinase interacting protein and calsyntenin, which provides modulation of neurotransmitter release in hippocampal neurons (Rice *et al.*, 2019). This interaction reveals a new perspective drug target which is unique for $GABA_B$ receptors 1a. Another study by Rice et al. (Rice *et al.*, 2020) describes about contribution of GABAergic interneurons to Aβ pathology in an APP knock-in mouse model. It was showed that endogenous APP is highly expressed in a heterogeneous subset of GABAergic interneurons trough hippocampus, suggesting that these cells may have a reflective impact to Aβ plaque pathology in AD. Study was also emphasizing that APP expression differ between models. Therefore, using several AD models, it was determined that GABAergic interneurons contribute proportionally to Aβ production in the hippocampus. The mechanism underneath is associated with high firing rates of interneurons relative to excitatory neurons (Rice *et al.*, 2019; Martín-Belmonte *et al.*, 2020).

Another enzyme converting glutamate into GABA and has been implied in a number of neurological disorders is the glutamic acid decarboxylase 67 (GAD67). GAD contains two isoforms, GAD65 and GAD67. GAD67 is mainly is distributed throughout the cell and have mostly a cytoplasmic localization. In the brain, 90% of the basal GABA is synthesized by GAD67. Dysfunctionality of GAD67 has been associated with several neurological disorders,

including AD. Functionally, previous reports have demonstrated that GAD67 haploinsufficiency in AD mouse brains has significant beneficial effects on pathological and behavioural outcomes. Additional studies have established the role of GAD67 as the enzyme for the synthesis and uptake of GABAergic system, which regulates mood, cognition, higher-order functions, and social elasticity. Moreover, investigations of post-mortem brains tissues and rodents have shown decreased brain levels of GAD67and increased concentrations of TNF-α and IL-6 (Ruan *et al.*, 2020; Oladapo *et al.*, 2021).

Parallel studies in rodents have demonstrated somatostatin-expressed changes in neurons of GABAergic system. Decrease of the somatostatin-expressed GABAergic interneurons could result as distribution of their synchronized cellular and neuronal activity which further may lead to cognitive impairments. Specific studies with GABAergic cell-type markers reported a significant reduction in somatostatin-expressed gene appearance, and thus has been observed in various conditions, e.g., AD or bipolar disorders. Somatostatin-expressed neurons have been identified as GABAergic neuronal subtype that is vulnerable to biological adversity and frequently affected in several brain disorders and during aging. It has been stated that induced cognitive dysfunctions may activate reduced signalling of the somatostatin-expressed neurons on $GABA_A$ α5 receptor (Prévot and Sibille, 2021).

1.2.4.4. Dopaminergic system

Dopaminergic pathways include the nigrostriatal, mesolimbic, and tuberoinfundibular tracts. DA exerts slow inhibitory actions at synapses in specific neuronal system commonly via G-protein-coupled activation of K^+ channels (post-synaptic) or inactivation of Ca^{2+} channels (pre-synaptic). With dysfunction of the dopaminergic signalling may lead to numerous diseases, such us, AD or Parkinson's disease. The DA neurotransmitter undergoes various changes during the neuropathological aging process. Some studies are suggesting that DA has a major role to regulate synaptic plasticity. If mechanisms for synaptic plasticity and DA neurotransmission have been progressively disarranged and impaired, then these changes could induce the occurrence of extracellular Aβ plaques and NFTs, further developing pre-dementia like symptoms (hypoactivity, gait disturbances, cognitive decline) (Nobili, la Barbera and D'Amelio, 2021; Xiao *et al.*, 2021).

The main source of DA in the brain derives from dopaminergic neurons in the locus coeruleus (LC), ventral tegmental area and substantia nigra pars compacta. LC innervates sites in the brain, such us, the basolateral amygdala, ventral tegmental area and the prefrontal cortex and progressive degeneration of LC neurons may induce AD pathology. These all specific

regions have associations with the hippocampus and performs its functions in memory, attention, learning, sleep-wake cycle, anxiety, pain and brain energy metabolism. *In vivo* studies recently revealed LC connection to tau pathology, which in turn aggregates Aβ deposits, reducing clearance of Aβ. Current study explains that disturbance of the basolateral amygdala and its interaction with hippocampus, leads to impairments in social recognition via distribution of DA receptor 1 and DA receptor 5 receptors or β-adrenoreceptors in the CA1 region (James *et al.*, 2021; Kelly *et al.*, 2021).

There are at least 5 subtypes of DA receptors which are especially important in the brain, renal and splanchnic vessels. It has been revealed that DA receptor 2 correlates with memory making processes in AD. Existing data suggesting that DA acts by binding the DA_2-like receptors to increase cortical excitability. However, binding with DA receptor 1 it develops increase of cortical Ach, e.g., it has been found that administration of L-dopa, by modulating cholinergic neurotransmission, improved the cognition functions of AD patients. Recent research demonstrated that DA can reduce oxidative stress and inflammation, and emphasises that both processes are associated with pro-inflammatory signalling pathway induced Aβ deposition, during the progression of AD. Montoya et al. (Montoya *et al.*, 2019) indicated that pharmacologic-antagonism or genetic deficiency of DA receptor 3 have been linked to neuroinflammation and neurodegeneration. Results of this study shows that DA receptor 3 deficiency results as inflammation, induced by glial cell produced anti-inflammatory protein resistin-like molecule α1. Therefore, DA_3 receptor signalling may regulate the dynamic of the pro-inflammatory and anti-inflammatory signal molecules by glial cells (Pan et al., 2019; Yang et al., 2021).

Other studies indicate that DA beta-hydroxylase plays crucial role in process to convert DA to NE. The enzyme DA beta-hydroxylase is generally expressed by noradrenergic neurons in the LC and peripheral nervous system. Activity of this enzyme regulates produced NE levels. Neurotransmitter, as NE, also is an actual etiological factor of AD, as their reduction influences motor functions in humans. Mutations in DA beta-hydroxylase gene might participate in progressive neurodegeneration. There are numerous DA beta-hydroxylase loci (rs1611115, rs5320 and rs1611131) which are associated with AD risk. In the development of AD, the role of DA beta-hydroxylase loci rs1611115 might be influenced by several other factors, such as age, gender and gene-gene interactions (Hui *et al.*, 2020). Nonetheless, NE system has a remarkable compensatory capacity, which might be neurochemically suppressed or absent due to neuronal destruction. NE influences microglial functions, it triggers production of pro-inflammatory molecules and promotes anti-inflammatory molecules. Moreover, loss of LC

neurons correlates with NE metabolism. In addition, NE decrease induced by LC neurons may be associated with dysfunctionality of BBB. These observations suggest that an affected LC neuron associating with alterations in NE my form a threat, disturbing BBB and impairing Aβ clearance processes (James *et al.*, 2021).

1.2.4.5. Serotoninergic system

One of the biologically active amines that is found in many tissues is 5-HT. This neurotransmitter has a very complex physiologic and pathologic effects, and often released locally. The actions of 5-HT are mediated trough variety of cell membrane receptors. Seven most studied 5-HT receptor subtypes have been identified, including both G protein-coupled receptors and a ligand-gated ion channel. Most 5-HT pathways originate from neurons in the raphe or midline regions of the pons and upper brain stem. 5-HT is contained in unmyelinated fibres that diffusely innervate most regions of the CNS. In most areas of the CNS, 5-HT has a strong inhibitory action, which has been mediated by 5-HT_{1A} receptors and is associated with membrane hyperpolarization caused by an increase in K^+ conductance. It has been found that 5-HT_{1A} and $GABA_B$ receptors share the same K^+ channels. These receptors and K^+ channels are coupled using a guanosine triphosphate-binding protein. Both excitatory and inhibitory actions can occur on the same neurons (Mdawar, Ghossoub and Khoury, 2020; Gründer and Cumming, 2021).

Since, depletion of 5-HT may increase the risk for major depression and AD, the link between inflammation and depressive symptoms in the context of age-related neurological disorders has been studied. One study presents that depletion of 5-HT occur as a result of deficient synthesis from its precursor tryptophan. Neuroinflammation and chronic stress can increase tryptophan 2,3-diozygenase expression which shunts tryptophan trough kynurenine pathway. This kynurenine pathway can produce neurotoxic metabolites, which regulates Aβ plaque load in the AD. In additional, it has been reported that during AD there is an activation of kynurenine pathway at the periphery and makes tryptophan even more less accessible for the 5-HT synthesis (Mackin *et al.*, 2021; Whiley *et al.*, 2021).

Degeneration of the serotoninergic system can suppress an appetite and even cause impairments to regulate behaviour, energy intake, respiratory, motor functions, emotions, homeostasis and sleep-wake cycle. Additionally, 5-HT is also involved in cognitive mechanisms such learning and short- and long-term memory. In AD, it has been demonstrated that there is a decline in the cortical or serum 5-HT level and negative result of disruption in serotonergic neurotransmission. Also, disturbance in serotonergic signalling are reported to

enhance Aβ pathology *in vitro, in vivo* and in clinical studies. Additionally, in post-mortem studies on AD brains, it was confirmed a reduced number of serotonergic neurons in the dorsal and the median raphe nuclei, and that immense accumulation of Aβ and NFTs in those brain regions associates with a progression of AD clinical symptoms. More specific, investigations have been reported that there are several 5-HT receptors (5-HT_{1A}, 5-HT_{2A}, 5-HT_{2C}, 5-HT_4, 5-HT_6 and 5-HT_7), which are consistent with cognitive processing in hippocampal and cortical neurons, and a significant loss or stimulation of those receptors associates with neuroinflammation, cortical Aβ load, Aβ-induced mitochondrial dynamics, biogenesis, autophagy, mitophagy and synaptic toxicity in AD pathology (Sun *et al.*, 2021; Yuede *et al.*, 2021).

Activation of 5-HT neurotransmitter receptors can alter APP processing witch further impacts production of Aβ. It has been postulated, that 5-HT_{2A} may regulate Aβ levels. As 5-HT_{2A} receptors are G-protein-coupled receptors with α subunit they can activate ERK signalling cascade and increase α- secretase to reduce Aβ levels. In addition, loss of 5-HT_{2A} receptors affects sleep processes and suppressing their activity promotes slow-wave sleep. Interruptions in slow-wave sleep leads to Aβ aggregation. Disrupted sleep is a common problem in AD. Recent data revealed that inverse selective agonist and functional antagonists of 5-HT_{2A} receptors rapidly suppress Aβ production by up to 50% trough signalling pathway triggering NMDA receptors, EKR and increasing α-secretase activity. Other study showed that a selective antagonist of 5-HT_{2A} ameliorates pathology of AD by reducing Aβ plaque accumulation by promoting microglial Aβ phagocytosis and degradation. It was demonstrated that this antagonist improves microglial dysfunction and supresses neuroinflammation trough 5-HT2 receptor/cAMP/protein kinase A/ cAMP-responsive element-binding protein by activating sirtuin signalling pathway. This signalling pathway has been related not only with aging processes but also linked to neuronal activities including energy production, metabolic processes, synaptic plasticity and long-term memory. Almost 90% of the AD patients develops behavioural and psychological symptoms. The reduction of the genes coding the 5-HT_{2A} and 5-HT_{2C} receptors and are linked to the development of behavioural and psychological symptoms. Studies have found that the pathological accumulation of Aβ depends on the reduction of 5-HT_{2A} expression, but antagonization of 5-HT_{2C} receptors can prevent τP hyperphosphorylation and improve memory (Li *et al.*, 2021; Yuede *et al.*, 2021).

Like 5-HT_2 receptor, the 5-HT_4 performs it function by an increase of cAMP and activates adenylyl cyclase. Evidence reports that in AD patients there is a significant loss of 5-HT_4 receptors in hippocampal and cortical neurons, which are connected in synaptic plasticity

and involved in memory. The 5-HT_4 receptor activation may interact with α-secretase regulation and Aβ production. Recently, it was reported by Hashemi-Firouzi et al. that the chronic stimulation of the 5-HT_4 receptor modulated the Aβ-triggered impairments in synaptic plasticity and memory deficits via a decrease in the hippocampal neurons and develops AD. Similar, synaptic and cognitive defects can be induced by null mutation of 5-HT_6 receptor. Sun et al., in the current study presented 5-HT_6 receptor null mutant mice, were found to exhibit cognitive decline and increased anxiety levels. It has been suggested that loss of 5-HT_6 receptor affects the Sonic Hedgehog signalling pathway in the primary ciliary, where these receptors have been specifically localized. These finding highlights that the 5-HT_6 receptor functionality is very complex and that it might regulate neuronal morphology and transmission, and contributes to cognitive disability in AD. Also, literature include data about that one of the main effects of 5-HT_6 receptor activation is the decrease of Ach neurotransmission, which role in AD are also well-documented (Gründer and Cumming, 2021; Hashemi-Firouzi, Shahidi and Soleimani Asl, 2021).

1.2.4.6. Histaminergic system

It was firstly proposed by De Almeida and Izquierdo in 1986, that histamine play important role in the regulation of memory consolidation. The important functions of histamine in the brain are mediated by histamine receptors located on postsynaptic membranes - H_1, H_2 and predominantly presynaptic - H_3. However, the role of H_4 receptor in cognitive processes is still not fully clear. Several studies have been reported that histaminergic system involve in cognitive, the sleep-wake cycle, sensory and motor functions. Activation of presynaptic receptors is associated with a reduction of neurotransmitter release, such, histamine itself, 5-HT, NE and Ach. In particular, the H_3 receptor have important role in the CNS, inhibiting histamine release. In reviews articles it has been summarized that neurotransmitters, such NE, DA and Ach have been suggested to play key roles in social discrimination and memory. Histamine also is involved in the same type of memory processes, and that reduction of histamine production in the brain improved short-term memory. Data provided by Sadek's et al. suggested that the post-synaptic receptor that mediates the promnesic effect is H_1 receptor in the brain. Nonetheless, some research summarized and supported the concept that memory improvement by antagonizing H_3 receptor has been caused by increase endogenous histaminergic tone and activation of postsynaptic histaminergic receptors. Some studies demonstrated debateable results on the histaminergic system in AD. They revealed, that at some AD cases histamine levels in the CSF has been increase in the frontal cortex, basal ganglia

and hippocampus. On the other hand, decreased histamine levels were observed in the hippocampus of AD patients. Notably, a recent study showed that cognitive deficits has been detected among with changes in histamine signal transduction. Moreover, it has been published by Higuchi et al., that there is correlation between H_1 receptor decreased expression in AD patients. *In vivo* study, with adult H_1 receptor deficient mice demonstrated the severe impairment in learning and memory, and therefore may trigger also an increase in Ach concentration in the frontal cortex and amygdala (Provensi *et al.*, 2020).

1.2.4.7. Purinergic system

Purinergic signalling is involved in different pathological processes, such us Aβ accumulation, τP phosphorylation, oxidative stress and neuroinflammation. Thus, suggests the importance of nucleotide and adenosine receptors present on the CNS. It was shown that when Aβ accumulation in the brain induce the ATP production of cortical astrocytes in the extra-cellular space, which stimulates nucleotide receptors – P_{2X7}. There are other reports with indicates, that degradation of Aβ has been caused by protease of insulin-degrading enzyme. It was confirmed that the speed of Aβ degradation has been affected by ATP and that ATP activates the insulin-degrading enzyme deprivation of small peptides, but it decreases the rate of insulin-degrading enzyme activity of peptides, such, Aβ. Also, Aβ can interfere with P_{2X7} receptor which mediates circadian rhythms of the intracellular Ca^{2+} levels. Resents studies, revealed that activation of P_{2X7} might affect α-synuclein-mediated intracellular free Ca^{2+} deployment in neuronal cells and stimulates active complex by pannexin 1, who are responsible to release of ATP. Moreover, activation of P_{2X7} receptors induces production of pro-inflammatory molecules, e.g., cytokines and chemokines. Furthermore, this instigation of P_{2X7} decrease the activity of α-secretase. However, activation of P_{2Y2} receptor, can cause an opposite effect in AD, triggering a positive neuroprotective effect in neurons, glial and endothelial cells. Activation of P_{2Y2} receptor also affects reuptake of fibrillar and oligomeric Aβ42. Adenosine receptors, A_1 and A_2, demonstrates that adenosine trought these receptors affecting the dopaminergic and glutamatergic neurotransmission and brain-derived neurotrophic factor. The research demonstrated that adenosine receptors also can induce changes in synaptic plasticity. Activation of A_1 by adenosine or its analogues initiates the PKC, protein activator 1 and ERK1/2, and thus leading to increase accumulation of soluble Aβ. Some studies have been observed the protective effects which have been mediated trough A_{2A} receptors. Antagonization of these receptors can trigger in reverse cognitive impairment and reduce

synaptic toxicity by activating a p38 mitogen-activated protein kinase (MAPK) (Merighi *et al.*, 2021; Pietrowski *et al.*, 2021).

1.2.5. Epigenetics basis of AD

Pathology of AD is influenced trough malfunction in regulation of genes and micro ribonucleic acids (miRNAs), along with some environmental factors (oxidative stress, inflammation, nutrition, chemical exposure, smoking, traumatic brain injury). This gene transcription and expression can be affected via chromatin (complex made up of DNA, RNA and proteins) structural change. DNA methylation, histone modifications and noncoding RNAs are epigenetic modifications which have been associated with AD (Myers and McGonigle, 2019).

DNA methylation is one of the best-documented chromatin alterations, which occurs in the cytosine residues of DNA trough the addition of a methyl group to DNA. Methylation of DNA modify and repress the transcription of the genes. This methyl group can be removed with active DNA demethylation, which is mediated by the methylcytosine dioxygenase enzyme and oxidize 5-methylcytosine (5-mC) to 5-hydroxymethylcytosine (5-hmC). DNA methylation is detected by 5-mC marks which has been associated with transcriptional repression. In AD, the methylation and demethylation processes of DNA have been altered and carried out by set of proteins as DNA methyltransferases. In one study it was observed in the brain of aged 3xTg AD mice model a global reduction in 5-mC and an increase in 5-hmC, suggesting an abnormal establishment of chromatin, which further may activate pathology of AD. Similarly, decreased levels of 5-mC have been investigated in post-mortem brains from AD patients. Studied changes were evaluated in several regions of brain, in cortical neurons, hippocampus and cerebellum. Furthermore, in AD hippocampus has been found a decrease of DNA methyltransferase 1 and methylated DNA-binding 2. The amount of 5-hmC also were assessed in the hippocampus of a pair of monozygotic twins discordant for AD. Obtained results showed a significant loss of 5-mC and 5-hmC and have accusation with load of Aβ and NFTs in AD patients. Nevertheless, some studies suggest that several genes increase upon reduced DNA methylation. One example is including APP gene and that during aging this gene is demethylated and therefore promoting accumulation of Aβ in brain. Hypomethylation of gene BRCA1 also has been stated as one of the factors in the AD, by stating that expression and functions of this gene appears to be isolated by τP aggregates. Also, hypomethylation of intron 1 on myeloid cell 2 gene, expressed by microglia, may induce inflammation cascade associated with AD development (Alcalà-Vida *et al.*, 2021; Fan *et al.*, 2021).

Other DNA modification which has been related with AD is histone acetylation. In order to regulate the transcriptional machinery to the genes a parts of gene regulation, histone acetylation and deacetylation, are required processes. It has been presented that epigenetic regulatory actions involve histone acetyltransferase and deacetyltransferase (HDAC) enzymes. Exhibition of histone acetyltransferase activity are weakening a positive charge of histones and producing relaxation of chromatin to further promote gene expression. Also, histone acetylation is only one of epigenetic marks that includes various series of actions, e.g. histone phosphorylation, methylation, sumoylation, ubiquitination, as well as DNA methylation. Several studies have been demonstrated that numerous members of HDAC are highly expressed. The proteins which have been associated with AD are HDAC1, HDAC2, HDAC3, HDAC4, HDAC6 and HDAC9. In AD, researchers have been discovered that HDAC2 is primary expressed in the hippocampus and prefrontal cortex and reduces the numbers of synapses, synaptic plasticity and memory formulation. HDAC2 expression levels has been detected higher in the brain of AD transgenic mice model and reduced a histone acetylation for genes related to neuroplasticity and memory. In microglia from AD transgenic mice it has been showed that HDAC1 and HDA2 reduce expression further develop a decline of Aβ production. In addition, HDAC2 and HDAC9 were also higher expressed in peripheral blood cells in the AD patient. Also, increased HDAC3 expression is associated with a decreased memory in the brains in animal models of AD. Moreover, detected high levels of HDAC6 also has been observed in the cortex and hippocampus of AD patients and in vivo studies revealed that reduction of HDAC6 helps to limit the production and accumulation of τP and therefore improve cognitive activity (Berson *et al.*, 2018; Alcalà-Vida *et al.*, 2021).

Genome-wide studies have shown that another important epigenetic player are the small and long non-coding RNAs (ncRNAs). Small ncRNAs, as microRNAs are the well-characterized members. Recent studies in post-mortem AD brain tissues found, by IL-1β and Aβ42 induced inflammation and stress and NF-kβ regulated pathway, significantly up-regulated several brain-abundant microRNA species. Also, it has been detected that expression of some microRNA species (miRNA-29a, miRNA-29b and miRNA-29c) were decreased with an increase of BACE1 expression and may lead to production and aggregation of Aβ plaques. Furthermore, increased levels of miRNA-7, miRNA-9-1, miRNA-34a miRNA-125b-1 have been observed in post-mortem AD brains. Significant changes have been found in long ncRNA expression in the AD brain. Since long ncRNA-51 modulates the splicing of sortilin-related receptor 1, an important gene for regulating Aβ precursor, increase of expression can reduce synthesis of sortilin-related receptor 1 variant A. Increase of long ncRNA-17A induce changes

in slicing of GABAB receptor and promotes Aβ secretion in response to inflammatory signals (Zhang *et al.*, 2020; Alcalà-Vida *et al.*, 2021).

Generally, all above mentioned epigenetics studies provide important data about a possible epigenetic mechanism and report several modifications in the epigenome of brain cells under AD conditions. However, epigenetics should be studied more intensively and deeper to find a way toward potential biomarkers and target molecules for the prevention and control of AD (Alcalà-Vida *et al.*, 2021).

1.2.5.1. Transgenic mouse models of AD

In order to evaluate the epigenetic mechanisms a different transgenic AD mouse models with pathological features, such us, Aβ or hyperphosphorylation of τP, dystrophic synaptic and neuronal loss, gliosis, or CAA have been generated. These models are quite variable in the extent of cerebral amyloidosis, the time of deposition/disease onset and spatial promoter-specific expression characteristics (Myers and McGonigle, 2019).

The effort to obtain mouse amyloid and pathologies that mimic human AD has led to the generation of multi-transgenic mice models which includes, e.g., APP, PS1 (or PSEN1), tau mutations (Table 1). Notably, the AD-related proteins Aβ, tau and ApoE differ between rodents and humans in their sequence pathogenicity, number of isoforms and expression patterns of inflammation-related genes (Serneels *et al.*, 2020). In 1990, using DNA from pedigrees of families with FAD, the Dutch mutation in APP was reported. Moreover, shortly afterwards were described mutations the London, Swedish and Indian. Pathogenic APP mutations are categorized according to their relative proximity to cleavage sites for BACE1 or the y-secretase/presenilin complex and are named for the geographic location of the first identified carrier family (e.g., Swedish) as well as affected residue position (e.g., K670N/M671L). There are several mutation can lead to increased levels of Aβ production (Swedish (K670N/M671L)) and ratio of Aβ42:Aβ40 (London (V717I), Indiana (V717F), Florida (I716V), Arctic (E693G), Iberian (I716F), hPSEN1 (M146V, M146L, L286V, L166P) (Sakakibara *et al.*, 2019; Serneels *et al.*, 2020).

The first transgenic mouse model for AD were developed to express human APP (human amyloid precursor protein) harbouring single FAD-associated mutation, e.g., Indiana, Swedish and London. Furthermore, the Tg2576 model was engineered to express hAPP with Swedish double mutation (Hsiao *et al.*, 1996). As a result, these models mutations lead to 5 times higher overexpression of Swedish- mutated hAPP and inducing Aβ aggregation, exhibiting neuronal

loss and developing CAA. Several AD mouse models were developed in which endogenous murine APP was modified to express humanized hAPP and knocking in several combinations of Swedish, Artic and Iberian APP mutations. One of the knock-in model which combines all three mutations is APP $^{NL-G-F}$. These mice models might be more closely represent human amyloidogenic pathways and express normal pathological levels of hAPP with higher ratio of Aβ42:Aβ40 comparing with wild type (Myers and McGonigle, 2019; Sakakibara *et al.*, 2019). Widely used AD multi-transgenic models in research are APP + PS1 (APP/PS1) mice models, such us, APP/PS1-21, 5×FAD and 3×Tg. The APP/PS1 mice models carrying mutation in both APP and PS1. APP/PS1 model, e.g., APP/PS1-21 exhibit Aβ plaque formation as well as synaptic and neuronal loss (Myers and McGonigle, 2019; Sakakibara *et al.*, 2019). The most extreme APP/PS1 model used in research is the 5×FAD model (Oakley et al., 2006). This model combines Swedish, London and Florida APP mutations with PS1 mutations (M146L and L286V). Multiple FAD mutations expression leads to faster and more severe pathology (synaptic and neuronal loss) versus single FAD mutation. Moreover, it has been published that Aβ accumulation begins very early at ≈ 6 weeks of age (Drummond and Wisniewski, 2017; Drummond et al., 2020). Another, the most widely used AD mice model, which harbours the Swedish APP mutation, the M146V mutation in PS1, and the P301L MAPT mutation is 3×Tg (Oddo *et al.*, 2003). This model exhibits Aβ accumulation at 3 to 4 months of age, with plaque development by 6 months of age and NFTs by 12 months of age. This model at 6 months of age demonstrates cognitive impairments and are considered as the most complete transgenic AD mice model currently available. However, the same as other APP models, it remains to the same limitations, relying on overexpression of a combination of mutation not representative of AD in humans (Drummond *et al.*, 2020).

Table 1. **Mouse models used for the study of Alzheimer's disease.**

Strain	Genetics	Neuropathology	Reference
3xTg	Three mutant alleles, homozygous for the hPSEN1 (M146V (Exon 5, increased Aβ42:Aβ40 ratio)), co-injected hAPP (Swedish) and MAPT (P301L (Exon 10, increased paired helical filaments)), mouse Thy1.2 promoter	Aβ plaques, τP pathology and gliosis	Oddo et al., 2003

APP/PS1	Mutated co-injected hAPP (Swedish), hPSEN1 (L166P (Exon 6, plaques and tangles)), mouse Thy1.2 promoter	Aβ plaques, gliosis, synaptic and neuronal loss, CAA	Radde et al., 2006
5xFAD	Mutated hAPP (Swedish, Florida and London), hPSEN1 (M146L (Exon 5, increased Aβ42:Aβ40 ratio), L286V (Exon 8, increased Aβ42:Aβ40 ratio)), mouse Thy1.2 promoter	Aβ plaques, gliosis, synaptic and neuronal loss, CAA	Oakley et al., 2006
Tg2576	Mutated hAPP (Swedish, isoform 695), containing the double mutation K670N/M671L (BACE1 cleavage site, increased Aβ production)	Aβ plaques, gliosis, synaptic loss, CAA	Hsiao et al., 1996
APP^{NL-G-F} knock-in	Mutated hAPP (Swedish (K670N/M671L), Iberian (I716F; y-secretase cleavage site, increased Aβ42:Aβ40 ratio) and Artic (E693G, within Aβ region, increased propensity of Aβ40 to aggregate)), endogenous APP promoter	Aβ plaques, gliosis, synaptic loss	Saito et al., 2014

1.3. Treatment options for AD

1.3.1. Contemporary approved therapeutic approaches for AD

Until recently, there were only five options approved by the U.S. Food and Drug Administration for the treatment of AD. These include three AchE inhibitors (donepezil, galantamine and rivastigmine), one NMDA receptor antagonist (memantine) and the combination of donepezil and memantine. These drugs were first implemented based on cholinergic and glutamatergic hypothesis and have been long time considered as the first-line choice for targeting of mild to severe AD. However, these approved drugs were gradually discovered to be ineffective in removing the root of AD pathogenesis but manly targeting the symptoms. After all scientific efforts for almost two decades, Food and Drug Administration approved the first new drug, a monoclonal antibody – aducanumab, for AD with a putative disease-modifying mechanism by removing of Aβ plaques from the brain. There are still many unmet criteria and loopholes in available therapeutic approaches, limiting their efficacy (Cummings and Salloway, 2021).

The current treatment in AD involves a multipronged approach of combining pharmacological and non-pharmacological (e.g., deep-brain or vagus nerve stimulation) tactics. One of the pharmacological approaches for mild to severe AD includes donepezil, galantamine and rivastigmine in different dosages. Donepezil and galantamine inhibit selectively and reversibly the AchE, whereas rivastigmine is a "pseudo-irreversible" inhibitor of AchE and BChE inhibitors. The effectiveness of these drugs varies from person to person and it is limited in time. It has been reported that AchE inhibitors tend to mitigate decline in cognition at least during the first year of treatment. All approved AchE inhibitors have presented their treatment benefits in delaying decline and improving cognition up to 52 weeks duration. Therefore, it is highly recommended by initiating of AchE inhibitor treatment as soon as possible after the diagnosis. At the moment, more than one systematic review has postulated the clinical relevance of galantamine against mild to moderate AD. AD patients who were administered galantamine, with a dosage of 24 mg and 32 mg per day, exhibited significant increase in cognitive performance. Furthermore, a 26-week study examined the clinical effects of rivastigmine (3, 6 and 9 mg/day) on the brain activity and according to screening results, there were a noticeable improvement, increasing hippocampal metabolism. Moreover, donepezil exerts good efficacy and tolerability in mild to moderate AD patients. There are no notable differences in effectiveness between approved AchE inhibitors, but as the most tolerated and commonly prescribed is Donepezil. This agent has been long approved as symptomatic treatment for AD, significantly slowing down progressive cognitive decline. In general, AchE inhibitors, except tacrine, are well tolerated and adverse effects are dose related. The most common adverse effects often include diarrhoea, nausea and vomiting, primarily triggered by the cholinomimetic action of the AchE inhibitors on the gastrointestinal tract and therefore are contraindicated in patients with active peptic ulcer or with gastrointestinal bleeding history. Some individuals have been also remarked with side effect, such us, rapid eye movement sleep behaviour disorder. These inhibitors may also induce bradycardia and increase the risk of orthostatic hypertension and are contraindicated in conditions, such us, including severe cardiac arrythmias. Adverse reactions affect usually a 5% to 20% of patients but are mostly mild and can be minimized by administrating drugs after a meal, nevertheless all patients should be monitored for changes in cognitive function, symptoms of gastrointestinal intolerance and weight loss. Furthermore, there are scientific reports concluding combinatorial treatment, memantine and AchE inhibitor, to potentially improve to treat from moderate to severe AD. The effectiveness of combination by making progress in cognitive functioning, has been repeatedly explored in various double-blind, randomized controlled trials and reported in

systematic reviews. This NMDA receptor antagonist, memantine, also can be administered alone. Memantine monotherapy has demonstrated short- and long-term benefits for patients with moderated to severe AD. Nevertheless, their combination benefits patients usually additive effects, without any increase in adverse effects (Bortolami *et al.*, 2021; Gąsiorowski *et al.*, 2021).

At the moment, none of approved drugs, that are used to counterbalance the neurotransmitter imbalance, are able to stop or modify the AD. The first disease-modifying treatment, aducanumab, was approved on 7 June 2021, for the treatment of mild cognitive impairment or mild-dementia stage of AD. Aducanumab is a human IgG1 anti-Aβ monoclonal antibody selective for Aβ fibrils and soluble oligomers. This therapeutic approach was developed of an antibody-based immunotherapeutic approach by selecting human B-cell clones triggered by neo-epitopes present in pathological Aβ aggregates. The preclinical study showed that aducanumab significantly increased recruitment of Iba-1-positive microglia, suggesting that Fc gamma receptor-mediated phagocytosis as a possible clearance mechanism (Sevigny *et al.*, 2016). This newly approved therapeutic approach showed substantial reduction of Aβ plaques in all cortical brain regions examined in a dose-dependent and time-dependent manner with prodromal or mild AD patients. It has been reported that the most common adverse effects were amyloid-related imaging abnormalities, e.g., headache, urinary tract infection, and upper respiratory tract infection. Nonetheless, the approval of aducanumab has raised and sparked some arguments, as the results from two phase III randomized clinical trials demonstrated conflicting evidence. The clinical trials revealed that aducanumab was associated with amyloid-related imaging abnormalities and that side effect profile in patients with mixed or more advanced disease has not been properly and clearly established (Cummings *et al.*, 2021; Walsh *et al.*, 2021).

1.3.2. Future therapeutic approaches for AD

As prevalence of AD continuous to increase, there is an urgent need for developing a new potential and affordable ways to treat AD, since currently approved medication provides either symptomatic relief or acquires deeper investigation. AD has been observed as multifactorial disorder, thus has shifted the research focus from a single pathological target to a more complex mechanism, such us, neuroinflammation, synaptic plasticity, insulin dysregulation and neurodegenerative processes. Overall, the novel therapeutic approaches includes a variety of strategies, which could be prospective candidates for the treatment of AD,

such us, anti-amyloid (secretase inhibitors, Aβ aggregation inhibitors and Aβ immunotherapy), anti-tau (phosphatase modifiers, kinase inhibitors, tau aggregation inhibitors, microtubule stabilizers, tau immunotherapy), anti-neuroinflammatory therapy (microglia and astrocyte modulators, insulin resistance management and microbiome therapy) and neuroprotective agents (antiepileptic drugs and NMDA receptor modification) (Srivastava, Ahmad and Khare, 2021; Yu, Lane and Lin, 2021). Nevertheless, new drug development process can be expensive and time consuming, that comes with a high risk of failure or abandonment because of therapeutic agent inefficacy. Additional potential method for accelerating pharmacological development is drug repurposing. This method not only reduces the risk of disintegration, but also have a shorter time frame cycle. In fact, safety and tolerance of existing drugs have already been investigated and it is easier for these drugs to achieve advanced clinical stages to examine the therapeutic effect in AD. These repurposed drugs in short time of period can move from preclinical investigation to phase II clinical trials. Up to now, some of the potential candidates were proposed in this way, such us, anti-inflammatory (ibuprofen and naproxen) anti-convulsants (levetiracetam, gabapentin and riluzole), anti-diabetics (metformin, liraglutide and intranasal insulin therapy), antidepressants (escitalopram and mirtazapine) drugs and mood stabilizer (lithium) (Sabbagh, 2020; Gąsiorowski *et al.*, 2021).

1.3.2.1. Repositioning existing anti-inflammatory therapy

The role of neuroinflammation is recognized as a promising ethological target which is now accepted due the consensus of preclinical, epidemiological, neuroimaging and genetic evidence. There are several anti-inflammatory strategies which may directly or indirectly influence key cellular functions of microglia and astroglia. One of the earliest anti-inflammatory therapeutic approaches to treat AD was suppression of neuroinflammation with nonsteroidal anti-inflammatory drugs (NSAIDs) (Rivers-Auty *et al.*, 2020). Numerous observational studies have elucidated NSAIDs role reducing or manipulating AD-associated impaired neurogenesis (Chandra, Jana and Pahan, 2018; Ozben and Ozben, 2019). These studies presented that NSAIDs increased liposomal activity, reduced cerebral Aβ plaque load, and, therefore improved spatial learning and memory, and non-selective NSAID, such us, naproxen, prevented Aβ-mediated inhibition of long-term hippocampal plasticity and showed neuroprotective effect in the transgenic and non-transgenic AD mice and rat models (van Bokhoven *et al.*, 2021). Moreover, it was studied, that some NSAIDs including, ibuprofen, diclofenac, indomethacin, piroxicam have effect of ɣ-secretase modulation lowering Aβ42

production. It has been complemented that long-term NSAIDs use may be beneficial only in the very early stages of the AD pathogenesis, coincident of initial Aβ aggregation, microglia activation and release of pro-inflammatory mediators. Previously studied anti-inflammatory drugs that target Rho-GTPases, peroxisome proliferator-activated receptors and maintain Ca2+ homeostasis have demonstrated cognition-enhancing effects (Ali *et al.*, 2019). However, because of its known low exposure in the brain, gastrointestinal toxicity and proved ineffectiveness, few clinical trials have evaluated the general use of NSAIDs in symptomatic individuals with AD based on the fact that non-specific suppression of both the pro-inflammatory and anti-inflammatory phenotypes might not be an entirely effective strategy. Thus, highlights the need to find a way for more appropriate therapy that specifically could target pro-inflammatory microglia phenotypes, such us, NF-kB/nod-like receptor family pyrin domain containing 3 and p38/MAPK pathways (Rivers-Auty *et al.*, 2020; Leng and Edison, 2021; van Bokhoven *et al.*, 2021).

There is growing evidence that the anti-rheumatic gold-containing medication auranofin has anti-inflammatory properties via inhibiting the NF-B-IL-6-STAT3 signalling pathway, which reduces IL-6 levels (Rothan *et al.*, 2020; Sonzogni-Desautels and Ndao, 2021; Yamashita, 2021). Auranofin has been used to treat patients for over 30 years and is well tolerated in humans. In fact, auranofin shows much accumulation in various tissues and the ability to penetrate the BBB and make it a promising candidate for the treatment of other diseases, such as neurodegenerative disorders (AD) (Madeira, Schindler and Klegeris, 2015; Feng *et al.*, 2020; Jang and Eom, 2020). The anti-inflammatory activity of auranofin currently remains unclear. Nevertheless, several studies specify that main mechanisms of action of auranofin could be inhibiting thioredoxin reductase. Furthermore, thioredoxin reductase regulates NF-B factor, which is involved in inflammation and cell survival (Zhang *et al.*, 2019). In addition, nuclear factor NF-B regulates the induction of cyclooxygenase 2 and inducible nitric oxide synthase. Several in vitro study, using cultured in vitro rodent cell and cell lines revealed that auranofin inhibits the production of prostaglandins E2, which has been produced trough cyclooxygenase 2 and regulated by NF-kB factor (Yamashita, 2021). Equally important, auranofin inhibits IL-6-induced phosphorylation of Janus kinase 1 and signal transducer and activator of transcription 3 signalling. As a result, auranofin inhibits many stages in the NF-B-IL-6-STAT3 signalling pathway (Hwangbo *et al.*, 2021). Auranofin also inhibits homodimerization of TLR4 and TL4-mediated activation of NF-kB. Several studies have been demonstrated that receptors by which microglia recognize Aβ aggregates are TLR, such, us, TLR2, which promotes expression of IL-8 and TNF (Hwangbo *et al.*, 2021; Sonzogni-

Desautels and Ndao, 2021). In addition to this, in vitro study, using primary human astrocytes and U-373 astrocyte cells toward human neuronal cells demonstrated that auranofin, demonstrated that auranofin can inhibit the neurotoxic effects and the neuronal cells from the microglia toxins TNF-a and nitric oxide in low micromolar concentrations. It has been suggested, that auranofin may have neuroprotective activity in addition to the previously described anti-inflammatory activity although the mechanisms for this are not fully clear (Madeira *et al.*, 2014; Madeira, Schindler and Klegeris, 2015).

Considering that AD patients exhibit neuroinflammation and that auranofin has an impact on the secretion of cytokines, protects neurons by inhibiting astrocyte toxicity and demonstrates antibacterial activity, it may be beneficial to test the activity of auranofin *in vivo* in a neurodegenerative disease model. Although, auranofin has an impact on the secretion of cytokines, protects neurons by inhibiting astrocyte toxicity and demonstrates antibacterial activity auranofin effects have never been studied in transgenic AD rodent models. Auranofin effects in transgenic AD mouse model have first been studied by our team. We demonstrated that auranofin significantly decreased Aβ deposition in the hippocampus and the number of Aβ plaques in the cingulate cortex, but it did not have memory-enhancing effects or induce changes in the expression of the studied proteins (Upīte *et al.*, 2020).

1.4. Techniques and strategies for CNS drug delivery

The safe, appropriate, and targeted delivery of drug compounds to CNS is an exceptional goal for achieving optimal therapeutic outcomes against neurological diseases. Administration of pharmacological agents in experimental animals, to investigate effects on the brain and behaviour, is performed via a variety of routes, e.g., intracerebrally (via implanted catheters in the brain), by injections (intraperitoneal (ip), subcutaneous, intravenous or intramuscular), transdermal (via a skin-patch or onto mucous membrane), by inhalation, orally (by gavage – insertion directly into the stomach) and intranasal (al Shoyaib, Archie and Karamyan, 2020). Each route of drug administration offers advantages and limitations depending on specific goals of the study. It is well-recognized that the route chosen will impact the final pharmacokinetics, pharmacodynamics as well as toxicity of pharmacological agents. Additionally, bioavailability of a small or large experimental compound could influence the selection of most suitable route of administration. Moreover, the main barrier which limits therapeutic efficacy and becomes one of the biggest challenges in new drug development for neurodegenerative diseases is BBB (Ding *et al.*, 2020; Pandit, Chen and Götz, 2020).

One of the more commonly used routes in rodent studies is the ip route. This technique is easy to master, more reproducible and less stressful as well as safer for experimental animals. Furthermore, a large volume of solution can be safely administered to rodent's trough this route, which might be advantageous for agents with poor solubility (al Shoyaib, Archie and Karamyan, 2020; Jain, 2020). This route is especially common in subchronic and chronic studies involving mice for which repetitive intravenous access is challenging. For example, studies have shown that subchronical and chronical ip administration (daily saline injections ≥ 30 days) are well-tolerated in laboratory animals (Alipour *et al.*, 2016; Nielsen *et al.*, 2017). Moreover, several experimental studies indicate that small to medium size molecules (molecular weight < 5000) and fluids are predominantly absorbed from visceral peritoneum by diffusion trough the splenic, inferior and superior mesenteric capillaries and drain into portal vein. Other experimental studies indicate that ip administration of small molecule pharmacological agents results in faster and more complete absorption to oral and subcutaneous routes. It is noteworthy, that brain exposure of most compounds where higher after ip or subcutaneous administration in comparison to intravenous infusion which could be due to saturation of transporters at the BBB and rapid elimination rate after intravenous infusion. However, this route as any other, has certain limitations. One limitation is the first pass metabolism and it is generally considered that, pharmacokinetics of small molecular drugs administered have lower systemic exposure. The others important factor is that inaccurate ip administration might also deposit drugs into gastrointestinal tract or retroperitoneum of the urinary bladder which may present an issue for potential pharmacological agents for neurological disease to fully cross the BBB (Pandit, Chen and Götz, 2020). In fact, for long-term experiments with purified drugs, systemic administration by ip injection is not considered the preferred choice for targeting the brain. The most direct method for targeting brain tissue is drug delivery by intracerebral infusion, where the agents are diffused with minimal systemic exposure and toxicity. This approach has been applied to increase the brain delivery efficiency of small molecular compounds, large biomolecules, and even nanoparticles. Intracerebral administration provides a way to overcome the BBB (Jain, 2020; Taylor *et al.*, 2021). Even thought, this approach effectively delivers therapeutics to the brain, it is also important to deliver treatment with a continuous and constant concentration. Therefore, several drug delivery systems are widely used to provide long-term continuous intracerebral infusion of test substances. The most promising systems for controlled and long-term drug delivery are osmotic pumps (e.g. ALZET® mini-osmotic pumps). This precision drug administration tool release drug at a rate that is independent of the pH and hydrodynamics of the dissolution medium,

providing more precise drug delivery and distribution of the fixed volume (Domínguez-García *et al.*, 2020; Parks *et al.*, 2020).

1.4.1. Intracerebral drug delivery by mini-osmotic pumps

Long-term continuous intracerebral infusion of test substances by using mini-osmotic pumps is an interesting approach in neurodegenerative disease research. This technique allows researchers to overcome difficulties of drug-delivery across physiological barriers such as the BBB (Saeedi *et al.*, 2019). Additionally, they are useful for targeted delivery, where the effects of a drug or test agent are localized in a particular tissue or organ. The miniaturized infusion sets consist of two main parts: a mini-osmotic pump and a brain infusion kit that contains the brain infusion cannula, catheter tube, and depth adjustment spacers. These miniaturized drug delivery systems, e.g., manufactured by ALZET, are available with a variety of delivery rates between 0.11 and 10 µL/hr and durations between 1 day and 6 weeks. ALZET pumps work due to the osmotic pressure. The high osmotic pressure allows water to flow into the pump through the semipermeable membrane. As the water enters the osmotic layer, it compresses the flexible reservoir and moves the test solution from the pump at a controlled and constant rate. Furthermore, injections often produce plasma levels well above the effective concentration, which can result in toxicity and waste of the compound. The ALZET pump enables researchers to understand and optimize key determinants of drug action, including the level and duration of drug exposure and spatial distribution of the drug to the target tissue. By manipulating these variables, drug efficacy can be optimized early in preclinical development (Keraliya *et al.*, 2012; Singh *et al.*, 2013).

For targeted delivery of substances towards the CNS, the pumps can be used with special brain infusion kits. This brain infusion kit can be used in two ways: a) infusion into the cerebral ventricles exposes a wide variety of brain regions and b) direct microperfusion of discrete brain structures. For this purpose, the pump is placed under the skin on the back of the animal which reduces the chance of infections compared to externalized infusion systems and only minimally hinders normal animal movement. The pump is connected through polyvinylchloride tubing to a metal infusion cannula, which can penetrate approximately 5 mm below the surface of the skull. Depending on the animal size, skull thickness, and desired site for infusion, this depth may need to be altered. To fix the cannula onto the skull, two different methods are widely used. The use of small anchoring screws combined with dental cement. However, a major disadvantage of using dental cement during the surgery is its time-consuming nature.

Additionally, it requires a substantial amount of product, which often makes the product very difficult to work with in mice, which have significantly smaller skulls than rats. Considering the above-mentioned disadvantages of using dental cements, cyanoacrylate adhesive gel has become popular to secure the cannula in rodent studies, especially in mice (Nikam *et al.*, 2012; Missaghi *et al.*, 2014). Nevertheless, in mice the relatively big and flat surface of the cannula's pedestal does not fit properly onto the relatively small and round-shaped skull surface. Therefore, it is needed to invent a completely new or improved approaches to make stereotactic brain infusion experiments more secure and easier to reproduce. In fact, for the first time it was reported by our team that even using the cyanoacrylate gel the fixation of the cannula is not completely satisfying and cause damage for the brain tissue (Sike *et al.*, 2017; Upite *et al.*, 2021).

1.5. Histological quantification of Aβ pathology in transgenic mouse models of AD

A wide range of techniques has been applied over the past decades to characterize Aβ pathology in brain tissue. These techniques include microscopic methods that enable visualization and structural determination, separation techniques to analyse and obtain Aβ species of certain sizes, spectroscopic techniques to follow the aggregation process and determine protein shape, and immunology-based methods for quantification of Aβ aggregates (Su *et al.*, 2015; Christensen and Pike, 2020). Obtaining quantitative data from histological sections represents a formidable challenge. In the past decade, there has been a growing interest for tools able to reduce human subjectivity and improve workload. Therefore, the whole slide scanning technology combined with automated object orientated image analysis can offer the capacity of generating fast and reliable results. However, processing of high-resolution, large images requires digital imaging software (Uslu *et al.*, 2020). For automated image analysis different processing and analysing programs exists (e.g., AxioVision®, ImageJ®, Image-Pro Plus® and DeePathology™ STUDIO) (Uslu *et al.*, 2020; Bascuñana, Brackhan and Pahnke, 2021; Upite *et al.*, 2021). These various imaging software tools for microscopy offer a unique range of additional options, for instance, high content object-based image analysis method for quantification of Aβ plaques in post-mortem brains of AD subjects and in Tg mice overexpressing Aβ (Gao *et al.*, 2021).

1.5.1. Automated quantification of Aβ pathology for new therapeutic approaches

Not surprisingly, much effort has been devoted to quantification of histological structures in various disease models. Advances in imaging technology have enabled and automated approaches for quantitative image analysis, which delivers more descriptive and biologically relevant data. The digital imaging software, e.g., AxioVision, ImageJ or Image-Pro Plus, offers a powerful spectrum of additional modules for image analysis to obtain faster results, uncompromising reliability and maximum reproducibility (Huss and Coupland, 2020; Thinh, Hoang Tung and Ha, 2020). Modules for image analysis can determine interactively the specimen (e.g. size), analyse structures interactively and create fully automatic measuring routines. One such routine is an object-based segmentation approach which can be applied to quantify Aβ plaques from immunohistochemically stained sections after digital imaging (Möhle *et al.,* 2021; Upite *et al.,* 2021). This function offers threshold operators for monochrome and colour images that are necessary to identify objects, e.g., Aβ. The objects can also be identified using „Region Growing“ (detection of associated regions). These two methods are supplemented by complex methods for segmentation, including dynamic and automatically generated threshold values as well as edge detection. In addition, it possible to determine morphometric measurement parameters from the contour of the specimen. The binary image is used as a mask to calculate geometric and densitometric parameters from the original image, which further can be imported into powerful tool, which generates statistical information about specimen details. In addition, in clinical and preclinical research, data from images must be quantitative to allow statistical analysis, needed for characterization of pathological changes and evaluation of potential new treatments. Nevertheless, some of mentioned software are not that powerful or precisely suitable to quantify Aβ pathology and obtain specific analytical values, which can be used to evaluate new therapeutic approaches (Dumitrascu *et al.,* 2020; Huss and Coupland, 2020). Accordingly, to the processing and analysing software user manuals, such us, AxioVision, the functionality beyond its basic core can be extend by developing plugins and creating custom tools using macros. Therefore, generating semi-automated analytic scripts might be useful to quantify Aβ pathology for new therapeutic approaches (Bascuñana, Brackhan and Pahnke, 2021; Upite *et al.*, 2021).

Some therapeutic approaches are not fully optimized to evaluate potential treatment by using Tg AD rodent models. One such method is long-term intracerebral infusion by using mini-osmotic pumps. Our previous study using ALZET mini-osmotic pumps has shown that inappropriate fixation of the ALZET cannula in a long-term continuous infusion experiment

could cause damage in the brain tissue. In addition, we also found a problem, that despite of how gently we tried to remove the metal cannula, a small piece of brain tissue which was attached to it was always removed from the surface of the cortex. Therefore, we developed an improved methodology, which provides better stability of the ALZET cannula (Sike *et al.*, 2017). However, most of the studies applying intracerebral injections focus on assessing the hippocampus or even smaller regions of interest (Diaz-Aparicio *et al.*, 2020; Tang and Guo, 2021). Considering the limited size of these regions, quantification of Aβ plaques and evaluation of a potential treatment are less complex, especially if the target tissue has not been traumatized. There is very limited data available regarding how the quantification of Aβ plaques should be performed in relation to intracerebral injection channels. Until now, there is no method available how to examine the spatial distribution of Aβ and thus, indirectly also the distribution of the test substances in the brain after local infusion with mini-osmotic pumps. Therefore, we developed a suitable analytical tool, which performs histopathological quantification, e.g., in the entire cortex area and compares the results of both hemispheres after continuous long-term intracerebral injection using mini-osmotic pumps (Upite *et al.*, 2021).

.

2. MATERIALS AND METHODS

2.1. Animals and ethics (Paper I, II and III)

For the paper I study, 14-month-old male $APP^{NL\text{-}G\text{-}F/NL\text{-}G\text{-}F}$ mice (n = 24) were used. The animals were obtained from the breeding colony and housed at the University of Alabama at Birmingham (USA).

In paper II - C57BL/6J (n = 36) and III - APPPS1-21 (n = 8), 50-days-old male mice were used and housed in the animal care facility of the Department of Comparative Medicine at the University Hospital in Oslo (Norway).

All animals were kept in controlled laboratory settings (temperature 21–22 °C and 12 h light/dark cycle) with free access to food and water. All experiments were conducted in accordance with the local laws and policies on the protection of animals used for scientific purposes (Paper I - University of Alabama at Birmingham Institutional Animal Care and Use Committee and local laws and policies on the protection of animals used for scientific purposes and Paper II;III - EU (Directive 2010/63/EU) and local animal ethics guidelines according to the state law for animal welfare of Norway). All efforts were made to minimize animal suffering and to reduce the number of animals used.

2.2. Chemicals and antibodies (Paper I and III)

Auranofin (10 mg and 50 mg, catalog No. A6733), dimethyl sulfoxide (DMSO) solution (catalog No. D8418), ExtrAvidin (catalog No. E2886) and Congo Red (CR) stain (catalog No. C6767) were obtained from Sigma-Aldrich (St. Louis, MO, USA). The following antibodies were used: mouse anti-human Aβ4–10 (W0-2; 1:2000; catalog No.MABN10; Millipore, Temecula, CA, USA), glial fibrillary acidic protein (mouse anti-GFAP; 1:1000; catalog No. MAB360; Sigma, St. Louis, MO, USA), ionized calcium binding adaptor molecule-1 (rabbit anti-Iba-1; 1:5000; catalog No. AB5076; Wako, Richmond, VA, USA), glutamic acid decarboxylase (mouse anti-GAD67; 1:1000; catalaog No. MAB5406; Millipore, Temecula, CA, USA), Homer-1 (rabbit anti-Homer-1; 1:500; Catalog No. ABN37; Millipore, Temecula, CA, USA) and anti-human Aβ clone 4G8 antibody (1:4000, BioLegend, USA).

2.3. Intraperitoneal injections of compounds and the use of ALZET® mini-osmotic pumps for the intracerebroventricular administration (Paper I, II and III)

In paper I, the mice were randomly allocated into three groups of 8 animals each. The experimental drug, auranofin was dissolved in 5% DMSO. Further, mice received once daily intraperitoneal (ip) injections of either 5% DMSO 1 ml/kg, which served as a control or auranofin (1 mg/kg or 5 mg/kg). Administration of control or auranofin was done for 30 experimental days in 14-month-old male $APP^{NL-G-F/NL-G-F}$ mice.

For paper II and III, ALZET® mini-osmotic pumps (model 2006) were used with ALZET® brain infusion kit 3 (Cupertino, CA, USA). In paper II, 36 animals and in paper III - 8 animals were used for the experiments. ALZET® mini-osmotic pumps were filled with infusion solutions - 1 x phosphate-buffered saline (PBS) with 1:100 black ink (Paper II) and 1 x PBS (Paper III) according to the manufacturer's instructions. Filled pumps with attached tubing were primed in sterile saline solution at 37°C for 60 h before implantation. Mini-osmotic pumps assured 42 days continuous delivery at a rate of 0.15 µl/h and were implanted when mice reached an age of 50 days by intracerebroventricular surgery.

2.3.1. Intracerebroventricular surgery (Paper II and III)

2.3.1.1. Silicone spacer preparation for intracerebroventricular surgery (Paper II)

To perform long-term intracerebral brain infusion using mini-osmotic pumps, a soft and elastic silicone spacer were invented to better secure a fixation of the cannula. An example of the 50-days-old male C57BL/6J mouse skull was prepared to produce the silicone spacers. Mouse was sacrificed by cervical dislocation. After decapitation, we skinned the head, removed the eyes, the cheek muscles and the tongue using a several surgical instruments.

Further, we "scrambled" the brain with a mounted needle inserted through the foramen magnum and then removed the residuals by repeated syringing with phosphate buffered saline. The skull with the remaining soft tissues was macerated at 60 °C for 48 h, by using commercially available kitchen detergent solution. After the incubation period the skull was thoroughly rinsed under running water and dried at room temperature overnight. Next, the cleaned skull was scanned using an 1172 microCT (Bruker microCT, Kontich, Belgium) at a resolution of 2160 × 960 pixels with a pixel size of 8.54 µm. The parameters for the 360° scan were selected to obtain optimal scans with a source output of 60 kV at 167 µA (10W) and no

filter applied. Later, the scan was reconstructed using NRecon (Bruker microCT, Kontich, Belgium), re-sectioned, and analysed with DataViewer (Bruker microCT, Kontich, Belgium).

To produce mold for the skulls and to produce spacers we used certified skin safe and platinum cure liquid silicone compound Dragon Skin 20 (Smooth-On, USA). Components A and B of this product in equal quantities were mixed. Finally, a vacuum manifold (Millipore, Germany) was used to completely eliminate the entrapped air bubbles at −0.2 MPa for 20 min.

2.3.2.2. Intracerebroventricular surgery and mini-osmotic pump implantation

For intracerebroventricular surgery mice were anesthetized by subcutaneous injection of Zoletil (Vibrac, France) using a dosage of 2.5 µl/g body weight. During the surgery a fully anesthetized mice were placed in a stereotaxic apparatus (Stoelting, USA) on a heating pad (37°C) to maintain normal body temperature. Veterinary ophthalmic lubricants (Lubtithal, Dechra, UK) were applied to maintain corneal hydration. Then, a midline incision was made to expose the skull, and a small subcutaneous pocket was opened on the back of the body using a two hemostats. A hole was drilled into the skull and the mini-osmotic pumps were implanted into the subcutaneous pocket. The cannula with the attached silicone spacer was implanted into the left lateral ventricle of the brain (coordinates: anteroposterior –0.8 mm, mediolateral –2 mm, dorsoventral –2.0 mm (Paper I) or – 1.5mm (Paper II) from bregma). The suture thread (Ethilon, 5-0, AgnThos, Sweden) or metal wound clips (Stoelting, USA) were used to close the incision. At the end of the surgery, mice were removed from the stereotaxic frame, put back to individual cages, and placed on a heating water apparatus (37°C) until they woke up.

2.4. Behavioural and cognitive assessment (Paper I)

In paper I, to assess the changes in animal memory and cognition behaviour as well as in locomotor activity, 19 days after the start of treatment, we performed 4 behavioural tasks (the open field test, elevated zero-maze test, object location task and eight-arm radial water maze test). To record the test parameters a video tracking device coupled with EthoVision 7.1 and 11.5 (Noldus, The Netherlands) were used. The apparatus for open field test, elevated zero-maze test, object location task was wiped with chlorhexidine solution and air-dried between trials.

2.4.1. Open field

To test for changes in animal locomotor activity, open field test was conducted. The open field test apparatus was a 42 cm by 42 cm square arena with 20-cm-high sides that was subdivided into two areas, the border and the centre. The mice were observed for 4 min with a video tracking software system. The total distance (cm) moved and the time (sec) spent in the centre zone of the arena were recorded (van Groen *et al.*, 2017).

2.4.2. Elevated zero-maze tests

The elevated zero-maze test was carried out to determine the anxiolytic action of tested drugs in mice. In this task, the apparatus consisted of a circular maze 70 cm in diameter that was raised 40 cm above the table and divided into two opposite areas (two open and two closed areas) with non-transparent material sidewalls. The closed areas had 15-cm-high sides, whereas the open areas had only 0.5-cm-high sidewalls. At the beginning of each trial, each animal was gently put inside a maze for 4 min. The distance (cm) moved, the time (sec) spent in the closed and open areas, and the total number of arm entries into the open areas were recorded and analysed with video tracking software (van Groen *et al.*, 2017).

2.4.3. Object location task

The ability of the mice to recognize that an object had experienced before had changed location was assessed in this test by using a oval arena (62 cm x 42 cm) with 30-cm-high sides and 20 cm high two small and irregularly shaped types of objects (A1 and A2). Both objects were appropriate for object location task testing in mice. In the acquisition phase, the mice were exposed to objects A1 and A2 (Fig.5), which were placed in a similar position in the arena. The mice were allowed to explore both objects for 8 min, and the amount of exploration of each object. After 1 h, the test phase in which object A2 was placed in the different position began for 4 min (Vogel-Ciernia and Wood, 2014). Thus, both objects in the test phase were equally familiar, but one was in a new location. All mice were placed at the same starting point and tracked with a video tracking system. The exploration time and discrimination index of the moved object were analysed and calculated using mathematical formula = $\frac{time\ with\ novel\ location - time\ with\ familiar\ location}{time\ with\ familiar\ location + time\ with\ novel\ location}$ (Denninger, Smith and Kirby, 2018).

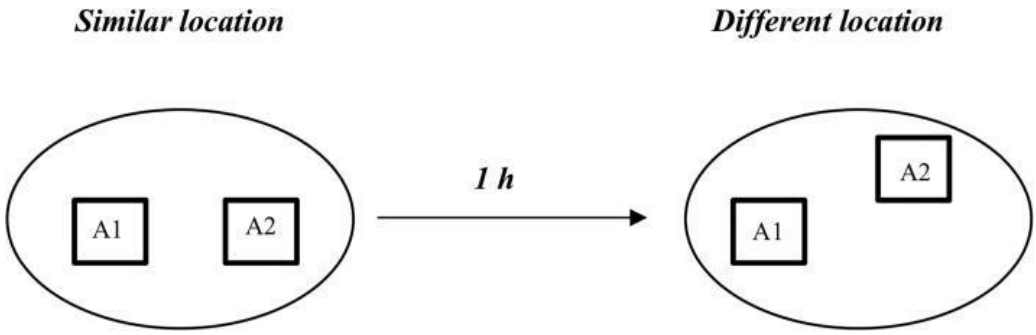

Fig. 5. **Schematic representation of the object location task.**

2.4.4. Eight-arm radial water maze test

To examine the spatial learning and memory capacity of the mice the eight-arm radial water maze test trainings were performed for 6 days (on experimental days 25–30). The apparatus consisted of a blue circular tank (d = 120 cm) that was filled with clear water (23 ± 1 °C) to a depth that would cover a round blue platform (d = 10 cm) and located 0.5 cm below the water surface. The pool included an eight-arm radial maze (d = 100 cm). The mice were trained to swim from one of the seven starting points of the maze to find a hidden platform in one of the eight-arms of the radial maze (an escape platform was situated in the SE arm). Each animal underwent 3 trials (60 sec for trial) per day for 5 consecutive days. If the platform was not found, the animal was gently placed on the platform and left there for 10 sec. In the probe trial, the platform was taken out of the pool and each animal was allowed to swim for 60 sec. The mice that had learned the platform position needed a shorter time to look for the "correct" arm. The latency to find the hidden platform (escape latency) and the swimming speed were recorded for each trial with video tracking software. For the probe trial (the starting point was localized in the North East (NE) arm), the time spent in the target arm, each arm and swimming speed were analysed.

2.5. Histopathological techniques (Paper I and III)

In paper I, following the behavioural testing, on day 31 after the start of the treatment two histopathological techniques - immunohistochemistry and histochemical staining, were performed. The mice were deeply anesthetized with Fatal-Plus solution and perfuses transcardially with cold saline. The brains were removed and fixed in 4% paraformaldehyde (PFA) for 24 h. After fixation, the brains were placed in 30% sucrose for 24 h for cryoprotection

and subsequently placed in an antifreeze solution. The brains were coronally sectioned (six series) at 35 μm on a freezing sliding microtome. The free-floating sections were then stained with primary antibodies (mouse anti-human W0–2 (1:2000), mouse anti-GFAP (1:1000), rabbit anti-Iba-1 (1:5000); mouse anti-GAD67 (1:1000) and rabbit anti-Homer1 (1:500)). For histochemical staining, the sections stained with the W0-2 antibody were double stained with CR. Brain sections were mounted on slides, air-dried and then placed in 4% PFA for 24 h. After 24 h, the slides were rinsed twice for 5 min in dH2O and then treated for 20 min with ethanol-saturated sodium chloride solution with 1% sodium hydroxide (1 ml per 100 ml). Then, the slides were transferred to the CR staining solution (80% ethanol-saturated sodium chloride solution with 0.2 g CR per 100 ml) for 25 min. Afterwards, all slides were rinsed for 20 sec in 95% ethanol and for 1 min in 100% ethanol, cleared in xylene, air dried and coverslipped (van *et al.*, 2011). The other series were stored in antifreeze solution for later use. The free-floating sections were transferred to a solution containing the primary antibody in Tris-buffered saline with 0.5% Triton X-100. After an 18 h incubation in the antibody, the sections were then rinsed and transferred to a solution containing an appropriate biotinylated secondary antibody for 2 h. After a 2 h incubation with the secondary antibody, the sections were rinsed and transferred to a solution containing ExtrAvidin-Peroxidase for 2 h. After rinsing, the sections were incubated with Ni-enhanced 3, 3′ diaminobenzidine tetrahydrochloride solution for 3 min. To obtain comparable staining across sections, all animals were processed simultaneously in the same staining tray. All stained sections were mounted on gelatin-coated slides and coverslipped.

For paper III, mice reaching an age of 100 days were sacrificed by cervical dislocation and transcardially perfused with PBS. The brains were removed and fixed in 4% PFA and transferred into 1x PBS supplemented with 0.01% sodium azide after seven days. PFA-fixed brains were embedded in paraffin and cut in 4μm thick coronal sections. Sections for Aβ staining were pre-treated for 5 min with 98% formic acid before being stained with primary antibody anti-human Aβ clone 4G8 (1:4,000, BioLegend, USA) using a fully automated immunostaining system BOND-III (Leica Biosystems GmbH, Germany). All incubations with primary antibodies were followed by the development with ‘Bond Polymer Refine Detection’ kit (DS9800, Leica Biosystems GmbH, Germany).

2.6. Quantification methods of *ex vivo* data (Paper I and III)

2.6.1. Quantification method using Olympus DP70 and ImageJ (Paper I)

The mounted and stained brain sections were digitized using an Olympus DP70. The optical density of glial GFAP, neuronal GAD67, Iba-1 and Homer-1 was measured in the cingulate cortex and hippocampal CA1 region. The percentage of the area covered by the Aβ reaction product and the number of plaques stained with CR were determined in the anterior cingulate cortex and hippocampal area - CA1 region. The threshold for the measurements was set at the appropriate level to avoid measuring background staining and was used for all images. Using a similar procedure, digital images were used to overlay the defined measurement area, and plaques in the same brain area from the CR-stained sections were counted. Two sections from each brain were analysed in one session. The quantification of both immunohistochemical and histochemical data was performed using open source image-processing software (ImageJ, Germany).

2.6.2. Quantification method using AxioVision (Paper III)

In paper III, all tissue sections were digitized using a Pannoramic MIDI II slide scanner (3DHistotech, Budapest, Hungary). The quantification of immunohistochemical data, to obtain raw data about plaques, was performed using the AxioVision viewer V4.8.1.0 (Carl Zeiss Vision GmbH, Germany) with the add-in "Mirax2AxioVision Converter Utility" (further referred to as "M2AV", Carl Zeiss Vision GmbH, Germany). The add-in "M2AV" (pre-release software) was installed separately. We generated and provided our custom script - M2AV-script "Abeta Pump Animals" (see - A New Tool for the Analysis of the Effect of Intracerebrally Injected Anti-Amyloid-β Compounds - IOS Press -Supplementary material 2). The M2AV-script "Abeta Pump Animals" uses several built-in commands for automated measurements, documentation of measured objects and data storage by saving of measurement data in an Excel-compatible file format (CSV).To install it we copied the files to the "Carl Zeiss" folder (usually located under "C:\Users\Public\Documents\Carl Zeiss\". It can then be called by selecting the script from the menu "Commander" and submenu "Scripts". After all components have been installed, the AxioVision Script Editor found in the menu "Commander" can be used to edit the provided script. This is necessary, as certain folder locations are hardcoded into the script and need to be customized.

2.6.2.1. Acquiring raw data using AxioVision software

The following systematic protocol was generated to describe in detail how to use the M2AV-script “Abeta Pump Animals” in AxioVision. This protocol explains how to import images, how to apply slide-specific settings, how to quantify Aβ plaques and how to obtain raw data that is required to proceed with the analysis in Excel.

1. Load the image (scanned slide) into AxioVision. Since AxioVision does not support the MRXS file format natively, use the add-in “M2AV”.

2. Start the script “Abeta Pump Animals”. This script will guide you through the whole process and show relevant information for each step. Complete and confirm each step to proceed with the next one.

3. Enter a unique slide name (e.g., “BlockID_SlideNo”). This name will be used to identify all data from this slide in later steps in Excel. Note: When importing the data to Excel, the underscore will be used to split the slide title. If you want to follow another naming convention, you need to edit the PowerQuery in the PowerQueryEditor.

4. Select the region of interest (ROI) by using the option “draw annotation” (Fig. 6). Carefully outline the entire area that you want to analyse. The area should contain equal parts from the ipsilateral and the contralateral hemisphere. Do not include any area that does not contain tissue. After finishing the outline, any point can be edited to improve the outline before proceeding to the next step. Important: Note the ipsilateral side for each slide, i.e., does the left or the right hemisphere contain the injection channel. This information will be needed later on when processing the data in Excel.

Fig. 6. **Sample ROI selection: selection of the ROI, outlined in red, using our custom script in AxioVision.**

5. Define the hemisphere border by marking two points as seen in Fig. 7. First, mark the upper point where both hemispheres meet. Second, mark the lower point where both hemispheres meet. Use the circle tool. Note: Only the coordinates of the center will be used for further calculations, the size of the circle is irrelevant.

Fig. 7. **Defining the hemisphere border: the upper and lower points where the hemispheres meet (red circles) using the circle tool in our custom script in AxioVision**

6. Define the injection point and a corresponding point in the contralateral hemisphere as seen in Fig. 8. First, mark the end of the injection needle. Second, mark a corresponding contralateral point. Similar to the previous step, the circle tool and center coordinates are used.

Fig. 8. **Defining the injection point: the injection point and a corresponding point in the contralateral hemisphere (red circles) using our custom script in AxioVision. The previously selected points are displayed in yellow.**

7. Next, AxioVision automatically detects all plaques within the selected ROI. When two plaques are located closely together, AxioVision may recognize them wrongly as a single plaque. You have to correct this mistake manually in the image editor by drawing a line to separate the two plaques as shown in Figure 9.

Fig. 9. **Separation of plaques: how to separate two plaques that have been detected as one object using the line tool in our custom script in AxioVision.**

8. In addition to "fused" plaques, some detected plaques may actually be other objects like spots of unspecific background staining or tissue folds with higher staining intensity. These false positives have to be removed manually. Objects outlined in green will be included in subsequent analyses, while objects outlined in red will be ignored (Fig. 10). In the image editor, click on an object to change its colour.

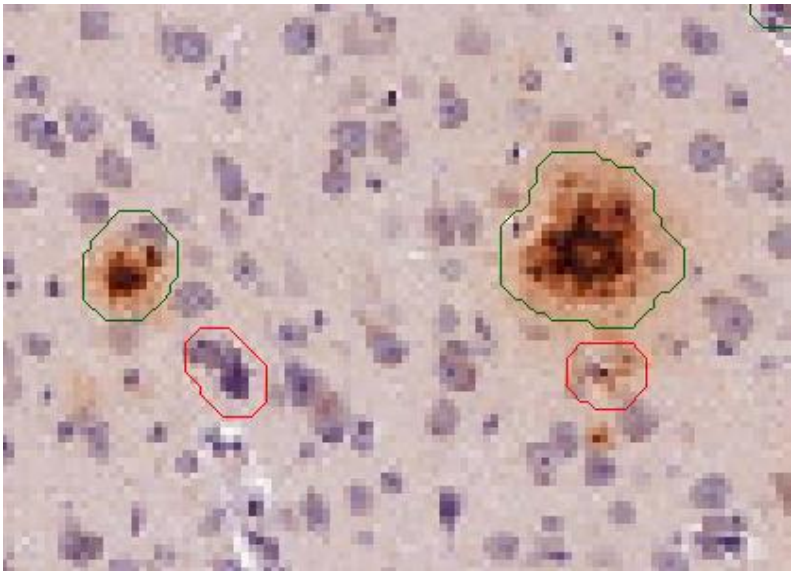

Fig. 10. **Separation of plaques: how to separate two plaques that have been detected as one object using the line tool in our custom script in AxioVision.**

9. When you have completed and confirmed the last step, AxioVision will analyse the ROI and save the raw data into different files. “Area.csv” contains the area of the ROI. “Measured Points.csv” contains information about all analysed plaques. “Ref Hemisphere.csv” contains the coordinates of the reference points dividing the two hemispheres (hemisphere border). “Ref Injection.csv” contains the coordinates of the reference points where the injection was made. An alert window “Done!” will appear once the data export is completed. AxioVision generates in total 10 files per slide, but only the CSV files are needed for the next part.

2.6.2.2. Processing raw data using Microsoft Excel software

To processed and analysed the raw data output from AxioVision we developed the Excel tool “Pump_Animal-Analysis_Tool_Template.xltm” using Microsoft Excel 2016. In this newly designed tool, we used Power Query data connection technology, and made several folder queries to load the raw data from the exported CSV files. We have included two versions of our tool. We provide an Excel macro-enabled template (XLTM) empty version (see - A New Tool for the Analysis of the Effect of Intracerebrally Injected Anti-Amyloid-β Compounds - IOS Press -Supplementary Material 3) and a version containing sample data for demonstration purposes (see - A New Tool for the Analysis of the Effect of Intracerebrally Injected Anti-Amyloid-β Compounds - IOS Press - Supplementary Material 4). To describe in detail how to use the custom Excel tool the following systematic protocol was generated.

1. Open the Excel tool “Pump_Animals_Analyzing_Tool_Template.xltm”. When double-clicking onto the file, Excel will open a new instance of the template (Fig. 11).

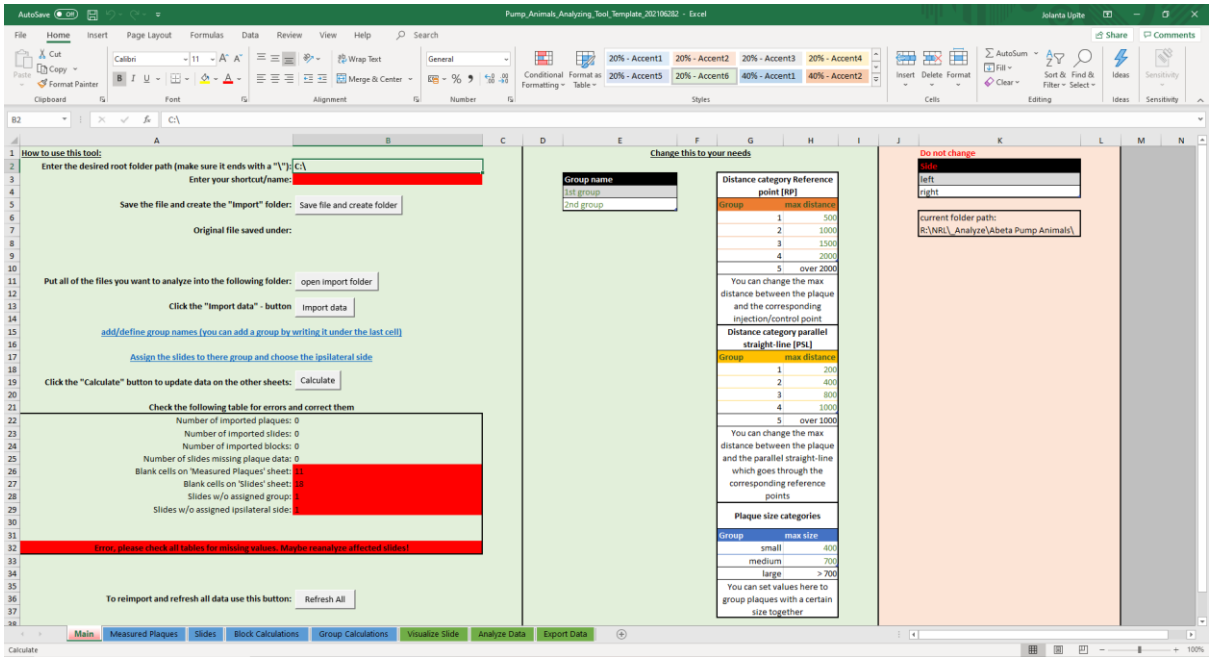

Fig. 11. **Excel tool. Screenshot of the worksheet “Main” with different settings and customizable options. Image shows a new instance of the template in Microsoft Excel.**

2. Before you can import your AxioVision raw data, the file needs to be saved. To this end, enter the path where all files should be saved to (“desired root folder” in the worksheet “Main”) and your name/shortcut. Then, click on “Save file and create folder”. This step will create a folder in the selected root folder (“Username_YYYYMMDD”), save the Excel tool as XLSM file (Excel macro-enabled workbook) and create a subfolder “Import”.
3. Next, you have to provide the raw data that you have obtained from AxioVision. Open the import folder and move or copy all CSV files that have been generated during the first part of this protocol into this folder (4 CSV files per slide).
4. You can now start the data import by clicking on the button “Import data”. A macro will extract all data from the files and save them inside the current Excel file.
5. If your data originates from animals in different groups, you can define and label all groups (table “Group name” in the worksheet “Main”). If you have more than two groups, expand the table as needed.
6. Next, provide information about each imported slide. Clicking “Assign the slides to their group and choose the ipsilateral side” brings you to the worksheet “Slides”. Assign

each slide to a group (column “Group”) and select the ipsilateral side as noted in section 3 (column “Ipsilateral side”). You can note additional slide-specific comments in the column “info”.

7. Finally, you can customize the distance categories for the following analyses (worksheet “Main”, tables “Distance group reference point [RP]” and “Distance group parallel straight line [PSL]”). We explain the meaning of these categories in Section 5.1. Initially, we recommend keeping the default values.
8. Once you have filled in all required information, start the analysis by pressing the button “Calculate”. You have to repeat this step, if new data is added or any information on the worksheet “Slides” is changed.
9. Note: Should you experience problems or inconsistencies, you can re-calculate everything (worksheet “Main”, button “Refresh all”). During a refresh, all information given in the worksheets “Main” and “Slides” is preserved. Use this script also to add more slides later (after you copied the new CSV files to the “Import” folder).
10. In the worksheet “Main”, you can find basic plausibility checks to verify that all data is imported correctly and has been labelled. If any check fails, the cell will be highlighted in red.

2.7. Statistical analysis (Paper I and III)

The statistical analysis were performed for paper I and III. GraphPad Prism® software was used to conduct the statistical analysis. All data are presented as the mean values ± (S.E.M.). Statistical significance was set at $P < 0.05$.

For paper I, the eight-arm radial water maze training data were analysed using two-way analysis of variance (ANOVA) followed by Holm-Sidak's multiple comparisons test. The eight-arm radial water maze test probe trial data, elevated zero-maze test data, object location task data and quantitative histopathological data were analysed using one-way ANOVA followed by Holm-Sidak's test.

In paper III, the statistical analysis of the immunohistochemical quantification of plaques by distance groups RP and PSL one-way analysis of variance (ANOVA) followed by post hoc Holm-Sidak's and Kruskal-Wallis followed by post hoc Dunn’s tests were used. In other cases of the immunohistochemical quantification of plaques were analysed with Student’s t-test.

3. RESULTS

3.1. Effect of subchronically administred compound - auranofin (Paper I)

3.1.1. Behavioral Outcome tested in 14-month-old male APP$^{NL-G-F/NL-G-F}$ mice

3.1.1.1. Auranofin does not influence the activity of the mice in the open field test

No significant differences were observed between groups in the total distance walked ($F(2, 21) = 1.963$, $p = 0.1$; Fig. 12A) and the time spent in the centre zone ($F(2, 21) = 0.6912$, $p = 0.5$; Fig. 12B). For the total distance traveled, the mean values were as follows: control: 1371.0 ± 133.7 cm; auranofin 1 mg/kg: 1834.4 ± 230.7 cm; auranofin 5 mg/kg: 1505.3 ± 125.7 cm; Fig. 12A. For the time spent in the center zone, the mean values were as follows: control: 135.1 ± 9.3 sec; auranofin 1 mg/kg: 152.7 ± 13.5 sec; auranofin 5 mg/kg: 142.5 ± 8.5 sec; Fig. 12B).

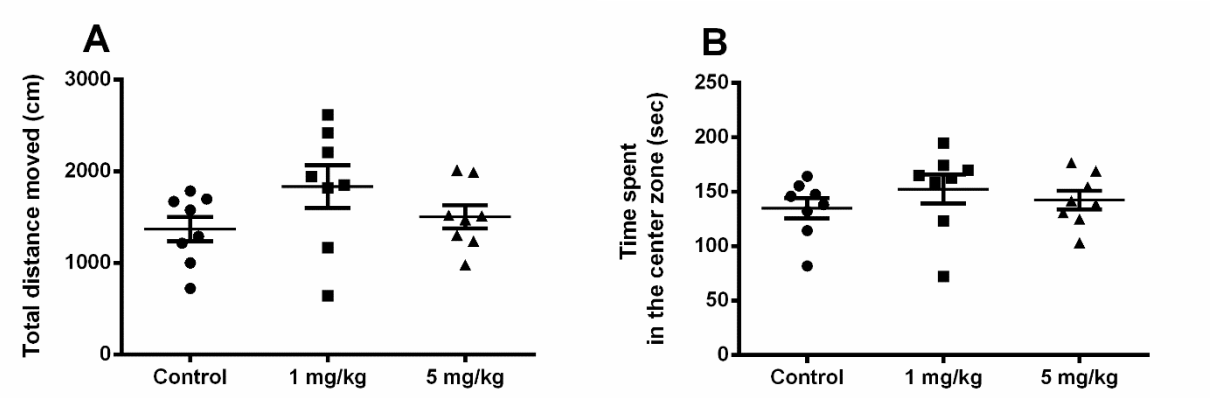

Fig. 12. **Influence of auranofin (1 or 5 mg/kg, ip) on the performance of APP$^{NL-G-F/NL-G-F}$ mice in the open field test (n = 8/group). (A) The data represent the total distance moved. (B) The data are expressed as the time spent in the centre zone. One-way analysis of variance (ANOVA) followed by Holm-Sidak's multiple comparisons test was used to account for inter-group variations. The data are shown as the mean values ± standard errors of the means (S.E.M.). Statistical significance was set at $P < 0.05$.**

3.1.1.2. Auranofin does not influence anxiety-related behaviour in the elevated zero-maze test

In the elevated zero-maze test, there was no significant difference, in the number of total entries into the open areas ($F(2, 21) = 3.201$, $p = 0.06$; control: 14.6 ± 2.5; auranofin 1 mg/kg: 24.9 ± 3.7; auranofin 5 mg/kg: 15.5 ± 3.2; Fig. 13A), and the time spent in the open areas (F

(2, 21) = 2.842, p = 0.08; control: 87.6 ± 12.3 sec; auranofin 1 mg/kg: 98.5 ± 14.5 sec; auranofin 5 mg/kg: 98.9 ± 16.5 sec; Fig. 13B), and in the closed areas (F (2, 21) = 0.2487, p = 0.78; control: 152.4 ± 12.3 sec; auranofin 1 mg/kg: 141.6 ± 14.5 sec; auranofin 5 mg/kg: 138.5 ± 16.7 sec; Fig. 13C) were observed between the treatment and control group. There were no significant differences in the total distance moved between the treatment groups (auranofin 1 mg/kg and 5 mg/kg and the control group (F (2, 21) = 3.095, p = 0.06; control: 957.5 ± 100.3 cm; auranofin 1 mg/kg: 1185.0 ± 145.4 cm; auranofin 5 mg/kg: 784.5 ± 52.6 cm; Fig. 13D).

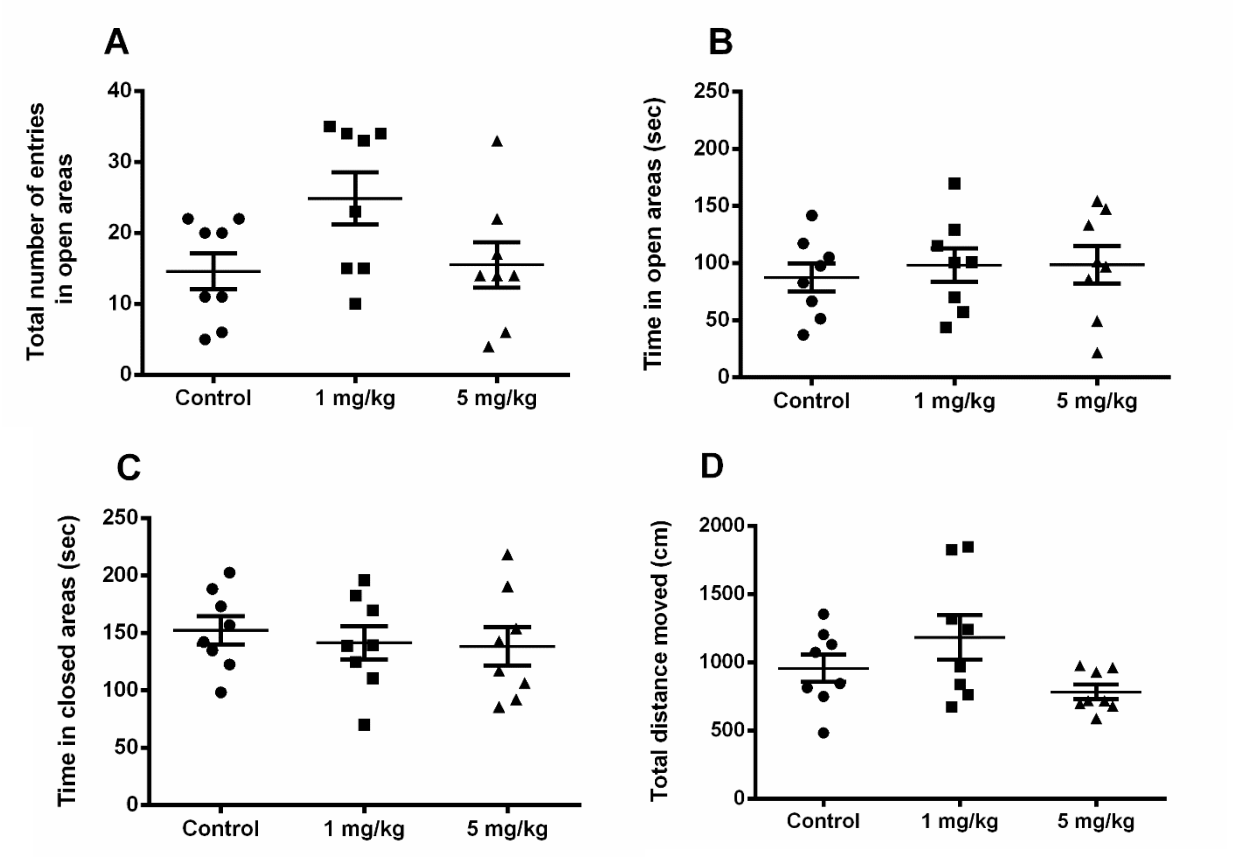

Fig. 13. **Effect of auranofin administration (1 or 5 mg/kg, ip) for 30 days on the performance of APP$^{NL\text{-}G\text{-}F/NL\text{-}G\text{-}F}$ mice in the elevated zero-maze test (n = 8/group). The data are expressed as the time spent in the open areas (A) and closed areas (B) in seconds. The data represent the total number of entries into the open areas (C). The total distance moved (D). One-way analysis of variance (ANOVA) followed by Holm-Sidak's multiple comparisons test was used to account for inter-group variations. The data are presented as the mean values ± standard errors of the means (S.E.M.). Statistical significance was set at P < 0.05.**

3.1.1.3. Auranofin does not have effect on hippocampus-dependent spatial memory in the object location task

As shown in Fig. 14 (A) and (B), no significant differences were observed between groups in the object location task following a 1-h delay. None of the treatment groups showed significant investigation time of the moved object (F (2, 21) = 0.2685, p = 0.7; Fig. 14A) or discrimination between the moved object (F (2, 21) = 0.2473, p = 0.7; Fig. 14B).

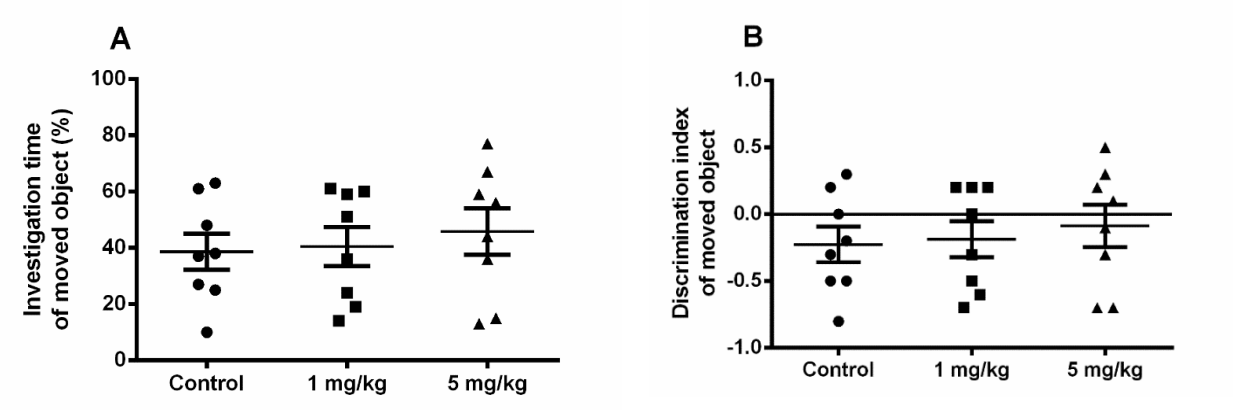

Fig. 14. **Effect of auranofin administration (1 or 5 mg/kg, ip) for 30 days on the performance of APP$^{NL\text{-}G\text{-}F/NL\text{-}G\text{-}F}$ mice in the object location task (n = 8/group). (A) The investigation time and (B) discrimination index of the moved object. One-way analysis of variance (ANOVA) followed by Holm-Sidak's multiple comparisons test was used to account for inter-group variations. The data are presented as the mean values ± standard errors of the means (S.E.M.). Statistical significance was set at P < 0.05.**

3.1.1.4. Auranofin does not influence spatial learning in the eight-arm radial water maze test

The performance of APP$^{NL\text{-}G\text{-}F/NL\text{-}G\text{-}F}$ mice that were treated with auranofin 1 or 5 mg/kg in the eight-arm radial water maze test is shown in Figure 15. Compared to the control group, the auranofin 1 mg/kg and 5 mg/kg treatment groups showed no significant improvement in their performance during the five days of training. The auranofin 1 mg/kg group shortened platform latency on day 3 (F (2, 21) = 0.923, auranofin 1 mg/kg vs. control, p = 0.5; auranofin 5 mg/kg vs. control, p = 0.7; auranofin 1 mg/kg vs. auranofin 5 mg/kg, p = 0.5; Fig. 15A), but no significant difference was present. Similarly, on day 4 (F (2, 21) = 0,671, auranofin 1 mg/kg vs. control, p = 0.6, auranofin 5 mg/kg vs. control, p = 0.8; auranofin 1 mg/kg, p = 0.6; Fig. 16A) and day 5 (F (2, 21) = 0.796, auranofin 1 mg/kg vs. control, p = 0.6; auranofin 5 mg/kg

vs. control, p = 0.7; auranofin 1 mg/kg vs. auranofin 5 mg/kg, p = 0.6; Fig. 15A) no significance was observed. The swimming speed of the mice showed, no significant difference between 1 mg/kg or 5 mg/kg auranofin treated mice and control mice on day 1 (F (2, 21) = 1.519, p = 0.2; control: 13.61 ± 1.00 cm/sec; auranofin 1 mg/kg: 15.27 ± 0.81 cm/sec; auranofin 5 mg/kg: 17.28 ± 2.24 cm/sec; Fig. 4B), day 2 (F (2, 21) = 2.542, p = 0.1; control: 11.50 ± 0.52 cm/sec; auranofin 1 mg/kg: 13.51 ± 0.74 cm/sec; auranofin 5 mg/kg: 12.83 ± 0.64 cm/sec; Fig. 15B), day 4 (F (2, 21) = 1.587, p = 0.2; control: 11.90 ± 0.75 cm/sec; auranofin 1 mg/kg: 14.11 ± 0.87 cm/sec and auranofin 5 mg/kg: 14.50 ± 1.55 cm/sec; Fig. 15B), or day 5 (F (2, 21) = 0.5852, p = 0.5, control: 13.90 ± 1.10 cm/sec; auranofin 1 mg/kg: 14.13 ± 0.76 cm/sec and 5 mg/kg: 14.95 ± 1.47 cm/sec; Fig. 15B); there were only significant differences in the swimming speed between the 1 mg/kg auranofin-treated mice and the control mice (p = 0.01) and between the 1 mg/kg auranofin-treated mice and 5 mg/kg auranofin-treated mice (p = 0.01) (control: 13.09 ± 0.51 cm/sec; auranofin 1 mg/kg: 15.81 ± 0.71 cm/sec; auranofin 5 mg/kg: 13.37 ± 0.51 cm/sec; Fig. 15B) on day 3. There was no statistically significant difference in the ability to find the correct arm (an escape platform was situated in the South East (SE) arm during the training sessions) in the probe trial (F (2, 21) = 2.268, p = 0.1; control: 9.70 ± 2.33 sec; auranofin 1 mg/kg: 10.97 ± 1.82 sec; auranofin 5 mg/kg: 4.23 ± 1.23 sec; Fig. 15C and 15D) and the swimming speed on the probe trial day (F (2, 21) = 0.6942, p = 0.5; control: 12.04 ± 0.86 cm/sec; auranofin 1 mg/kg: 13.09 ± 0.54 cm/sec; auranofin 5 mg/kg: 13.00 ± 0.65 cm/sec; Fig. 15B) among experimental groups.

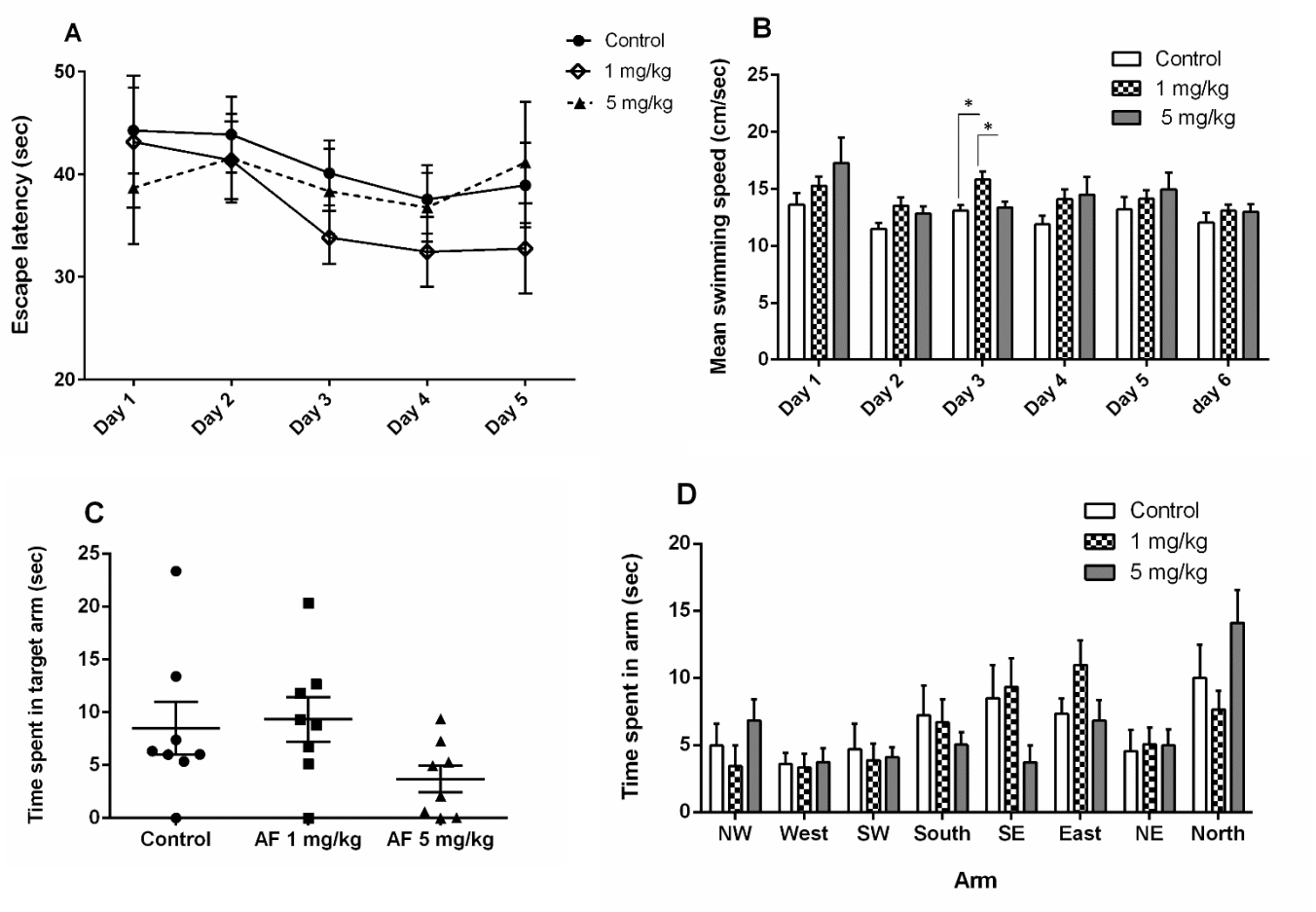

Fig.15. **Effect of auranofin administration (1 or 5 mg/kg) on the performance of APP$^{NL-G-F/NL-G-F}$ mice in the eight-arm radial water maze test (n = 8/group). Spatial learning is represented by the mean escape latency on each training day (A) and the average swimming speed (B) of the mice on each day. Two-way analysis of variance (ANOVA) with repeated measures was used to account for inter-group variations (group and training day as factors). In the probe trial test, the time spent in the eight-arm radial water maze arms (target arm (SE)) was recorded (C and D). One-way analysis of variance (ANOVA) followed by Holm-Sidak's multiple comparisons test was used to account for inter-group variations. The data are presented as the mean values ± standard errors of the means (S.E.M.). Statistical significance was set at P < 0.05. *P < 0.05**

3.1.2. Immunohistochemical Data

3.1.2.1. Chronic administration of auranofin reduces Aβ load and plaque number in in 14-month-old male APP$^{NL-G-F/NL-G-F}$ mice, as determined by W0-2 and CR staining

AD pathology was assessed by measuring the Aβ plaque load in the cingulate (Cg) cortex (Fig. 16A and B top row) and hippocampus (stratum radiatum of CA1) (Fig. 16A and B, second

row). The chronic administration of auranofin at 1 mg/kg ($p = 0.0004$) and 5 mg/kg ($p = 0.01$) resulted in a significant decrease in Aβ accumulation in the hippocampus compared to that in the control group (percentage load: control: 6.38 ± 0.26; auranofin 1 mg/kg: 4.71 ± 0.29; auranofin 5 mg/kg: 5.38 ± 0.18; Fig. 16B, second row). No significant differences were observed in the Aβ plaque load in the Cg cortex ($p = 0.9$ for auranofin 1 mg/kg; $p = 0.6$ for auranofin 5 mg/kg) compared to that in the control group (percentage load: control: 7.29 ± 0.68; auranofin 1 mg/kg: 7.25 ± 0.31; auranofin 5 mg/kg: 6.50 ± 0.42; Fig. 16B, top row). A significant difference was observed in the level of Aβ (measured as the number of plaques) in the Cg cortex region (Fig. 16A and B, third row) but not in the hippocampus (Fig. 16A and B, bottom row) upon CR staining. Multiple comparisons showed that there was only a significant decrease in the Aβ plaque number in the Cg cortex ($p = 0.3$ for auranofin 1 mg/kg; $p = 0.03$ for auranofin 5 mg/kg) compared to the control group (control: 60.63 ± 2.61; auranofin 1 mg/kg: 51.50 ± 7.75; auranofin 5 mg/kg: 43.25 ± 2.27; Fig. 16B, third row). No significant differences were observed between the treatment groups and the control group in the hippocampus ($p = 0.9$ for auranofin 1 mg/kg vs. control; $p = 0.6$ for auranofin 5 mg/kg vs. control; control: 72.13 ± 1.61; auranofin 1 mg/kg: 59.60 ± 6.34; auranofin 5 mg/kg: 69.25 ± 3.59; Fig. 16B, bottom row). For W0-2 and CR staining, tissues from only five or six animals from the control and 1 mg/kg auranofin-treated groups were measured because of uneven staining due to 2 – 3 tissues sticking to the staining tray wall (Fig. 16B).

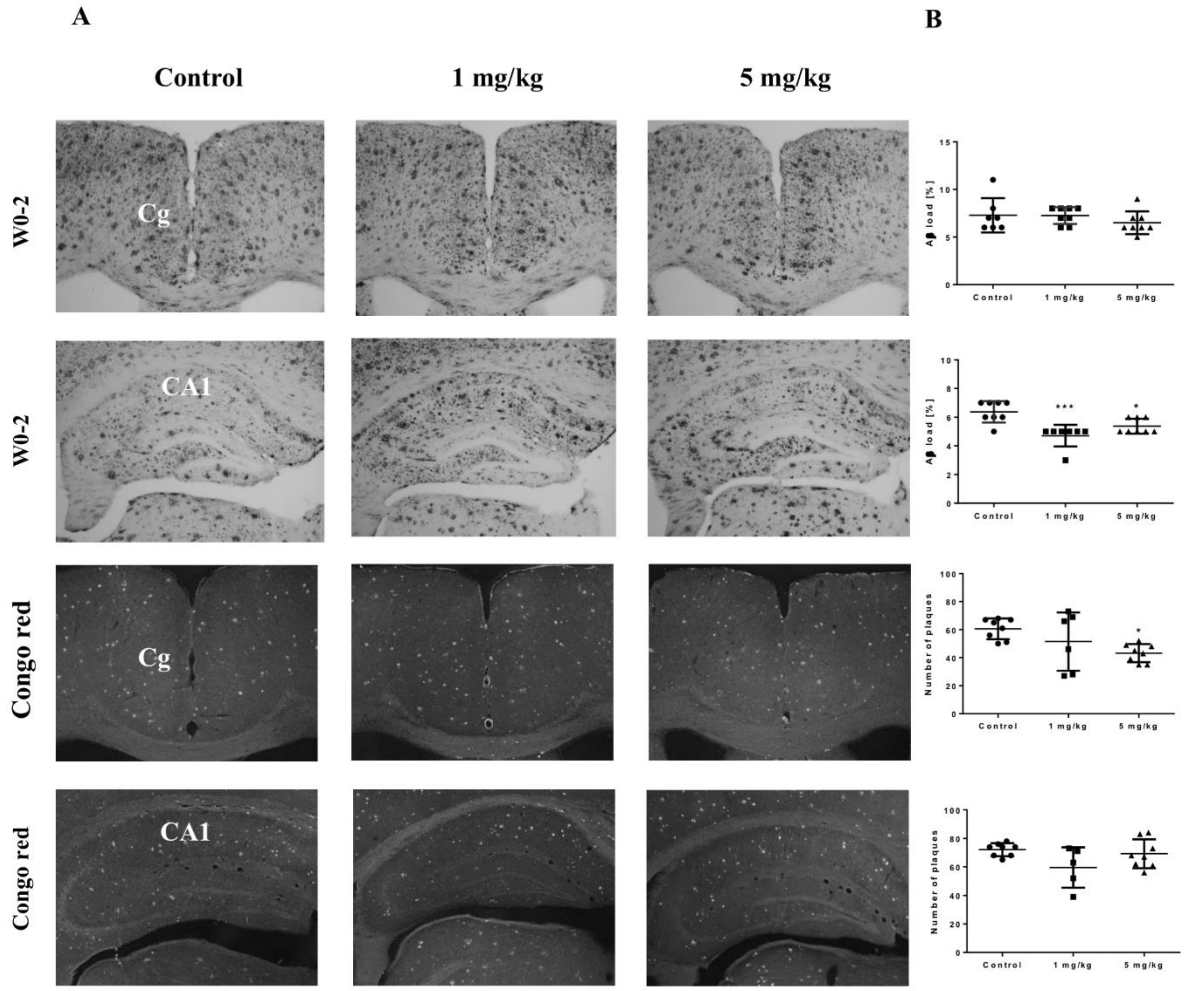

Fig. 16. **Photomicrographs of W0-2 and Congo Red staining of the hippocampus and cingulate cortex of APP$^{NL-G-F/NL-G-F}$ mice after treatment with control, auranofin 1 mg/kg or 5 mg/kg (n = 5 – 8/group). (A) Top row: three photomicrographs of the Cg cortex stained for W0-2. Second row: three photomicrographs of the hippocampus stained for W0-2. Third row: three photomicrographs of the Cg cortex stained for Congo Red. Bottom row: three photomicrographs of the hippocampus stained for Congo Red. (B) Bar graphs showing the quantification of the density measurements of immunohistochemical staining. One-way analysis of variance (ANOVA) followed by Holm-Sidak's multiple comparisons test was used to account for inter-group variations. The data are presented as the mean values ± standard errors of the means (S.E.M.). Statistical significance was set at $P < 0.05$. *$P < 0.05$ and ***$P < 0.0005$ vs. control.**

3.1.2.2. Effects of auranofin on Iba-1 and GFAP density in the brains of $APP^{NL\text{-}G\text{-}F/NL\text{-}G\text{-}F}$ mice

The chronic administration of 1 mg/kg and 5 mg/kg auranofin did not produce significant changes in staining density for Iba-1 in the Cg cortex ($F(2, 21) = 0.4699$, $p = 0.6$; auranofin 1 mg/kg: 56.73 ± 0.77; auranofin 5 mg/kg: 55.45 ± 0.83; control: 55.76 ± 1.25; Fig. 17A and B, top row) and in the hippocampus ($F(2, 20) = 1.293$, $p = 0.2$, auranofin 1 mg/kg: 61.26 ± 1.38; auranofin 5 mg/kg: 62.74 ± 0.71; control: 60.43 ± 1.38; Fig. 17A and B, second row). Furthermore, neither dose of auranofin significantly decreased the GFAP density in $APP^{NL\text{-}G\text{-}F/NL\text{-}G\text{-}F}$ mice compared to control mice in the Cg cortex ($F(2, 21) = 0.4429$, $p = 0.6$; auranofin 1 mg/kg: 79.18 ± 3.07; auranofin 5 mg/kg: 77.09 ± 2.26; control: 75.41 ± 3.10; Fig. 17A and B, third row) or in the hippocampus ($F(2, 17) = 0.1559$, $p = 0.8$; auranofin 1 mg/kg: 106.67 ± 3.76; auranofin 5 mg/kg: 105.28 ± 3.26; control: 108.16 ± 3.77; Fig. 17A and B, bottom row). For Iba-1 and GFAP staining, tissues from only seven animals from the control and 1 mg/kg auranofin-treated groups were measured because of uneven staining due to tissues sticking to the staining tray wall (Fig. 17B, second and bottom row).

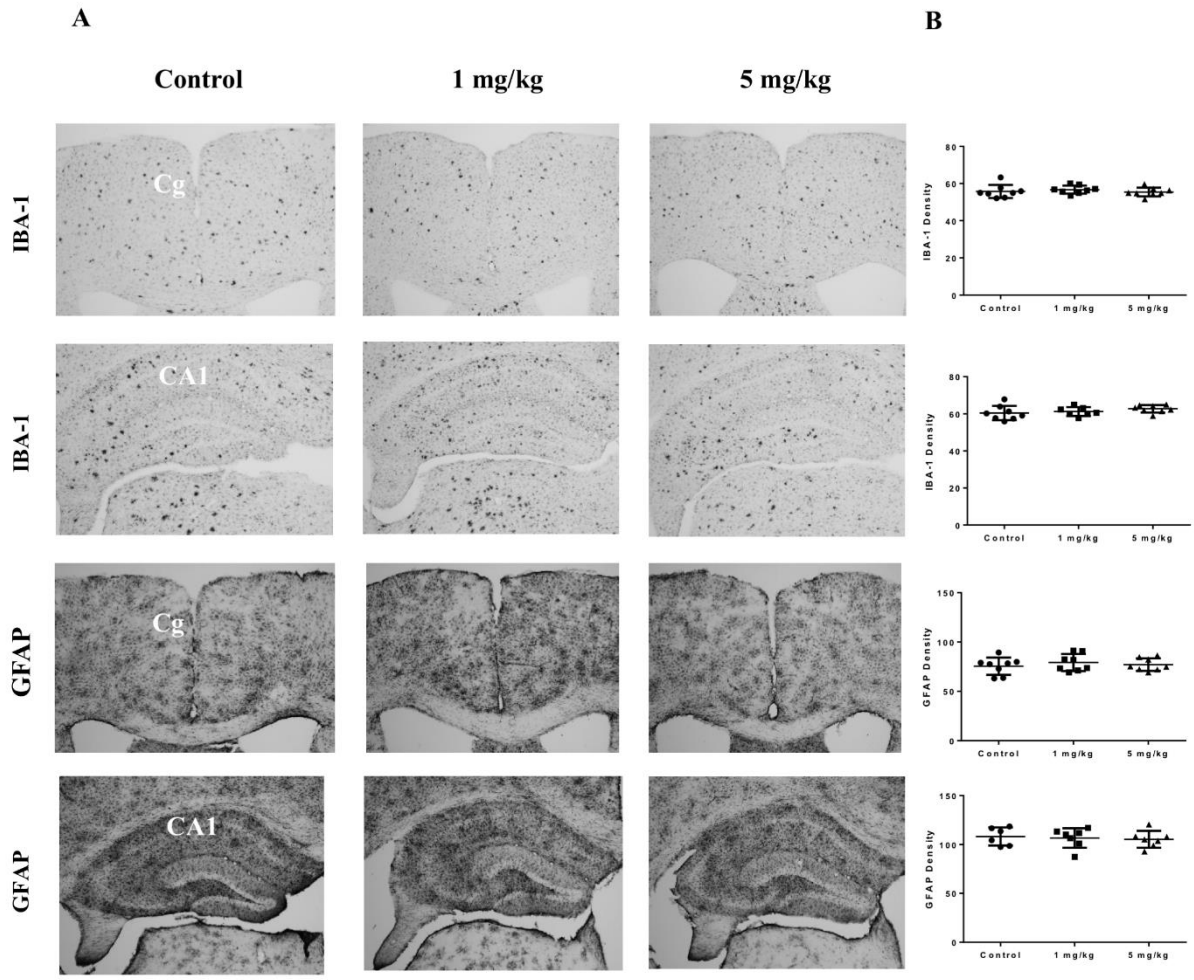

Fig. 17. **Photomicrographs of Iba-1 and GFAP staining of the hippocampus and cingulate cortex of APP$^{NL-G-F/NL-G-F}$ mice after treatment with control, auranofin 1 mg/kg or 5 mg/kg (n = 7 – 8/group). Cg – cingulate cortex. (A) Top row: three photomicrographs of the Cg cortex stained for Iba-1. Second row: three photomicrographs of the hippocampus stained for Iba-1. Third row: three photomicrographs of the Cg cortex stained for GFAP. Bottom row: three photomicrographs of the hippocampus stained for GFAP. (B) Bar graphs showing the quantification of the density measurements of immunohistochemical staining. One-way analysis of variance (ANOVA) followed by Holm-Sidak's multiple comparisons test was used to account for inter-group variations. The data are presented as the mean values ± standard errors of the means (S.E.M.). Statistical significance was set at $P < 0.05$.**

3.1.2.3. Effects of auranofin on GAD67 and Homer-1 desity in the brains of $APP^{NL\text{-}G\text{-}F/NL\text{-}G\text{-}F}$ mice

Similarly, the expression of GAD67 and Homer-1 in the brain was determined in the $APP^{NL\text{-}G\text{-}F/NL\text{-}G\text{-}F}$ mice. There were no significant changes in GAD67 expression in the Cg cortex ($F(2, 21) = 0.9147$, $p = 0.4$; auranofin 1 mg/kg: 102.78 ± 4.20; auranofin 5 mg/kg: 96.01 ± 2.54; control: 99.74 ± 3.70; Fig. 18A and B, top row) or the hippocampus ($F(2, 20) = 0.8521$, $p = 0.4$ auranofin 1 mg/kg: 78.10 ± 1.63; auranofin 5 mg/kg: 75.05 ± 1.57; control: 76.87 ± 1.74; Fig. 18A and B, second row) of the treated mice compared with the control mice. No significant differences were observed in Homer-1 expression in the Cg cortex ($F(2, 21) = 1.057$, $p = 0.3$; auranofin 1 mg/kg: 94.14 ± 3.05 and 5 mg/kg: 88.57 ± 3.34; control: 91.63 ± 1.28; Fig. 18A and B, third row) or the hippocampus ($F(2, 19) = 0.1197$, $p = 0.8$, auranofin 1 mg/kg: 87.40 ± 2.55 and 5 mg/kg: 89.32 ± 1.79; control: 87.99 ± 3.45; Fig. 18A and B, bottom row) of the treated mice compared with the control mice. For Homer-1 staining, tissue from only seven animals from the l and 5 mg/kg auranofin treated groups were measured because of uneven staining.

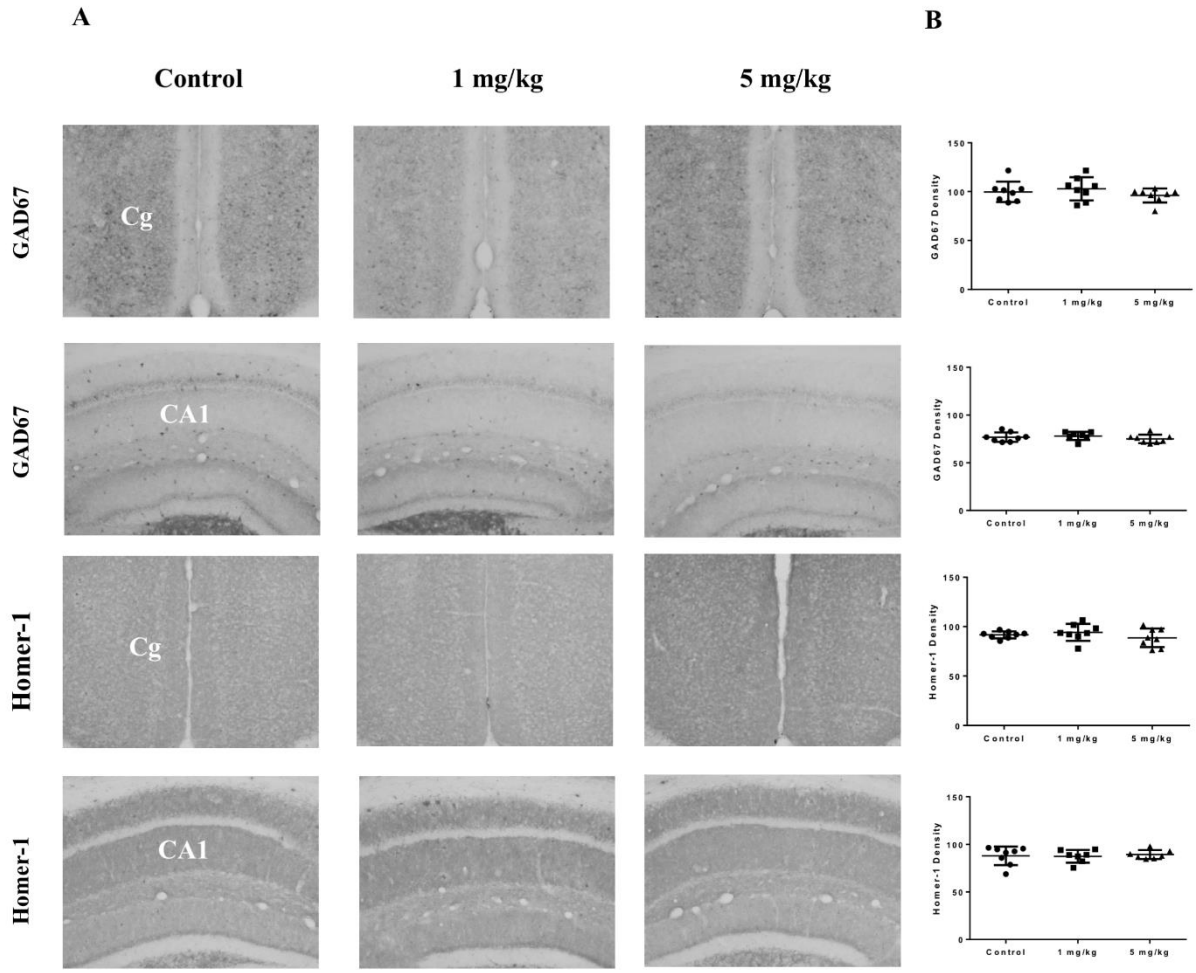

Fig. 18. **Photomicrographs of GAD67 and Homer-1 staining of the hippocampus and cingulate cortex of APP$^{NL-G-F/NL-G-F}$ mice after treatment with control, auranofin 1 mg/kg or 5 mg/kg (n = 7 – 8/group). Cg – cingulate cortex. (A) Top row: three photomicrographs of the Cg cortex stained for GAD67. Second row: three photomicrographs of the hippocampus stained for GAD67. Third row: three photomicrographs of the Cg cortex stained for Homer-1. Bottom row: three photomicrographs of the hippocampus stained for Homer-1. (B) Bar graphs showing the quantification of the density measurements of immunohistochemical staining. One-way analysis of variance (ANOVA) followed by Holm-Sidak's multiple comparisons test was used to account for inter-group variations. The data are presented as the mean values ± standard errors of the means (S.E.M.). Statistical significance was set at $P < 0.05$.**

3.2. Improved cannula fixation methodology and histopathological quantification tool for the intracerebral infusion experiments using mini-osmotic pumps (Paper II and III)

3.2.1. Modified method for a better fixation of the cannula holder (Paper II)

3.2.1.1. Three-dimensional print and preparation of gypsum skulls

First, we produced a solid model of the skull to serve a casting template. MicroCT scanner with high resolution was used to produce a 3D plastic print of a 50-days-old mouse skull. After reconstruction of the CT scan the skull was 3D-printed (Fig.19). As the skull bone was far too thin to be printed and stable it collapsed under slightest pressure, even when printed 5-times as big as the original mouse skull. To prevent this the obvious idea would be to print a filled skull. However, even the thinnest possible resin layering of 25 µm with the printer used produced a "stair treads"- surface too prominent to allow smooth fitting to a skull.

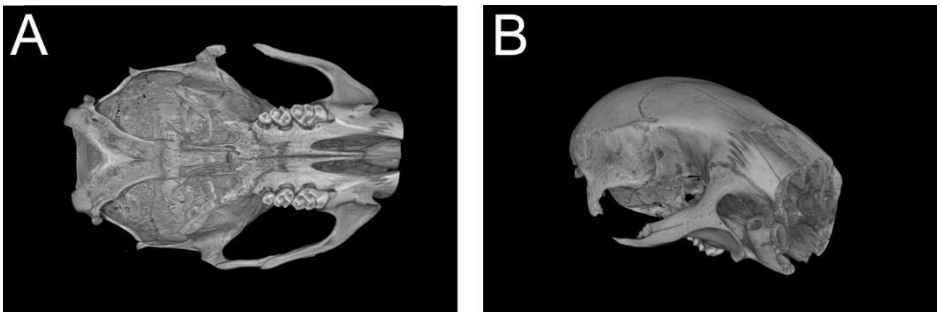

Fig.19. **CT scan and 3D-reconstruction of a of a 50-days-old mous skull using a microCT scanner.**

With the above in mind, we applied a more appropriate approach to produce a solid skull model. For that reason, a cleaned skull as a positive model was used to create a flexible silicone mold. The A and B components of the Dragon Skin silicone were mixed for 3 minutes and poured into a containment field made of plastic. Further, a vacuum degassing was used to eliminate entrapped air bubbles. Next, we dipped the skull into the silicone and allowed the rubber turn from a liquid to a flexible solid for 4 hours at room temperature. After the silicone has cured, the skull was removed (Fig. 20A) and the mold filled with a very fluid gypsum-water mixture. After 1-hour incubation at room temperature the gypsum has cured, and the gypsum skull easily removed from the silicone mold. Finally, we used sandpaper to produce a flat basal skull surface and adjust the height to 5.5 mm at coordinates AP -2 mm to bregma and

ML 0 mm to bregma (Fig. 20B). The base was prepared in a way that its surface was in parallel to the area AP 0.0 mm to bregma to AP 2 mm to bregma.

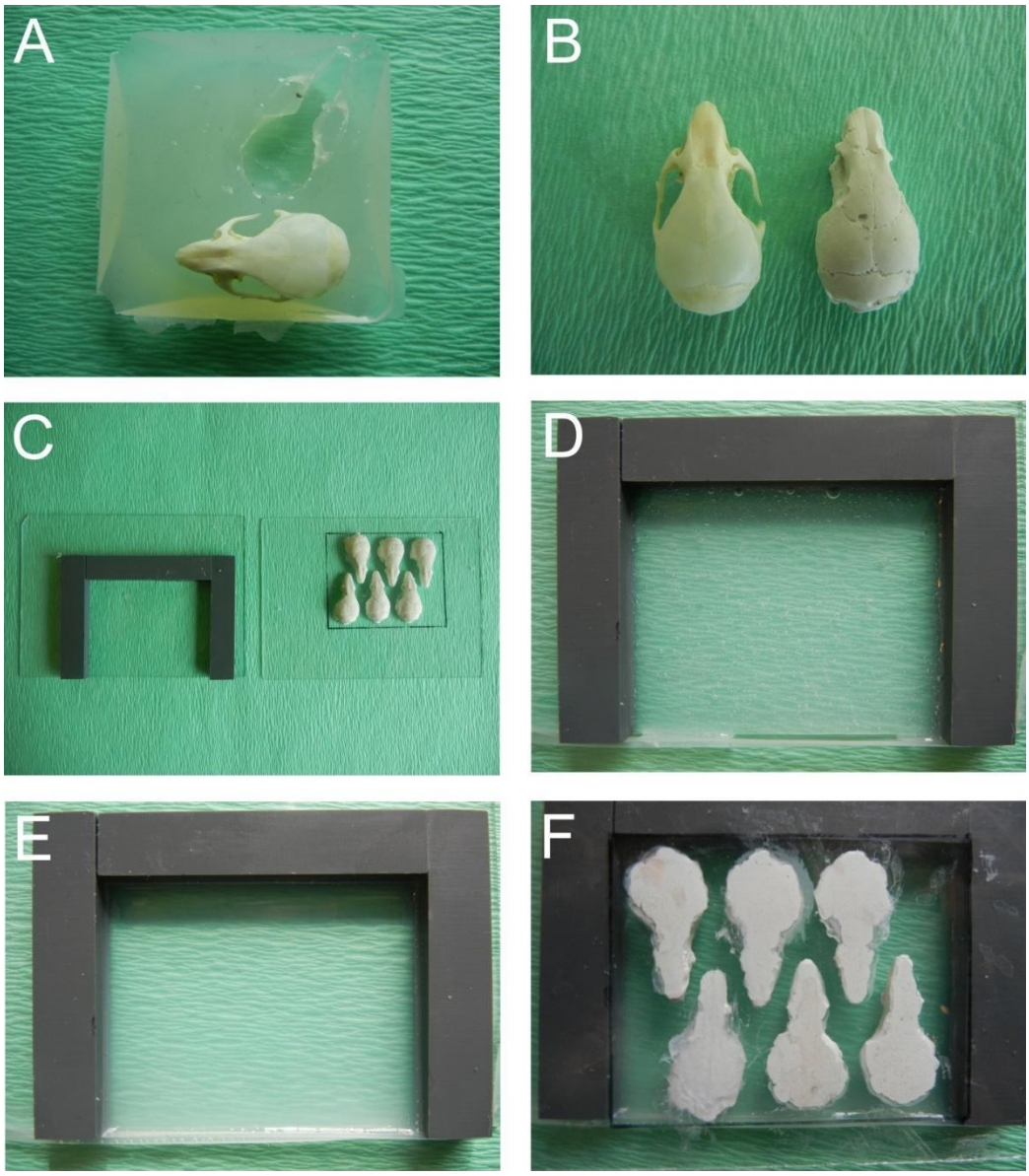

Fig. 20. **(A) Photograph of the silicone mold made by using a cleaned skull in order to produce the gypsum skulls. (B) The gypsum skull (right) and the model skull of a 50-days old mouse (left). (C) The mold system. The casting chamber with the plastic spacers (left side) and the gypsum skulls glued onto the glass surface (right side). (D) the mixed silicone poured into the casting chamber still containing entrapped air bubbles. E: the silicone mixture after de-gassing. (F) The assembled mold system.**

3.2.1.2. Preparation of the mold system and silicone spacers

To continue production of the skull-shaped silicone spacers, a special mold system was built. First, three plastic spacers with height of 6 mm were glued onto a glass surface to make a containment field (Fig. 20C, left side). Next, we fixed six gypsum sculls onto another glass surface using cyanocrylate (Fig. 20C, right side). Further, we made enough silicone to fill the containment field to 2mm height (Fig. 20D). Then it was vacuum degassed to completely eliminate all entrapped air bubbles (Fig. 20E). In the next step, we placed the glass surface with the gypsum skulls upside-down onto the top of the spacers of the containment field so that the dorsal-most part of the skulls dipped into the silicone (Fig. 20F). After 4 hours the rubber has cured and the glass surface with the skulls was gently removed. Finally, we got a silicone spacer with a flat surface on the skulls' (Fig. 21A) and with the shape of the skull on the other (Fig. 21B). Before surgery, the silicone spacers were autoclaved, served as post-curing and leads to the elimination of all remaining silicone monomers.

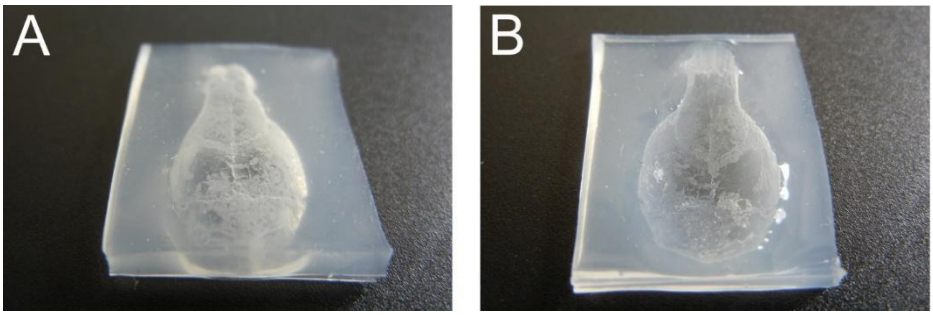

Fig. 21. **The silicone spacer. (A) the flat upper surface. (B) the skull-shaped bottom surface.**

3.2.1.3. Application of the silicone spacer during the surgery

Before surgery, the silicone spacer was prepared to about the size of the cannula base platform and according to the coordinates of the infusion point. As can be seen in Fig. 21, the mold and silicone nicely reproduce all skull fissures. Therefore, it is possible to determine which part of the spacer will be needed. Additionally, the spacer could be tailored to the proper size and shape, which on the one hand is big enough to provide an attachment surface for the cannula, but on the other hand is small enough to allow closing the wound without problems. To implant the mini-osmotic pump connected to a brain cannula, a standard stereotactic operation was performed. After drilling the hole, the silicone spacer was carefully placed onto the skull above the hole using a cyanoacrylate adhesive. To avoid cyanoacrylate getting into

the borehole, it was applied onto the skull only. By using the micromanipulator and a sharp needle, a hole was punched through the silicone over the burr hole to allow the blunt infusion cannula going through the silicone. Then, the pump was placed into the subcutaneous pocket and cyanoacrylate adhesive was introduced onto the cannula's pedestal. Further, the cannula was placed into the cannula holder of the stereotactic frame and lowered into position using the micromanipulator (Fig. 22A). After 2 minutes, the cannula head was removed, and the wound was closed.

After the operation, the animals recovered quickly. All animals were monitored closely during infusion period of 42 days. Some of the animals tried to scratch the wound but they were not able to open the wound and remove the cannula from the skull. After 2-3 weeks, the hair grew back (Fig. 22B). Overall, the implanted pump and the cannula caused minimal discomfort to the animals and it had no effect on the moving ability. After 50 days, the mice were sacrificed, and the cannula was still securely attached to the skull with the silicone spacer (Fig. 22C). On the surface of the removed brains only a small hole is visible (Fig. 22D) which indicates that the cannula was properly fixed and there was no lateral movement.

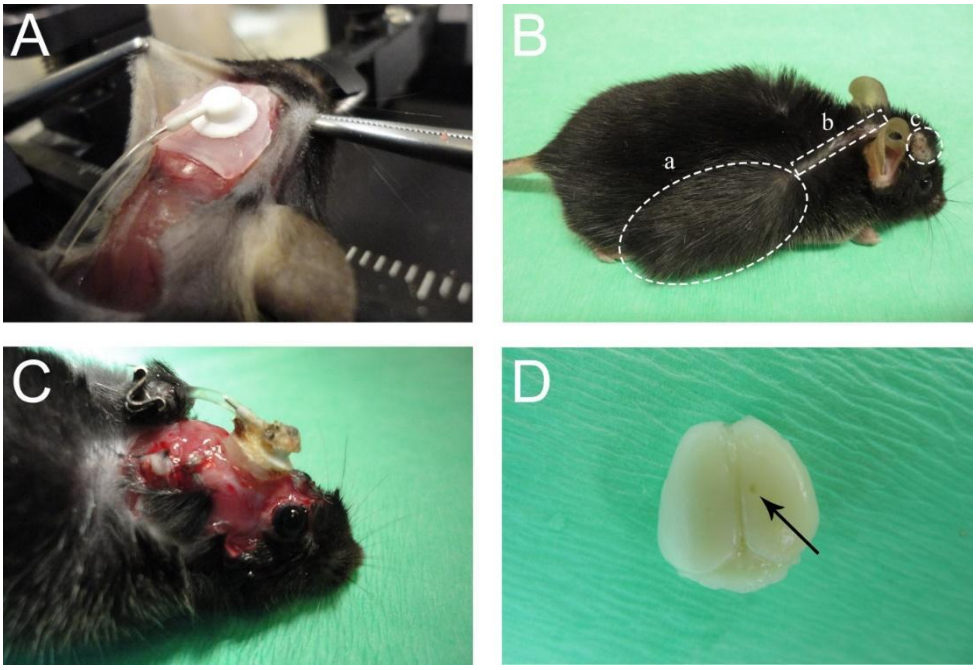

Fig. 22. **(A) The application of the silicone spacer during the surgery. (B) A 100-days–old mice carrying an implanted pump (a: pump. b: plastic tubing c: encased cannula). (C) After transcardial perfusion; the cannula is still securely attached. (D) A small hole in the brain indicates where the cannula was inserted.**

3.2.2. New analytic toolbox for quantitative histological assessment in relation to intracerebral injection channels (Paper III)

For the visualization and interpretation of the data, our custom Excel tool ("Pump_Animal-Analysis_Tool_Template.xltm") provides different charts and tables (worksheets "Visualize Slide" and "Analyze data"). In the following sections, more details about these worksheets have been provided. Additionally, the worksheet "Export Data" provides several pre-defined filters to export specific sets of values for the analysis in third-party software, e.g. statistical analysis in Prism (GraphPad Software, San Diego, USA).

3.2.2.1. Plaque categorization

This work present two different approaches how to characterize plaques based on their distance to a reference point (RP) or to a reference line (parallel straight line, PSL). Both approaches (RP/PSL) categorize plaques in five predetermined distances that can be customized (worksheet "Main"). The detailed mathematical calculations are described in **Supplementary Material 1**.

The RP approach categorizes plaques in a circular manner according to their distance from a reference point (Fig. 23A). On the ipsilateral side, this reference point is the tip of the injected cannula. On the contralateral side, it is the previously selected reference point. The distance categories are defined in the "Main" worksheet. By default, these categories are distances smaller than (1) 500 µm, (2) 1000 µm, (3) 1500 µm, (4) 2000 µm, and (5) more than 2000 µm.

The PSL approach categorizes plaques according to their distance from a reference line. This reference line is calculated as a parallel to the previously defined hemisphere border that goes through the reference point in the respective hemisphere (Fig.23B). By default, the distance categories are distances smaller than (1) 200 µm, (2) 400 µm, (3) 800 µm, (4) 1000 µm, and (5) more than 1000 µm.

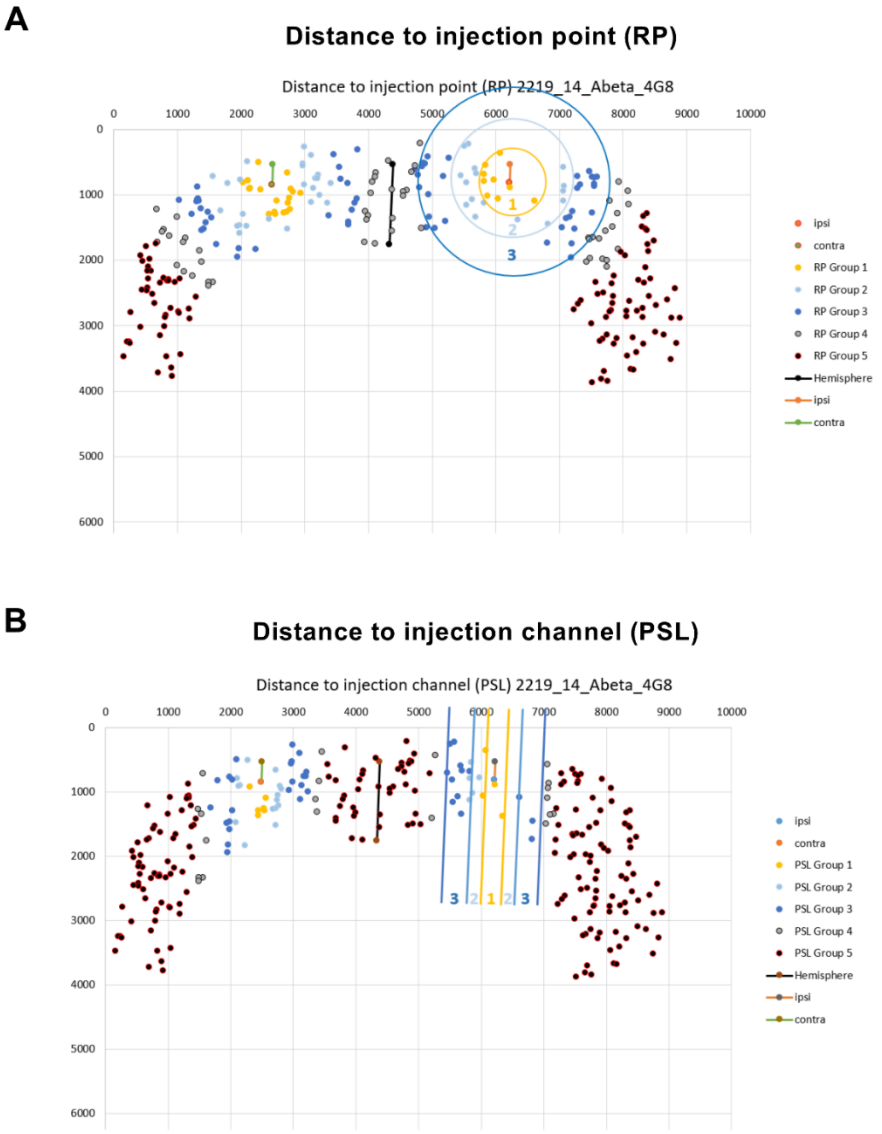

Fig.23. **Schematic representation of the categorization approaches for amyloid plaques. (A) Distance between plaques and the injection point (RP). The RP approach categorizes plaques in a circular manner according to their distance from a reference point. The distance categories are smaller than (1) 500 µm, (2) 1000 µm, (3) 1500 µm, (4) 2000 µm, and (5) more than 2000 µm. (B) The distance between the plaque and the injection channel (PSL). The PSL approach categorizes plaques according to their distance from a reference line. The distance categories are distances smaller than (1) 200 µm, (2) 400 µm, (3) 800 µm, (4) 1000 µm, and (5) more than 1000 µm. The circles/lines were added manually to visualize the approach and are not used for the actual classification. Representative pictures have been obtained from our custom Excel tool.**

3.2.2.2. Visualization of detected plaques

The obtained raw data in AxioVision contains precise two-dimensional coordinates for each plaque, which are used to calculate their distance (RP or PSL). Moreover, these coordinates are used to generate graphical visualizations for one slide at a time (worksheet "Visualize Slide").

After selecting the slide/animal of interest, the user obtains three different graphs: plaques accumulated across the whole cortex (Fig. 24A), plaques accumulated across the cortex from RP (Fig. 24B) and plaques accumulated across the cortex from PSL (Fig. 24C). Each data point represents one detected plaque, regardless of its size. In Figure 24A, B and C, the color of the data points represents their distance to the injection point or channel based on the pre-defined distance groups for RP and PSL.

These graphical representations allow the user to visualize plaque location around the injection point or channel and to detect potential calculation errors, e.g. if quantified plaques do not belong to a particular distance group.

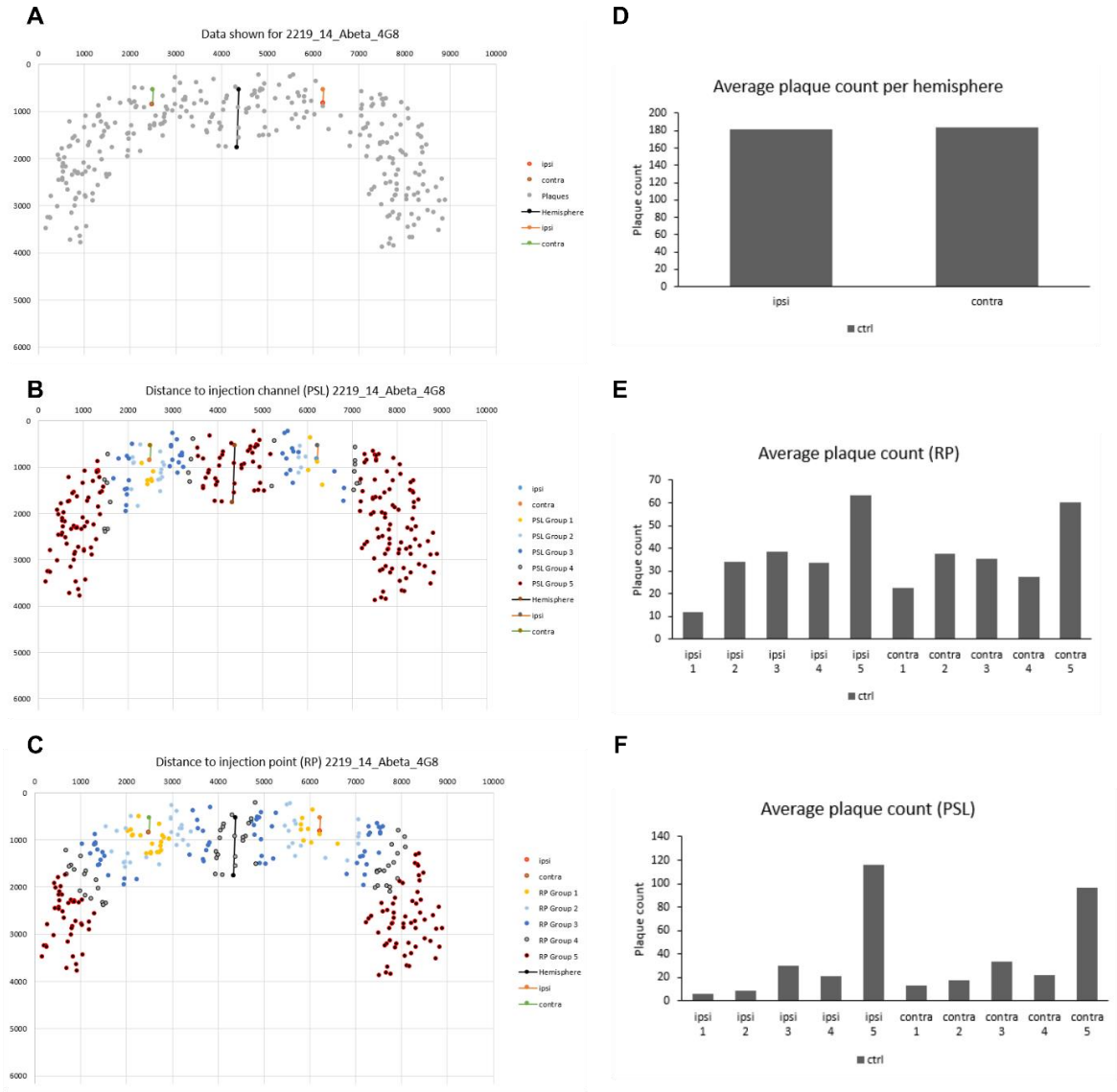

Fig. 24. **Graphical visualization of plaques in the cortex of a mouse in Excel. (A) The plaques accumulated across the cortex as detected by AxioVision. (B) The plaques accumulated in the cortex categorized by distance group RP. (C) The plaques accumulated in the cortex categorized by distance group PSL. (D, E and F) Distance histograms showing the number of plaques. Representative pictures have been obtained from our custom Excel tool.**

3.2.2.3. Quantification of detected plaques

Custom made Excel tool - "Pump_Animal-Analysis_Tool_Template.xltm" (see - A New Tool for the Analysis of the Effect of Intracerebrally Injected Anti-Amyloid-β Compounds - IOS Press -Supplementary Material 3) assess plaques based on their location alone or in combination of location and size categories (small, medium, large). In the worksheet "Analyze Data", the user finds several automatically generated charts that display group means of these quantifications. For biological relevance, group means are calculated by first calculating values per slide (worksheet "Slides"), subsequently averaging all slides of one block (i.e. animal, worksheet "Block Calculations"), and calculating the mean counts of all animals in the respective group (worksheet "Group calculations"). By default, all groups are selected, but it can be deselected to display fewer groups in the charts. To exclude individual slides from subsequent calculations, users can remove the group label of the respective slide in the worksheet "Slides". Obtained charts include the number of plaques (Fig. 24D), and distance histograms based on the pre-defined distance categories for RP (Fig. 24E) and PSL (Fig. 24F).

3.2.2.4. Sample data set

To demonstrate the functionality of the Excel tool- "Pump_Animal-Analysis_Tool_Template.xltm", a sample data set is included. Raw data are provided (see - A New Tool for the Analysis of the Effect of Intracerebrally Injected Anti-Amyloid-β Compounds - IOS Press - Supplementary Material 4) and specific graphs (**Supplementary Material 2**). The sample data was obtained from 16 immunohistochemically stained brain sections from eight animals that received intracerebral injections of PBS using mini-osmotic pumps. We present the quantitative measures: number of plaques, cortex area covered by plaques and size of plaques, obtained from 1-2 IHC stained brain sections per animal (slides, n = 14; animals, n = 8).

Furthermore, the sample data were statistically analysed, comparing the ipsi- and contralateral hemispheres (**Supplementary Material 2)**. There are four different quantitative measurements present: number of plaques, size of plaques, number of plaques by size groups, and cortex area covered by plaques. The Excel template categorizes plaques according to their size: 1) small, ≤ 400 μm^2; 2) medium, 401 – 700 μm^2; 3) large, > 700 μm^2, according to Bolmont *et al.* (Bolmont *et al.*, 2008). Moreover, the number of plaques for each size group in the pre-defined distance groups: RP and PSL were calculated in the Excel template. The in-

depth analysis of plaques according to size and location allows to detect whether a certain plaque category has decreased around the injection site induced by the administered compound.

4. DISCUSSION

Age-associated diseases, including sporadic AD, are an increasing global health care challenge. AD exhibits a many pathological and clinical features. These clinical features have been linked to detrimental changes in the brain - neocortex, e.g., a large number of neuritic plaques and NFTs, consisting of Aβ peptide and hyperphosphorylated τP. Listed pathological hallmarks are thought to disrupt normal synaptic functions and triggering downstream toxic pathways such as inflammation, as well as tau hyperphosphorylation and the formation of NFTs at specific brain regions, leading to eventual neurodegeneration (Koutsodendris *et al.*, 2021; Blanchard, Victor and Tsai, 2022; Ju and Tam, 2022; Mahaman *et al.*, 2022; "2022 Alzheimer's disease facts and figures," 2022). Therefore, interest in the therapeutic properties of molecules that target multiple different pathogenic mechanisms has been well-justified (Maramai *et al.*, 2020; Nguyen *et al.*, 2021; Nowak, Slupski and Rutkowska, 2021; Austad *et al.*, 2022). However, to evaluate potential new treatments, in preclinical research, some diagnostical approaches (visual evaluation, semi-quantitation and morphology) can be subjective and may lead to inaccuracies in the interpretation of the obtained results Moreover, to characterize pathological changes the obtained data from images must be quantitative to allow highly accurate statistical analysis (Falk *et al.*, 2019; Bascuñana, Brackhan and Pahnke, 2021; Möhle *et al.*, 2021). The pathological assessment may also depends on the selected drug administration route *in vivo* models, especially if it harmfully affects the brain tissue that is needed to perform a quantitative histological analysis. Thus, not only an evaluation of possible treatment but also optimized methods to perform drug administration for long-term intracerebral infusion experiments and Aβ pathological assessment in relation to injection channels are described below.

4.1. Auranofin, as a potential anti-inflammatory agent influences Aβ pathology AD preclinical model (Paper I)

Neuroinflammation contributes to the pathogenesis of a wide range of neurodegenerative disorders, particularly during their early stages before irreversible changes, such us plaque formation, have occurred (Cornell *et al.*, 2022; Ju and Tam, 2022). Earlier studies indicate that auranofin possesses both anti-neuroinflammatory and neuroprotective activity (Madeira, Schindler and Klegeris, 2015). Sulphur-containing gold compound – Auranofin, has been used to treat inflammation associated with rheumatoid arthritis. It is well known that auranofin

inhibits particular inflammatory pathways including NF-kB activation and TNF-α production and secretion (Rothan *et al.*, 2020; Abdalbari and Telleria, 2021). Extensive clinical used of auranofin has shown that this drug has a safe pharmacological profile in humans. Therefore, auranofin could potentially slow the progression of neurological disorders including AD. Besides, by repurposing an effective anti-inflammatory drug, the process of development of novel therapeutics and put into clinical trials could be significantly reduced. There are no published data regarding whether the administration of auranofin affects Aβ deposition or cognition in transgenic mouse models of AD. To study this molecule, was used novel $APP^{NL-G-F/NL-G-F}$ AD mice that carried three mutations (Swedish (NL), Beyreuther/Iberian (F), and Arctic (G)), known as mutations in familial AD, which lead to Aβ deposition, plaque formation as well as cognitive deficits (Saito *et al.*, 2014). In our study we evaluate the effects of subchronic (30 days) administration of auranofin at low doses (1 mg/kg and 5 mg/kg) on behaviour and biochemical parameters (Aβ deposition, GAD67, Homer-1, GFAP and Iba-1) in Cg cortex and hippocampal area- CA1 regions in 14-month-old male $^{APPNL-G-F/NL-G-F}$ AD mice.

We hypothesize that auranofin might decrease the abundance of non-cored and cored amyloid plaques because it directly targets fibrillar Aβ aggregates and promotes their dissociation and degradation. This activity could also be responsible for the compound's effect on immune hyperactivity, caused by Aβ plaque-associated microglia.

Extracellular and, in some cases, intracellular accumulations of aggregated Aβ deposits are detected by immunochemistry. In addition, histological approaches with several amyloid dyes, such as, CR, have the strength of precise and larger regional quantification of aggregated Aβ. In additional, CR staining can be complementary method to characterize the dense-cored plaques, that forms as central mass surrounded by an outer sphere of Aβ plaques (Sarkar *et al.*, 2020; Setti *et al.*, 2021). To detect and present differences between cored and non-cored Aβ plaque load in the brain, two stains, W0-2 antibody and CR dye, were used. We assessed AD pathology by measuring the Aβ plaque pathology in the Cg cortex and hippocampal area - CA1. The involvement of these selected brain regions in different cognitive and motor functions is well documented (Preston and Eichenbaum, 2013; Guo and Yang, 2020).

The obtained data demonstrated that the subchronic for 30 days ip administration of auranofin at doses 1 mg/kg and 5 mg/kg, significantly reduced the density of Aβ plaques in the CA1 hippocampal region but not in the Cg cortex of 14-month-old $APP^{NL-G-F/NL-G-F}$ mice, upon the staining with W0-2 antibody. Whereas, after conducting the CR staining, multiple comparison showed significant decrease in the total number of Aβ plaques also in the Cg cortex at dose 5 mg/kg (higher dose) of auranofin, but no change was detected in the CA1 region. Our

studies indicate that the anti-Aβ compound auranofin might has potential effects on the disease process in $APP^{NL\text{-}G\text{-}F/NL\text{-}G\text{-}F}$ mice and in the future, it could be beneficial to measure the amount of different oligomeric forms of Aβ.

Some studies have described that $APP^{NL\text{-}G\text{-}F/NL\text{-}G\text{-}F}$ mice model (at the age 3 – 10 months) show a decline in motivation in tandem with cored Aβ plaque aggregation in the subcortical brain area including the striatum (CPu) (Hamaguchi *et al.*, 2019; Mehla *et al.*, 2019). Moreover, recently it is noted that this impairment in relation with cored Aβ plaques, may be associated with Aβ43 generation, which as an isoform is typically found within the cores of amyloid plaques and in the brains of AD patients (Jäkel *et al.*, 2019; Ruiz-Riquelme *et al.*, 2021). Some studies suggest that an increase in cored Aβ plaques in the hippocampus produces significant neurotoxicity, cause synaptic and neuronal loss and are associated with a stronger decline in cognitive performance (Hamaguchi *et al.*, 2019; Boon, 2020; Boon *et al.*, 2020). In fact, another study has showed that anti-inflammatory compound - Triflusal significantly reduced cored Aβ plaque load and decreased risk of cognitive impairment in Tg AD mice model (Coma *et al.*, 2010). Therefore, it could be beneficial to measure the amount of different oligomeric forms of Aβ testing therapeutical approach with the ability to reduce e.g. cored Aβ plaques, might rescue the impaired motivation and be a breakthrough treatment.

$APP^{NL\text{-}G\text{-}F/NL\text{-}G\text{-}F}$ mice model develops age-dependent microgliosis and astrocytosis around the Aβ plaques in the cortex and hippocampus starting from the age of approximately 6-12 months. In addition, a significant change in Aβ load and astrocytosis were also found in LC, CPu, hindbrain and cerebellum layers (Mehla *et al.*, 2019). Moreover, it has been suggested that reactive gliosis might have a potential involvement of neuroinflammation by causing NE axonal degeneration in the LC, which was frequently detected with Aβ plaques surrounded by activated microglia, in $APP^{NL\text{-}G\text{-}F/NL\text{-}G\text{-}F}$ mice model (Sakakibara *et al.*, 2019). Even newer studies indicate that low-grade peripheral inflammation results in a higher Aβ accumulation, affects Aβ phagocytosis by microglial cells and induces neuronal dysfunction over time in $APP^{NL\text{-}G\text{-}F/NL\text{-}G\text{-}F}$ mice at the age of 6 months. It has been also revealed with morphometric analysis that there is an increase in small plaques (<10 μm^2) in the cortex and different size of plaques (<10 μm^2 - 20 μm^2) in the hippocampus. Next, it was found that low-grade peripheral inflammation affects microglial activation, migration and motility and reduces microglia Aβ phagocytosis in the cortex and hippocampus (Xie *et al.*, 2021).

Even though $APP^{NL\text{-}G\text{-}F/NL\text{-}G\text{-}F}$ mice's can be conveniently used to analyse the downstream events such as neuroinflammation and spatial memory impairment, however the findings of recently performed study revealed that this particular mice strain might be not the best choose

for preclinical studies to investigate Aβ metabolism, clearance and aggregation due to expressed Arctic (G) mutation. The reason is based on the fact that Arctic mutation might discrete affinity for anti-Aβ antibodies and interfere with direct or indirect interactions between Aβ deposition and APOE genotype, but, so far, no experimental reports have been published. Therefore, the generation of mice model that aggregates wild-type human Aβ without Arctic mutation and targeting mechanisms upstream of Aβ deposition could be more appropriate to investigate AD pathology in preclinical testing (Saito *et al.*, 2014; K. Sato *et al.*, 2021).

The present data demonstrated that auranofin can reduce Aβ load in the hippocampus and decrease the plaque number in the cortex, however showed no significant improvement for cognition and memory. Auranofin with doses 1mg/kg and 5 mg/kg, showed no significant change in the object location task, open field and eight-arm radial water maze tests in male $APP^{NL\text{-}G\text{-}F/NL\text{-}G\text{-}F}$ mice model. Although, the auranofin 1 mg/kg and 5 mg/kg treated mice in the eight-arm radial water maze test showed no significant improvement, during the five days of training, it was observed that 1 mg/kg group on day 3 and 4 shortened platform latency. This phenomenon may be associated with age-dependent impairment of learning and memory functions in $APP^{NL\text{-}G\text{-}F/NL\text{-}G\text{-}F}$ mice model.

It has been determined that at the age 6 – 12 months $APP^{NL\text{-}G\text{-}F/NL\text{-}G\text{-}F}$ mice demonstrated severe impairment in the learning ability, but no significance in the latency to reach the platform in the Morris water maze test (Mehla *et al.*, 2019). Similar results in the behavioural changes were determined at 6 – 14 months of age in the $APP^{NL\text{-}G\text{-}F/NL\text{-}G\text{-}F}$ mice, performing the Y-maze test, novel object location task and utilizing the IntelliCage system. In the novel object location task mice at the age of 9 – 12 months significantly spent less time exploring the novel objects as compared to control mice, indicating a progressive memory impairment. Meanwhile, the novelty-induced behaviour such as horizontal activity, total distance travelled and time moved did not change markedly in $APP^{NL\text{-}G\text{-}F/NL\text{-}G\text{-}F}$ mice when they were 3 – 12 months old (Masuda *et al.*, 2016; Mehla *et al.*, 2019). In contrast, some other published data stated that impairment change was not observed in the operant training and testing sessions (6 month-old) and time-dependent effect on behaviour (4 – 9 month-old) was not affected when Aβ production increased in $APP^{NL\text{-}G\text{-}F/NL\text{-}G\text{-}F}$ mice (Hamaguchi *et al.*, 2017). We assume that these discrepancies between obtained data from behavioural outcome might depend on several factors, such as, the age of the animals and due to pre-selected and performed behavioural. Suppose to assess the efficacy of auranofin by detecting cognitive improvement, other behavioural tests should be also considered, such us, sociability, fear conditioning and novelty-associated general locomotor activity. However, there is a possibility that effect of

subchronically administered auranofin and improvement in behavioural responses could be determine in much younger Tg AD mouse model, in prodromal stages, where dementia might be still curable.

Numerous epidemiologic and prospective studies published between 1995 and 2016 have described nonsteroidal anti-inflammatory drugs (NSAIDs) (e.g., ibuprofen, indomethacin) as putative protective agents whose use diminishes the development and progression of neurodegenerative disorders (Miguel-Alvarez *et al.*, 2015; Calsolaro and Edison, 2016). Even newer studies indicate that anti-inflammatory drugs such us, flufenamic acid effectively inhibit activation of the microglial inflammasome and ginsenoside compound K exhibit anti-inflammatory effect by reducing amyloid-induced microglia inflammation (Jung *et al.*,2022; Jiao and Jia, 2022).

In turn, reviewing the obtained histological results, auranofin administered for 30 days had no statistically significant impact on the levels of GFAP, Iba-1 or synaptic plasticity markers - GAD67 and Homer-1 expression in our selected $APP^{NL\text{-}G\text{-}F/NL\text{-}G\text{-}F}$ AD mouse model. As this particular Tg AD mice model expresses the low-grade peripheral inflammation, now we suggest that testing of several neuroinflammatory markers such as expression or levels of proinflammatory cytokines and CD68 markers might be beneficial to detect possible anti-inflammatory effects of auranofin. The strong correlation between oxidative stress and inflammation in Aβ pathology is now well-documented, so an assessment of ROS levels and whether they could be significantly reduced with auranofin should be evaluated (G. *et al.*, 2021). Other markers of Aβ pathology associated with inflammation in the AD, such as the extracellular matrix glycoprotein - Tenascin-C, may also be used in the future. The deficiency of the Tenascin-C ameliorates and has been linked to inflammatory processes in the AD-related pathology. Published data also reveals that Tenascin-C is associated with cored Aβ plaques in AD, as it deposits surrounded selectively cored neuritic Aβ plaques, by suggesting as a potential biomarker in neuropathological evaluation of AD (G. *et al.*, 2011; Mi *et al.*, 2016). Keeping in mind all the above factors mentioned, the further experiments should be required to add additional data and possible demonstrate the anti-inflammatory effect of auranofin on Aβ pathology in a Tg $APP^{NL\text{-}G\text{-}F/NL\text{-}G\text{-}F}$ mouse or another Tg AD mouse model.

4.2. Development of new application technique and analysis approach for long-term intracerebral brain infusion experiments (Paper II and III)

The development of new drugs targeted into the brain are important strategies for studying mechanisms underlying brain diseases, such us, AD. However, tested drug delivery to the brain is challenging due to the selective permeability of BBB to the certain compounds. There are several routes of administration of tested compounds depending on specific goals of the preclinical studies (Pardridge, 2020; Whelan, Hargaden and Knox, 2021). In this context, mini-osmotic pumps represent a suitable delivery system for studying long-term treatments into the brain and enhance transport across the BBB by direct intracerebroventricular administration. The osmotic pump system consists of guide cannula to provide precise drug delivery in the brain (Weil *et al.*, 2017; Rechberger *et al.*, 2020). However, one of the disadvantages using this method is as consequence of the inappropriate approach of the cannula fixation, which causes detachment from the skull before the end of the study or damage to brain tissue. Moreover, it is critically important for preclinical research to have reliable and accurate technique to examine indirectly the distribution of the test substances in the brain after intracerebral infusion. Therefore, we have developed two novel and experimentally validated methods. With first, an optimized fixational approach to minimized possible damage from the inserted brain cannula was created. With the second method advanced methodological quantification tool to examine local distribution of Aβ (identification, quantification, visualization, and characterization) after intracerebral infusion of experimental compounds was generated.

4.2.1. A newly designed fixation adapter improves the long-term brain infusion experiments (Paper II)

During the long-term continuous brain infusion experiments the brain cannula is encased in a polycarbonate platform that encompasses a removable attachment point for the stereotactic device, serves as platform for fixation to the skull. Currently, there are two methods of choice to fix the cannula onto the skull by using superglue or cement. Previous studies indicated that fixing the brain cannula with small anchoring screws combined with dental cements “white” (zinc-polycarboxylate) and “pink” (methyl-methacrylate), have been associated with an increased incidence of surgical problems, such us, skin necrosis, respiratory system irritation, headcap loss and infections (Poole *et al.*, 2019; Nicholson, Sidhu and Czarnecka, 2020). There are no official guidelines for dental cement selection for cannulation. In fact, to prevent

bacterial colonization multiple new active ingredients for dental cement have been previously added to dental cements, such as, hexametaphosphate microparticles, calcium phosphate, and silver ions. These agents showed improvement in the antimicrobial effect, amount of fluoride delivered, and rate of demineralization, however, it has caused a decrease in the mechanical properties of the cements. Also, dental cements modified with magnesium oxide nanoparticles showed significant antimicrobial properties (Naguib, Nassar and Hamed, 2022). Applying dental cements during the surgery could be time-consuming process. To apply this method for small laboratory animals, e.g., mice and rats, it requires a large volume of product, which complicates the surgical process. The powdered dental cement can be mixed with its acrylic solvent and applied. Alternatively, the powder can be placed first and the solvent carefully added to it, taking care to limit both to the implantation site. Meanwhile, new active ingredients have been tested and investigated for appealing purposes, many researchers in place of dental cement use cyanoacrylate adhesive. The use of cyanoacrylate gel has many advantages as compared to dental cements. As cyanoacrylate adhesive is a single component product, there is no need to prepare it and provides greater stability, may obviate the need for anchor screws and therefore markedly reduce surgical time for the intracerebral implantation. Above all, even using cyanoacrylate gel, we have found that the fixation of the cannula is not fully satisfying, because the relatively small and round-shaped mice skull does not properly fit with the big and flat platform of the cannula (**Supplementary Figure 1**).

Hence, we invented a new nontoxic soft and elastic silicone adapter which has the form of the mouse skull and is tear resistant despite its thinness. Our improved method provides a perfect fixation of the cannula while being seamlessly attached to the skull surface at the same time, during long-term intracerebral brain infusion experiments by using mini-osmotic pumps. Moreover, it can be produced to fit any skull of any age. The spacer also serves as a spacer to adapt the depth of the infusion point, which can easily be changed to fit different infusion depths by changing the height of the casting chamber with spacers thinner. Additionally, we founded that choosing the proper superglue is an important aspect. Based on our experiments superglues which are more viscous than fluid provides better fixation. We also found that removing the brain cannula even with the slightest pressure a small piece of brain tissue was always removed from the surface of the cortex.

To conclude, we assume that this new improved method will make brain infusion experiments more secure and provided step-by-step protocol for the production and application of silicone spacer, as well as have a positive effect on animal welfare as well.

4.2.2. Development of new analytical toolbox facilitates the analysis of long-term intracerebral infusion experiments (Paper III)

Up to date, there is no method available how to examine the spatial distribution of Aβ plaques and thus, also the distribution of the experiment test substances after local into the brain infusion.

Intracerebroventricular administration of agents using mini-osmotic pumps (e.g. ALZET) is a well-established method (Sheeler *et al.*, 2021). Currently, the available data indicate on different neuroanatomical sites of interest that are close to the cannula insertion point or channel (e.g. various hippocampal regions) as regions of interest (cortex and hippocampus) (Chen *et al.*, 2018). Most of the studies focuses on assessing the hippocampus or even smaller regions of interest by applying intracerebral injections. Therefore, quantification of Aβ plaques and evaluation of a potential treatment are less complex, if the target tissue has not been traumatized. There are several other quantitative methods require homogenized brain tissue or the separation of both hemispheres of the brain to perform immunohistochemistry or biochemical studies. These methods can provide a complete visual comparison of the spatial distribution of Aβ between the control and the injected hemisphere (Wen *et al.*, 2018; Zhou and Li, 2019). However, there is very limited data available regarding how the quantification of Aβ plaques should be performed in specific brain areas based on their location relative to the point of injection or the injection channel. Therefore, we developed a suitable analytical tool, which performs histopathological quantification e.g. in the entire cortex area and compares the results of both hemispheres after continuous long-term intracerebral injection using mini-osmotic pumps. This tool reports of additional data based on the ROI, number and sizes of the selected Aβ plaques. In addition, we developed Excel worksheets for quality control and graphical visualization of data obtained in AxioVision.

It is important to find out whether a potential treatment could reduce the number of specific plaque sizes based on the ROI. Therefore, the core functionality of our tool is the classification of Aβ plaques in pre-defined distance groups by RP and PSL approaches and different plaque sizes (small, medium, and large). That allows us to more specifically and accurately determine the distribution and efficacy of the newly tested substances. Furthermore, several other methods exist that have been used to assess Aβ pathology, but these processing and analysing tools (e.g. AxionVisio, ImageJ) do not provide strategies for specific situations with lost tissue and injection trajectories.

The tool presented here can be applied to many types of injections (e.g., stereotactic microinjections, intracortical injections, and ventricular injections). Our method can be used to determine various other immunohistochemical markers, such as, NFTs of highly phosphorylated forms of the τP, or markers related to neuroinflammation (GFAP, IBA-1, IL-6, TNF-α) (Angiulli *et al.*, 2021). It might also be useful to analyse different *in vivo* approaches with side differences, for example, traumatic brain injuries, ischemic stroke and models could be tested after induction of a head injury, comparing the size of the traumatized tissue region and the non-traumatized brain hemisphere. Moreover, this tool could be applied to explore whenever other brain cannulation processes (e.g., Bi-lateral Brain Cannulation) could cause significant loss of brain tissues and, therefore, interacts with histological analysis.

Despite the tool's accuracy and wide application, we would also like to point out some limitations of our method. One limitation of the analytical tool is that the user has to manually segregate double plaques by drawing a line between the single plaques. Even more, the user needs to carefully check the automatic recognition and deselect/select the affected objects and decide whether the recognized object is a real plaque or not. As both mentioned aspects are involved in the analysis of the Aβ plaques, there is a possibility that the user engagement to identify errors and to separate plaques may lead to additional errors in the results. Using an automatic image analysis could increase objectivity and reduce time, e.g., machine learning-supported analyses (DeePathology™ STUDIO) (de Matos *et al.*, 2021; van der Laak, Litjens and Ciompi, 2021). Second, model performance is objective, i.e. independent of who uses it once the training phase has concluded. However, the model can become inherently biased if trained with inappropriate data. Equally important addition would be to recognize the plaque sizes (based on size groups small, medium, large) in distance groups and provides a graphical visualization of the Aβ plaques. From a technical standpoint, our method could be optimized for better comparison between experimental groups by calculating automatically the RP on the contralateral side (mirrored along the hemisphere border). As well as, different improvement would be to make the number of distance categories customizable.

In summary, our study has pointed that this analytic tool, gives improved performance of evaluation process for potential treatments after continuous long-term intracerebral injection *in vivo* studies. However, further studies would be necessary to generate representative results obtained with our new method that would increase its current usage and potential impact.

5. CONCLUSIONS

1. In transgenic AD mouse model, for the first time we demonstrated that the anti-inflammatory drug auranofin at low doses (1 mg/kg and 5 mg/kg) significantly reduces Aβ pathology (load and number of core plaques) but has no effect on spatial memory processes and on the expression of the studied inflammatory and synaptic plasticity proteins.
2. The improved method using an easily producible spacer facilitates the crucial step of long-term brain infusion experiments with intracerebral catheters in a highly secure and reproducible manner.
3. The developed analytic toolbox for histopathological assessment, generates reliable data for Aβ deposition characterization in relation to the distribution of experimental compounds in relation to intracerebral injection channels and provides an improved histopathological evaluation process for potential treatments after continuous long-term intracerebral injection.
4. The discovered effects of anti-inflammatory drug and the new developed methods enhance preclinical research in the AD field, and further studies would increase their current usage and potential impact.

6. ACKNOWLEDGEMENTS

I would like to express my sincere gratitude to the following people, who in different ways have contributed in my doctoral work:

Professor Dr. **Baiba Jansone** my supervisor, I wish to thank you for your professional way of guiding me trought this thesis, support with excellent scientific knowledge, focused hard work, ideas and never-ending enthusiasms.

Professor Dr. **Jens Pahnke** my co-supervisor from the Translational Neurodegeneration and Neuropathology Laboratory at the University of Oslo, is acknowledged for his support throughout these years, for sharing your knowledge, for excellent guidance and training in neuroscience. I am thankful to all colleagues at the University of Oslo: **Ádám Sike, Thomas Brüning, Luisa Möhle, Mirjam Brackhan, Iván Eiriz, Markus Krohn, Kristin Paarmann, Pablo Bascuñana**, for teaching me the basic of neurosurgery, their help with scientific article preparation and all support since my first steps in the Translational Neurodegeneration and Neuropathology Laboratory.

Associated professor Dr. **Inga Kadish** and Dr. **Thomas van Groen** from the Department of Cell, Developmental and Integrative Biology at the University of Alabama at Birmingham (USA), I am grateful for their help during experimental work, scientific article preparation and great support.

My close colleagues from the Faculty of Medicine, University of Latvia Department of Pharmacology for creating great atmosphere and interesting scientific and non-scientific discussions at work and your friendship.

This work has been supported by the Latvian Council of Science Fund (lzp-2018/1-0275), National Institutes of Health (P30 NS 47466) and funding organizations under the aegis of JPND –PETABC (VIAA #ES RTD/2020/26 –Latvia).

My family and friends, for encouraging me and being with me wherever I am going, always believing in me and your love.

7.REFERENCES

1. “2022 Alzheimer’s disease facts and figures” (2022) Alzheimer’s and Dementia, 18(4). doi:10.1002/alz.12638.

2. Abdalbari, F.H. and Telleria, C.M. (2021) “The gold complex auranofin: new perspectives for cancer therapy,” Discover Oncology. doi:10.1007/s12672-021-00439-0.

3. Abg Abd Wahab, D.Y. et al. (2019) “Review on Cross Talk between Neurotransmitters and Neuroinflammation in Striatum and Cerebellum in the Mediation of Motor Behaviour,” BioMed Research International. doi:10.1155/2019/1767203.

4. Agrawal, I. and Jha, S. (2020) “Mitochondrial Dysfunction and Alzheimer’s Disease: Role of Microglia,” Frontiers in Aging Neuroscience. Frontiers Media S.A. doi:10.3389/fnagi.2020.00252.

5. Alcalà-Vida, R. et al. (2021) “Epigenetic mechanisms underlying enhancer modulation of neuronal identity, neuronal activity and neurodegeneration,” Neurobiology of Disease. doi:10.1016/j.nbd.2020.105155.

6. Ali, M.M. et al. (2019) “Recommendations for Anti-inflammatory Treatments in Alzheimer’s Disease: A Comprehensive Review of the Literature,” Cureus [Preprint]. doi:10.7759/cureus.4620.

7. Alipour, M. et al. (2016) “Effect of sub-chronic intraperitoneal administration of aminoguanidine on the memory and hippocampal apoptosis- -related genes in diabetic rats,” Bratislava Medical Journal, 117(8). doi:10.4149/BLL_2016_092.

8. Alzheimer’s Association and Association, A. (2020) Alzheimer’s Facts and Figures Report. https://www.alz.org/alzheimers-dementia/facts-figures?lang=en-US, Alzheimer’s & Dementia.

9. Angiulli, F. et al. (2021) “Blood-based biomarkers of neuroinflammation in alzheimer’s disease: A central role for periphery?,” Diagnostics. doi:10.3390/diagnostics11091525.

10. Apátiga-Pérez, R. et al. (2021) “Neurovascular dysfunction and vascular amyloid accumulation as early events in Alzheimer’s disease,” Metabolic Brain Disease [Preprint]. doi:10.1007/s11011-021-00814-4.

11. Austad, S.N. et al. (2022) “Targeting whole body metabolism and mitochondrial bioenergetics in the drug development for Alzheimer’s disease,” Acta Pharmaceutica Sinica B. doi:10.1016/j.apsb.2021.06.014.

12. Babaei, P. (2021) “NMDA and AMPA receptors dysregulation in Alzheimer’s disease,” European Journal of Pharmacology. doi:10.1016/j.ejphar.2021.174310.

13. Banks, W.A. et al. (2021) “Healthy aging and the blood–brain barrier,” Nature Aging, 1(3). doi:10.1038/s43587-021-00043-5.

14. Bascuñana, P., Brackhan, M. and Pahnke, J. (2021) “Machine Learning-Supported Analyses Improve Quantitative Histological Assessments of Amyloid-β Deposits and Activated Microglia,” Journal of Alzheimer’s disease : JAD, 79(2). doi:10.3233/JAD-201120.

15. Baumel, B.S. et al. (2021) “Potential Neuroregenerative and Neuroprotective Effects of Uridine/Choline-Enriched Multinutrient Dietary Intervention for Mild Cognitive Impairment: A Narrative Review,” Neurology and Therapy. doi:10.1007/s40120-020-00227-y.

16. Berson, A. et al. (2018) “Epigenetic Regulation in Neurodegenerative Diseases,” Trends in Neurosciences. doi:10.1016/j.tins.2018.05.005.

17. Binert-Kusztal, Z., Starek, M. and Dabrowska, M. (2021) “Neurodegenerative diseases; pharmacotherapeutic aspect of Alzheimer’s diseases,” Farmacja Polska, 77(7). doi:10.32383/farmpol/142108.

18. Blanchard, J.W., Victor, M.B. and Tsai, L.H. (2022) “Dissecting the complexities of Alzheimer disease with in vitro models of the human brain,” Nature Reviews Neurology. doi:10.1038/s41582-021-00578-6.

19. van Bokhoven, P. et al. (2021) “The Alzheimer’s disease drug development landscape,” Alzheimer’s Research and Therapy, 13(1). doi:10.1186/s13195-021-00927-z.

20. Bolmont, T. et al. (2008) “Dynamics of the microglial/amyloid interaction indicate a role in plaque maintenance,” Journal of Neuroscience, 28(16). doi:10.1523/JNEUROSCI.4814-07.2008.

21. Boon, B.D.C. (2020) “A novel type of amyloid-beta plaques discovered in early-onset AD patients,” Alzheimer’s & Dementia, 16(S2). doi:10.1002/alz.044558.

22. Boon, B.D.C. et al. (2020) “The coarse-grained plaque: a divergent Aβ plaque-type in early-onset Alzheimer’s disease,” Acta Neuropathologica, 140(6). doi:10.1007/s00401-020-02198-8.

23. Bortolami, M. et al. (2021) “Acetylcholinesterase inhibitors for the treatment of Alzheimer’s disease–a patent review (2016–present),” Expert Opinion on Therapeutic Patents. doi:10.1080/13543776.2021.1874344.

24. Busche, M.A. and Hyman, B.T. (2020) “Synergy between amyloid-β and tau in Alzheimer’s disease,” Nature Neuroscience. doi:10.1038/s41593-020-0687-6.

25. Cascella, R. and Cecchi, C. (2021) “Calcium dyshomeostasis in Alzheimer’s disease pathogenesis,” International Journal of Molecular Sciences. doi:10.3390/ijms22094914.

26. Chandra, S., Jana, M. and Pahan, K. (2018) “Aspirin induces lysosomal biogenesis and attenuates amyloid plaque pathology in a mouse model of Alzheimer’s disease via PPARα,” Journal of Neuroscience, 38(30). doi:10.1523/JNEUROSCI.0054-18.2018.

27. Chauhan, P.S. and Yadav, D. (2021) “Dietary Nutrients and Prevention of Alzheimer’s disease,” CNS & Neurological Disorders - Drug Targets, 20. doi:10.2174/1871527320666210405141123.

28. Chen, Y. et al. (2018) “Intranasal Insulin Ameliorates Cerebral Hypometabolism, Neuronal Loss, and Astrogliosis in Streptozotocin-Induced Alzheimer’s Rat Model,” Neurotoxicity Research, 33(4). doi:10.1007/s12640-017-9809-7.

29. Christensen, A. and Pike, C.J. (2020) “Staining and Quantification of β-Amyloid Pathology in Transgenic Mouse Models of Alzheimer’s Disease,” in Methods in Molecular Biology. doi:10.1007/978-1-0716-0592-9_19.

30. Clifton, N.E. et al. (2019) “Regulation and Function of Activity-Dependent Homer in Synaptic Plasticity,” Molecular Neuropsychiatry, 5(3). doi:10.1159/000500267.

31. Coma, M. et al. (2010) “Triflusal reduces dense-core plaque load, associated axonal alterations and inflammatory changes, and rescues cognition in a transgenic mouse model of Alzheimer’s disease,” Neurobiology of Disease, 38(3). doi:10.1016/j.nbd.2010.01.019.

32. Cornell, J. et al. (2022) “Microglia regulation of synaptic plasticity and learning and memory,” Neural Regeneration Research. doi:10.4103/1673-5374.322423.

33. Calsolaro,V. and Edison, P. (2016) “Neuroinflammation in Alzheimer's disease: current evidence and future directions,” Alzheimers Dement., 12. doi:10.1016/j.jalz.2016.02.010.

34. Cuervo-Zanatta, D. et al. (2021) “Modulation of the microbiota-gut-brain axis by bioactive food, prebiotics, and probiotics decelerates the course of Alzheimer’s disease,” in Studies in Natural Products Chemistry. doi:10.1016/B978-0-12-819489-8.00019-3.

35. Cummings, J. et al. (2021) “Aducanumab: Appropriate Use Recommendations,” Journal of Prevention of Alzheimer’s Disease, 8(4). doi:10.14283/jpad.2021.41.

36. Cummings, J. and Salloway, S. (2021) “Aducanumab: Appropriate use recommendations,” Alzheimer’s & Dementia [Preprint]. doi:10.1002/alz.12444.

37. Darling, A.L. and Shorter, J. (2020) “Atomic Structures of Amyloid-β Oligomers Illuminate a Neurotoxic Mechanism,” Trends in Neurosciences. doi:10.1016/j.tins.2020.07.006.

38. Dejakaisaya, H., Kwan, P. and Jones, N.C. (2021) “Astrocyte and glutamate involvement in the pathogenesis of epilepsy in Alzheimer’s disease,” Epilepsia. doi:10.1111/epi.16918.

39. Denninger, J.K., Smith, B.M. and Kirby, E.D. (2018) “Novel object recognition and object location behavioral testing in mice on a budget,” Journal of Visualized Experiments, 2018(141). doi:10.3791/58593.

40. Devkota, S., Williams, T.D. and Wolfe, M.S. (2021) “Familial Alzheimer s disease mutations in amyloid protein precursor alter proteolysis by γ-secretase to increase amyloid β-peptides of ≥45 residues,” Journal of Biological Chemistry, 296. doi:10.1016/j.jbc.2021.100281.

41. Diaz-Aparicio, I. et al. (2020) “Microglia actively remodel adult hippocampal neurogenesis through the phagocytosis secretome,” Journal of Neuroscience, 40(7). doi:10.1523/JNEUROSCI.0993-19.2019.

42. Ding, S. et al. (2020) “Overcoming blood–brain barrier transport: Advances in nanoparticle-based drug delivery strategies,” Materials Today. doi:10.1016/j.mattod.2020.02.001.

43. Domínguez-García, S. et al. (2020) “A novel PKC activating molecule promotes neuroblast differentiation and delivery of newborn neurons in brain injuries,” Cell Death and Disease, 11(4). doi:10.1038/s41419-020-2453-9.

44. Drummond, E. et al. (2020) “The amyloid plaque proteome in different subtypes of Alzheimer’s disease,” Alzheimer’s & Dementia, 16(S2). doi:10.1002/alz.044973.

45. Drummond, E. and Wisniewski, T. (2017) “Alzheimer’s disease: experimental models and reality,” Acta Neuropathologica. doi:10.1007/s00401-016-1662-x.

46. Du, H. et al. (2021) “A multifaceted role of progranulin in regulating amyloid-beta dynamics and responses,” Life Science Alliance, 4(7). doi:10.26508/lsa.202000874.

47. Dumitrascu, O.M. et al. (2020) “Sectoral segmentation of retinal amyloid imaging in subjects with cognitive decline,” Alzheimer’s and Dementia: Diagnosis, Assessment and Disease Monitoring, 12(1). doi:10.1002/dad2.12109.

48. van Erum, J., van Dam, D. and de Deyn, P.P. (2019) “Alzheimer’s disease: Neurotransmitters of the sleep-wake cycle,” Neuroscience and Biobehavioral Reviews. doi:10.1016/j.neubiorev.2019.07.019.

49. F., P. et al. (2019) “Pilot human study to define the impact of vascular and inflammatory risk factors in Alzheimer’s disease,” Journal of Neurochemistry, 150.

50. Falk, T. et al. (2019) “U-Net: deep learning for cell counting, detection, and morphometry,” Nature Methods, 16(1). doi:10.1038/s41592-018-0261-2.

51. Fan, C. et al. (2021) “Systematic analysis to identify transcriptome-wide dysregulation of Alzheimer’s disease in genes and isoforms,” Human Genetics, 140(4). doi:10.1007/s00439-020-02230-7.

52. Feng, L. et al. (2020) “Repurposing Auranofin and Evaluation of a New Gold(I) Compound for the Search of Treatment of Human and Cattle Parasitic Diseases: From Protozoa to Helminth Infections,” Molecules (Basel, Switzerland), 25(21). doi:10.3390/molecules25215075.

53. Finch, M.S., Bagit, A. and Marko, D.M. (2020) “Amyloid beta 42 oligomers induce neuronal and synaptic receptor dysfunctions,” Journal of Physiology, 598(17). doi:10.1113/JP280038.

54. Findley, C.A. et al. (2019) “Amyloid Beta-Related Alterations to Glutamate Signaling Dynamics During Alzheimer’s Disease Progression,” ASN Neuro. doi:10.1177/1759091419855541.

55. G., B. et al. (2011) “Reactive astroglia proliferation and neurosphere formation is limited in mouse models reflecting different aspects of alzheimer’s disease,” GLIA, 59.

56. G., S. et al. (2021) “OXIDATIVE STRESS IN ALZHEIMER’S DISEASE–EVALUATING THE AMYLOID BETA HYPOTHESIS,” International Journal of Current Pharmaceutical Research [Preprint]. doi:10.22159/ijcpr.2021v13i5.1906.

57. Gao, X. et al. (2021) “Quantitative imaging of amyloid beta peptide (Aβ) in Alzheimer’s brain tissue by laser ablation ICP-MS using gold nanoparticles as labels,” Analytica Chimica Acta, 1148. doi:10.1016/j.aca.2020.12.072.

58. Gąsiorowski, K. et al. (2021) “Current and Near-Future Treatment of Alzheimer’s Disease,” Current Neuropharmacology, 19. doi:10.2174/1570159x19666211202124239.

59. George, A.A. et al. (2021) “Implications of oligomeric amyloid-beta (oAβ42) signaling through α7β2-nicotinic acetylcholine receptors (nAChRs) on basal forebrain cholinergic neuronal intrinsic excitability and cognitive decline,” Journal of Neuroscience, 41(3). doi:10.1523/JNEUROSCI.0876-20.2020.

60. Gindorf, M. et al. (2021) “Meprin β: A novel regulator of blood–brain barrier integrity,” Journal of Cerebral Blood Flow and Metabolism, 41(1). doi:10.1177/0271678X20905206.

61. Govindpani, K. et al. (2020) “Impaired expression of gaba signaling components in the alzheimer’s disease middle temporal gyrus,” International Journal of Molecular Sciences, 21(22). doi:10.3390/ijms21228704.

62. Grangeon, L. et al. (2021) “Early-Onset Cerebral Amyloid Angiopathy and Alzheimer Disease Related to an APP Locus Triplication,” Neurology Genetics, 7(5). doi:10.1212/nxg.0000000000000609.

63. van Groen, T. et al. (2017) “The Aβ oligomer eliminating D-enantiomeric peptide RD2 improves cognition without changing plaque pathology,” Scientific Reports, 7(1). doi:10.1038/s41598-017-16565-1.

64. Gründer, G. and Cumming, P. (2021) “Serotonin and amyloid deposition: A link between depression and Alzheimer’s disease?,” Journal of Neurochemistry, 156(5). doi:10.1111/jnc.15269.

65. Guo, D. and Yang, J. (2020) “Interplay of the long axis of the hippocampus and ventromedial prefrontal cortex in schema-related memory retrieval,” Hippocampus, 30(3). doi:10.1002/hipo.23154.

66. Hahm, E.T. et al. (2018) “Cholinergic Homeostatic Synaptic Plasticity Drives the Progression of Aβ-Induced Changes in Neural Activity,” Cell Reports, 24(2). doi:10.1016/j.celrep.2018.06.029.

67. Hamaguchi, T. et al. (2017) “Yokukansankachimpihange increased body weight but not food-incentive motivation in wild-type mice,” Nagoya Journal of Medical Science, 79(3). doi:10.18999/nagjms.79.3.351.

68. Hamaguchi, T. et al. (2019) “AppNL-G-F/NL-G-F mice overall do not show impaired motivation, but cored amyloid plaques in the striatum are inversely correlated with motivation,” Neurochemistry International, 129. doi:10.1016/j.neuint.2019.104470.

69. Hampel, H. et al. (2019) “Revisiting the Cholinergic Hypothesis in Alzheimer’s Disease: Emerging Evidence from Translational and Clinical Research,” The journal of prevention of Alzheimer’s disease. doi:10.14283/jpad.2018.43.

70. Hashemi-Firouzi, N., Shahidi, S. and Soleimani Asl, S. (2021) “Chronic stimulation of the serotonergic 5-HT4 receptor modulates amyloid-beta-related impairments in synaptic plasticity and memory deficits in male rats,” Brain Research, 1773. doi:10.1016/j.brainres.2021.147701.

71. Hazen, J. et al. (2020) “The Association between Circulating Inflammatory Markers and the Progression of Alzheimer Disease in Norwegian Memory Clinic Patients with Mild Cognitive Impairment or Dementia,” Alzheimer Disease and Associated Disorders, 34(1). doi:10.1097/WAD.0000000000000342.

72. Hsiao, K. et al. (1996) “Correlative memory deficits, Aβ elevation, and amyloid plaques in transgenic mice,” Science, 274(5284). doi:10.1126/science.274.5284.99.

73. Hsien, L.C. et al. (2020) “Application of optogenetic amyloid-β distinguishes between metabolic and physical damage in neurodegeneration,” eLife, 9. doi:10.7554/eLife.52589.

74. Hui, L. et al. (2020) “Association between dopamine beta-hydroxylase polymorphism and attention function in suicide attempters with chronic schizophrenia,” Human Psychopharmacology, 35(6). doi:10.1002/hup.2755.

75. Huss, R. and Coupland, S.E. (2020) “Software-assisted decision support in digital histopathology,” Journal of Pathology. doi:10.1002/path.5388.

76. Hwangbo, H. et al. (2021) “Anti-inflammatory effect of auranofin on palmitic acid and lps-induced inflammatory response by modulating tlr4 and nox4-mediated nf-κb signaling pathway in raw264.7 macrophages,” International Journal of Molecular Sciences, 22(11). doi:10.3390/ijms22115920.

77. Jacinta, A.A., Ishola, I.O. and Adeyemi, O.O. (2019) “Cortico-Hippocampal Memory Enhancing Activity of Hesperetin on Scopolamine-Induced Amnesia in Mice: Role of Antioxidant Defense Systems, Cholinergic Neurotransmission and Expression of BDNF,” IBRO Reports, 7. doi:10.1016/j.ibror.2019.09.051.

78. Jain, K.K. (2020) “An Overview of Drug Delivery Systems,” in Methods in Molecular Biology. doi:10.1007/978-1-4939-9798-5_1.

79. Jäkel, L. et al. (2019) “Aβ43 in human Alzheimer’s disease: effects of active Aβ42 immunization,” Acta neuropathologica communications, 7(1). doi:10.1186/s40478-019-0791-6.

80. James, T. et al. (2021) “Locus coeruleus in memory formation and Alzheimer’s disease,” European Journal of Neuroscience. doi:10.1111/ejn.15045.

81. Jang, H.I. and Eom, Y. bin (2020) “Antibiofilm and antibacterial activities of repurposing auranofin against Bacteroides fragilis,” Archives of Microbiology, 202(3). doi:10.1007/s00203-019-01764-3.

82. Janoutová, J. et al. (2020) “Possible prevention of Alzheimer’s disease,” Ceska a Slovenska Neurologie a Neurochirurgie. doi:10.14735/amcsnn202028.

83. Jiang, J. et al. (2022) “Systemic LPS-induced microglial activation results in increased GABAergic tone: A mechanism of protection against neuroinflammation in the medial prefrontal cortex in mice,” Brain, Behavior, and Immunity, 99. doi:10.1016/j.bbi.2021.09.017.

84. Jiao, H. and Jia, J. (2022) “Ginsenoside compound K acts via LRP1 to alleviate Amyloid β42-induced neuroinflammation in microglia by suppressing NF-κB,” Biochem Biophys Res Commun. doi: 10.1016/j.bbrc.2021.12.071.

85. Ju, Y. and Tam, K. (2022) “Pathological mechanisms and therapeutic strategies for Alzheimer’s disease,” Neural Regeneration Research. doi:10.4103/1673-5374.320970.

86. Junakovic, A. and Telarovic, S. (2021) “The effects of art therapy on parkinson`s and alzheimer`s disease,” Medicina Fluminensis. doi:10.21860/medflum2021_261184.

87. Jung, E.S. et al. (2022) “Amyloid-β activates NLRP3 inflammasomes by affecting microglial immunometabolism through the Syk-AMPK pathway,” Aging Cell, e13623. doi: 10.1111/acel.13623.

88. Kalaria, R.N. and Sepulveda-Falla, D. (2021) “Cerebral Small Vessel Disease in Sporadic and Familial Alzheimer Disease,” American Journal of Pathology [Preprint]. Elsevier Inc. doi:10.1016/j.ajpath.2021.07.004.

89. Kazim, S.F. and Iqbal, K. (2016) “Neurotrophic αsmall-molecule mimetics mediated neuroregeneration and synaptic repair: Emerging therapeutic modality for Alzheimer’s disease,” Molecular Neurodegeneration. doi:10.1186/s13024-016-0119-y.

90. Kelly, L. et al. (2021) “Identification of intraneuronal amyloid beta oligomers in locus coeruleus neurons of Alzheimer’s patients and their potential impact on inhibitory neurotransmitter receptors and neuronal excitability,” Neuropathology and Applied Neurobiology, 47(4). doi:10.1111/nan.12674.

91. Kenkhuis, B. et al. (2021) “Co-expression patterns of microglia markers Iba1, TMEM119 and P2RY12 in Alzheimer’s disease Running title: Microglia markers in Alzheimer’s disease,” bioRxiv [Preprint].

92. Keraliya, R.A. et al. (2012) “Osmotic Drug Delivery System as a Part of Modified Release Dosage Form,” ISRN Pharmaceutics, 2012. doi:10.5402/2012/528079.

93. Khan, A.F. et al. (2020) “Whole brain generative model identifies neurotransmitter alterations underlying Alzheimer’s disease progression,” Alzheimer’s & Dementia, 16(S4). doi:10.1002/alz.041193.

94. Kleinberger, G. et al. (2017) “ The FTD -like syndrome causing TREM 2 T66M mutation impairs microglia function, brain perfusion, and glucose metabolism ,” The EMBO Journal, 36(13). doi:10.15252/embj.201796516.

95. Knopman, D.S. et al. (2021) “Alzheimer disease,” Nature Reviews Disease Primers, 7(1). doi:10.1038/s41572-021-00269-y.

96. Koola, M.M. (2020) “Galantamine-Memantine combination in the treatment of Alzheimer’s disease and beyond,” Psychiatry Research. doi:10.1016/j.psychres.2020.113409.

97. Koronyo-Hamaoui, M. et al. (2020) “Peripherally derived angiotensin converting enzyme-enhanced macrophages alleviate Alzheimer-related disease,” Brain, 143(1). doi:10.1093/brain/awz364.

98. Koutsodendris, N. et al. (2021) “Apolipoprotein E and Alzheimer’s Disease: Findings, Hypotheses, and Potential Mechanisms,” Annual Review of Pathology: Mechanisms of Disease. doi:10.1146/annurev-pathmechdis-030421-112756.

99. Kuhn, A.J. et al. (2020) “Alzheimer’s Disease ‘non-amyloidogenic’ p3 Peptide Revisited: A Case for Amyloid-α,” ACS Chemical Neuroscience, 11(11). doi:10.1021/acschemneuro.0c00160.

100. Kurokin, I. et al. (2021) “Targeted lipidomics of mitochondria in a cellular alzheimer’s disease model,” Biomedicines, 9(8). doi:10.3390/biomedicines9081062.

101. van der Laak, J., Litjens, G. and Ciompi, F. (2021) “Deep learning in histopathology: the path to the clinic,” Nature Medicine. doi:10.1038/s41591-021-01343-4.

102. Lautrup, S. et al. (2019) “Microglial mitophagy mitigates neuroinflammation in Alzheimer’s disease,” Neurochemistry International, 129. doi:10.1016/j.neuint.2019.104469.

103. Lee, H.N., Jeong, M.S. and Jang, S.B. (2021) “Molecular characteristics of amyloid precursor protein (App) and its effects in cancer,” International Journal of Molecular Sciences. MDPI AG. doi:10.3390/ijms22094999.

104. Leng, F. and Edison, P. (2021) “Neuroinflammation and microglial activation in Alzheimer disease: where do we go from here?,” Nature Reviews Neurology. doi:10.1038/s41582-020-00435-y.

105. Leyns, C.E.G. et al. (2019) “TREM2 function impedes tau seeding in neuritic plaques,” Nature Neuroscience, 22(8). doi:10.1038/s41593-019-0433-0.

106. Li, H., Knight, W. and Xu, J. (2022) “Striatal oxidative damages and neuroinflammation correlate with progression and survival of Lewy body and Alzheimer diseases,” Neural Regeneration Research, 17(4). doi:10.4103/1673-5374.322463.

107. Li, H.H. et al. (2021) “Serotonin 2 receptors, agomelatine, and behavioral and psychological symptoms of dementia in Alzheimer’s disease,” Behavioural Neurology. doi:10.1155/2021/5533827.

108. Lin, L., Zheng, L.J. and Zhang, L.J. (2018) “Neuroinflammation, Gut Microbiome, and Alzheimer’s Disease,” Molecular Neurobiology. doi:10.1007/s12035-018-0983-2.

109. Litke, R. et al. (2021) “Modifiable Risk Factors in Alzheimer Disease and Related Dementias: A Review,” Clinical Therapeutics. doi:10.1016/j.clinthera.2021.05.006.

110. Mackin, R.S. et al. (2021) “Late-Life Depression Is Associated With Reduced Cortical Amyloid Burden: Findings From the Alzheimer’s Disease Neuroimaging Initiative Depression Project,” Biological Psychiatry, 89(8). doi:10.1016/j.biopsych.2020.06.017.

111. Madeira, J.M. et al. (2014) “Gold drug auranofin could reduce neuroinflammation by inhibiting microglia cytotoxic secretions and primed respiratory burst,” Journal of Neuroimmunology, 276(1–2). doi:10.1016/j.jneuroim.2014.08.615.

112. Madeira, J.M., Schindler, S.M. and Klegeris, A. (2015) “A new look at auranofin, dextromethorphan and rosiglitazone for reduction of glia-mediated inflammation in neurodegenerative diseases,” Neural Regeneration Research. doi:10.4103/1673-5374.153686.

113. Mahaman, Y.A.R. et al. (2022) “Biomarkers used in Alzheimer’s disease diagnosis, treatment, and prevention,” Ageing Research Reviews. doi:10.1016/j.arr.2021.101544.

114. Maramai, S. et al. (2020) “Multitarget Therapeutic Strategies for Alzheimer’s Disease: Review on Emerging Target Combinations,” BioMed Research International. doi:10.1155/2020/5120230.

115. Martín-Belmonte, A. et al. (2020) “Reduction in the neuronal surface of post and presynaptic GABAB receptors in the hippocampus in a mouse model of Alzheimer’s disease,” Brain Pathology, 30(3). doi:10.1111/bpa.12802.

116. Masuda, A. et al. (2016) “Cognitive deficits in single App knock-in mouse models,” Neurobiology of Learning and Memory, 135. doi:10.1016/j.nlm.2016.07.001.

117. de Matos, J. et al. (2021) “Machine learning methods for histopathological image analysis: A review,” Electronics (Switzerland). doi:10.3390/electronics10050562.

118. Mattsson-Carlgren, N. et al. (2020) “Aβ deposition is associated with increases in soluble and phosphorylated tau that precede a positive Tau PET in Alzheimer’s disease,” Science Advances, 6(16). doi:10.1126/sciadv.aaz2387.

119. Mdawar, B., Ghossoub, E. and Khoury, R. (2020) “Selective serotonin reuptake inhibitors and Alzheimer’s disease,” Neural Regeneration Research. doi:10.4103/1673-5374.264445.

120. Mehla, J. et al. (2019) “Age-dependent behavioral and biochemical characterization of single APP knock-in mouse (APPNL-G-F/NL-G-F) model of Alzheimer’s disease,” Neurobiology of Aging, 75. doi:10.1016/j.neurobiolaging.2018.10.026.

121. Mendez, M.F. (2017) “Early-Onset Alzheimer Disease,” Neurologic Clinics. W.B. Saunders, pp. 263–281. doi:10.1016/j.ncl.2017.01.005.

122. Mendez, M.F. (2019) “Early-onset Alzheimer disease and its variants,” CONTINUUM Lifelong Learning in Neurology. doi:10.1212/CON.0000000000000687.

123. Merighi, S. et al. (2021) “Alzheimer and purinergic signaling: Just a matter of inflammation?,” Cells. doi:10.3390/cells10051267.

124. Mi, Z. et al. (2016) “Tenascin-C is associated with cored amyloid-b plaques in Alzheimer disease and pathology burdened cognitively normal elderly,” Journal of Neuropathology and Experimental Neurology, 75(9). doi:10.1093/jnen/nlw062.

125. Missaghi, S. et al. (2014) “Investigation of critical core formulation and process parameters for osmotic pump oral drug delivery,” AAPS PharmSciTech, 15(1). doi:10.1208/s12249-013-0040-4.

126. Miguel-Alvarez, M. et al. (2015) “Non-steroidal anti-inflammatory drugs as a treatment for Alzheimer's disease: a systematic review and meta-analysis of treatment effect.” Drugs Aging, 32. doi:10.1007/s40266-015-0239-z.

127. Möhle, L. et al. (2021) “Development of deep learning models for microglia analyses in brain tissue using DeePathologyTM STUDIO,” Journal of Neuroscience Methods, 364. doi:10.1016/j.jneumeth.2021.109371.

128. Montoya, A. et al. (2019) “Dopamine receptor D3 signalling in astrocytes promotes neuroinflammation,” Journal of Neuroinflammation, 16(1). doi:10.1186/s12974-019-1652-8.

129. Moreta, M.P.G. et al. (2021) “Efficacy of acetylcholinesterase inhibitors on cognitive function in alzheimer’s disease. Review of reviews,” Biomedicines. doi:10.3390/biomedicines9111689.

130. Myers, A. and McGonigle, P. (2019) “Overview of Transgenic Mouse Models for Alzheimer’s Disease,” Current Protocols in Neuroscience. doi:10.1002/cpns.81.

131. Naguib, G.H., Nassar, H.M. and Hamed, M.T. (2022) “Antimicrobial properties of dental cements modified with zein-coated magnesium oxide nanoparticles,” Bioactive Materials, 8. doi:10.1016/j.bioactmat.2021.06.011.

132. Nam, E., Nam, G. and Lim, M.H. (2020) “Synaptic Copper, Amyloid-β, and Neurotransmitters in Alzheimer’s Disease,” Biochemistry. doi:10.1021/acs.biochem.9b00775.

133. Nguyen, T.T. et al. (2021) “Advances in developing therapeutic strategies for Alzheimer’s disease,” Biomedicine and Pharmacotherapy. doi:10.1016/j.biopha.2021.111623.

134. Nicholson, J.W., Sidhu, S.K. and Czarnecka, B. (2020) “Enhancing the mechanical properties of glass-ionomer dental cements: A review,” Materials. doi:10.3390/ma13112510.

135. Nielsen, B.S. et al. (2017) “Subchronic, Low-Level Intraperitoneal Injections of Manganese (IV) Oxide and Manganese (II) Chloride Affect Rat Brain Neurochemistry,” International Journal of Toxicology, 36(3). doi:10.1177/1091581817704378.

136. Nikam, P.H. et al. (2012) “Osmotic pump: A reliable drug delivery system,” Research Journal of Pharmaceutical, Biological and Chemical Sciences, 3(3).

137. Nobili, A., la Barbera, L. and D’Amelio, M. (2021) “Targeting autophagy as a therapeutic strategy to prevent dopamine neuron loss in early stages of Alzheimer disease,” Autophagy, 17(5). doi:10.1080/15548627.2021.1909409.

138. Nowak, D., Slupski, W. and Rutkowska, M. (2021) “New therapeutic strategies for Alzheimer’s disease,” Postepy Higieny i Medycyny Doswiadczalnej, 75. doi:10.5604/01.3001.0014.9532.

139. Nuebling, G.S. et al. (2021) “Low-degree trisomy 21 mosaicism promotes early-onset Alzheimer disease,” Neurobiology of Aging, 103. doi:10.1016/j.neurobiolaging.2021.02.021.

140. Oakley, H. et al. (2006) “Intraneuronal β-amyloid aggregates, neurodegeneration, and neuron loss in transgenic mice with five familial Alzheimer’s disease mutations: Potential factors in amyloid plaque formation,” Journal of Neuroscience, 26(40). doi:10.1523/JNEUROSCI.1202-06.2006.

141. Oddo, S. et al. (2003) “Triple-transgenic model of Alzheimer’s Disease with plaques and tangles: Intracellular Aβ and synaptic dysfunction,” Neuron, 39(3). doi:10.1016/S0896-6273(03)00434-3.

142. Oladapo, O.M. et al. (2021) “Naringin Confers Protection against Psychosocial Defeat Stress-Induced Neurobehavioral Deficits in Mice: Involvement of Glutamic Acid Decarboxylase Isoform-67, Oxido-Nitrergic Stress, and Neuroinflammatory Mechanisms,” Journal of Molecular Neuroscience, 71(3), pp. 431–445. doi:10.1007/s12031-020-01664-y.

143. Olsen, I. and Singhrao, S.K. (2020) “Interaction between genetic factors, Porphyromonas gingivalis and microglia to promote Alzheimer’s disease,” Journal of Oral Microbiology. doi:10.1080/20002297.2020.1820834.

144. Onyango, I.G. et al. (2021) “Neuroinflammation in Alzheimer’s disease,” Biomedicines. doi:10.3390/biomedicines9050524.

145. Ozben, T. and Ozben, S. (2019) “Neuro-inflammation and anti-inflammatory treatment options for Alzheimer’s disease,” Clinical Biochemistry. doi:10.1016/j.clinbiochem.2019.04.001.

146. Pan, R.Y. et al. (2020) “Sodium rutin ameliorates Alzheimer’s disease-like pathology by enhancing microglial amyloid-β clearance,” Science Advances, 5(2). doi:10.1126/SCIADV.AAU6328.

147. Pan, X. et al. (2019) “Dopamine and dopamine receptors in Alzheimer’s disease: A systematic review and network meta-analysis,” Frontiers in Aging Neuroscience. doi:10.3389/fnagi.2019.00175.

148. Pandit, R., Chen, L. and Götz, J. (2020) “The blood-brain barrier: Physiology and strategies for drug delivery,” Advanced Drug Delivery Reviews. doi:10.1016/j.addr.2019.11.009.

149. Pardridge, W.M. (2020) “Blood-Brain Barrier and Delivery of Protein and Gene Therapeutics to Brain,” Frontiers in Aging Neuroscience. doi:10.3389/fnagi.2019.00373.

150. Park, D. et al. (2020) “Human neural stem cells encoding ChAT gene restore cognitive function via acetylcholine synthesis, Aβ elimination, and neuroregeneration in APPswe/PS1dE9 mice,” International Journal of Molecular Sciences, 21(11). doi:10.3390/ijms21113958.

151. Parks, E.E. et al. (2020) “Interleukin 6 reduces allopregnanolone synthesis in the brain and contributes to age-related cognitive decline in mice,” Journal of Lipid Research, 61(10). doi:10.1194/jlr.RA119000479.

152. Perea, J.R., Bolós, M. and Avila, J. (2020) “Microglia in Alzheimer’s disease in the context of tau pathology,” Biomolecules. doi:10.3390/biom10101439.

153. Pérez, M., Avila, J. and Hernández, F. (2019) “Propagation of tau via extracellular vesicles,” Frontiers in Neuroscience. doi:10.3389/fnins.2019.00698.

154. Pietrowski, M.J. et al. (2021) “Glial Purinergic Signaling in Neurodegeneration,” Frontiers in Neurology. doi:10.3389/fneur.2021.654850.

155. Poole, E.I. et al. (2019) “Stereotaxic surgery for implantation of guide cannulas for microinjection into the dorsomedial hypothalamus in young rats,” MethodsX, 6. doi:10.1016/j.mex.2019.07.005.

156. Preston, A.R. and Eichenbaum, H. (2013) “Interplay of hippocampus and prefrontal cortex in memory,” Current Biology. doi:10.1016/j.cub.2013.05.041.

157. Prévot, T. and Sibille, E. (2021) “Altered GABA-mediated information processing and cognitive dysfunctions in depression and other brain disorders,” Molecular Psychiatry. doi:10.1038/s41380-020-0727-3.

158. Provensi, G. et al. (2020) “Brain histamine modulates recognition memory: possible implications in major cognitive disorders,” British Journal of Pharmacology. doi:10.1111/bph.14478.

159. Quinn, J.P. et al. (2018) “Tau Proteolysis in the Pathogenesis of Tauopathies: Neurotoxic Fragments and Novel Biomarkers,” Journal of Alzheimer’s disease : JAD. doi:10.3233/JAD-170959.

160. Rabinovici, G.D. (2019) “Late-onset Alzheimer disease,” CONTINUUM Lifelong Learning in Neurology. Lippincott Williams and Wilkins, pp. 14–33. doi:10.1212/CON.0000000000000700.

161. Radde, R. et al. (2006) “Abeta42-driven cerebral amyloidosis in transgenic ... [EMBO Rep. 2006] - PubMed result,” EMBO reports, 7(9).

162. Rechberger, J.S. et al. (2020) “Evaluating infusate parameters for direct drug delivery to the brainstem: A comparative study of convection-enhanced delivery versus osmotic pump delivery,” Neurosurgical Focus, 48(1). doi:10.3171/2019.10.FOCUS19703.

163. Rey, F. et al. (2022) “Mitochondrial dysfunctions in neurodegenerative diseases: role in disease pathogenesis, strategies for analysis and therapeutic prospects,” Neural Regeneration Research. doi:10.4103/1673-5374.322430.

164. Rice, H.C. et al. (2019) “Secreted amyloid-b precursor protein functions as a GABA B R1a ligand to modulate synaptic transmission,” Science, 363(6423). doi:10.1126/science.aao4827.

165. Rice, H.C. et al. (2020) “Contribution of GABAergic interneurons to amyloid-β plaque pathology in an APP knock-in mouse model,” Molecular Neurodegeneration, 15(1). doi:10.1186/s13024-019-0356-y.

166. Rivers-Auty, J. et al. (2020) “Anti-inflammatories in Alzheimer’s disease—potential therapy or spurious correlate?,” Brain Communications, 2(2). doi:10.1093/braincomms/fcaa109.

167. Ror Maratha, S., Falls, N. and Vashist, N. (2019) “Alzheimer’s Disease: Neurotransmitters Involved and the Possible New Strategies,” Indo Global Journal of Pharmaceutical Sciences, 09(01). doi:10.35652/igjps.2019.9102.

168. Rothan, H.A. et al. (2020) “The FDA-approved gold drug auranofin inhibits novel coronavirus (SARS-COV-2) replication and attenuates inflammation in human cells,” Virology, 547. doi:10.1016/j.virol.2020.05.002.

169. Ruan, Z. et al. (2020) “Alzheimer’s disease brain-derived tau-containing extracellular vesicles: Pathobiology and GABAergic neuronal transmission,” bioRxiv [Preprint]. doi:10.1101/2020.03.15.992719.

170. Ruiz-Riquelme, A. et al. (2021) “Aβ43 aggregates exhibit enhanced prion-like seeding activity in mice,” Acta Neuropathologica Communications, 9(1). doi:10.1186/s40478-021-01187-6.

171. Sabbagh, M.N. (2020) “Alzheimer’s Disease Drug Development Pipeline 2020,” Journal of Prevention of Alzheimer’s Disease. doi:10.14283/jpad.2020.12.

172. Saeedi, M. et al. (2019) "Applications of nanotechnology in drug delivery to the central nervous system," Biomedicine and Pharmacotherapy. doi:10.1016/j.biopha.2018.12.133.

173. Saito, T. et al. (2014) "Single App knock-in mouse models of Alzheimer's disease," Nature Neuroscience, 17(5). doi:10.1038/nn.3697.

174. Sakakibara, Y. et al. (2019) "Amyloid-β plaque formation and reactive gliosis are required for induction of cognitive deficits in App knock-in mouse models of Alzheimer's disease," BMC Neuroscience, 20(1). doi:10.1186/s12868-019-0496-6.

175. Sarkar, S. et al. (2020) "Modification of methods to use Congo-red stain to simultaneously visualize amyloid plaques and tangles in human and rodent brain tissue sections," Metabolic Brain Disease, 35(8). doi:10.1007/s11011-020-00608-0.

176. Sato, K. et al. (2021) "A third-generation mouse model of Alzheimer's disease shows early and increased cored plaque pathology composed of wild-type human amyloid β peptide," Journal of Biological Chemistry, 297(3). doi:10.1016/j.jbc.2021.101004.

177. Sato, Y. et al. (2021) "Extracellular Zn2+-Dependent Amyloid-β1–42 Neurotoxicity in Alzheimer's Disease Pathogenesis," Biological Trace Element Research. doi:10.1007/s12011-020-02131-w.

178. Schwartzentruber, J. et al. (2021) "Alzheimer ' s disease risk genes," Nature Genetics, 53(March).

179. Serneels, L. et al. (2020) "Modeling the β-secretase cleavage site and humanizing amyloid-beta precursor protein in rat and mouse to study Alzheimer's disease," Molecular Neurodegeneration, 15(1). doi:10.1186/s13024-020-00399-z.

180. Setti, S.E. et al. (2021) "In vivo demonstration of Congo Red labeled amyloid plaques via perfusion in the Alzheimer disease rat model," Journal of Neuroscience Methods, 353. doi:10.1016/j.jneumeth.2021.109082.

181. Sheeler, C. et al. (2021) "Post-symptomatic Delivery of Brain-Derived Neurotrophic Factor (BDNF) Ameliorates Spinocerebellar Ataxia Type 1 (SCA1) Pathogenesis," Cerebellum, 20(3). doi:10.1007/s12311-020-01226-3.

182. Shekari, A. and Fahnestock, M. (2021) "Cholinergic neurodegeneration in Alzheimer disease mouse models," in Handbook of Clinical Neurology. doi:10.1016/B978-0-12-819973-2.00013-7.

183. al Shoyaib, A., Archie, S.R. and Karamyan, V.T. (2020) "Intraperitoneal Route of Drug Administration: Should it Be Used in Experimental Animal Studies?," Pharmaceutical Research. doi:10.1007/s11095-019-2745-x.

184. Sike, Á. et al. (2017) "Improved method for cannula fixation for long-term intracerebral brain infusion," Journal of Neuroscience Methods, 290. doi:10.1016/j.jneumeth.2017.07.026.

185. Singh, K. et al. (2013) “OSMOTIC PUMP DRUG DELIVERY SYSTEM: A NOVAL APPROACH,” Journal of Drug Delivery and Therapeutics, 3(5). doi:10.22270/jddt.v3i5.636.

186. Sonzogni-Desautels, K. and Ndao, M. (2021) “Will Auranofin Become a Golden New Treatment Against COVID-19?,” Frontiers in Immunology, 12. doi:10.3389/fimmu.2021.683694.

187. Srivastava, S., Ahmad, R. and Khare, S.K. (2021) “Alzheimer’s disease and its treatment by different approaches: A review,” European Journal of Medicinal Chemistry. doi:10.1016/j.ejmech.2021.113320.

188. Strodel, B. (2021) “Amyloid aggregation simulations: challenges, advances and perspectives,” Current Opinion in Structural Biology. doi:10.1016/j.sbi.2020.10.019.

189. Su, Y. et al. (2015) “Partial volume correction in quantitative amyloid imaging,” NeuroImage, 107. doi:10.1016/j.neuroimage.2014.11.058.

190. Sun, Z. et al. (2021) “5-HT6R null mutatrion induces synaptic and cognitive defects,” Aging Cell, 20(6). doi:10.1111/acel.13369.

191. Sung, P.S. et al. (2020) “Neuroinflammation and neurogenesis in alzheimer’s disease and potential therapeutic approaches,” International Journal of Molecular Sciences. doi:10.3390/ijms21030701.

192. Tang, B.L. (2019) “Amyloid Precursor Protein (APP) and GABAergic Neurotransmission,” Cells, 8(6). doi:10.3390/cells8060550.

193. Tang, C. and Guo, W. (2021) “Implantation of a mini-osmotic pump plus stereotactical injection of retrovirus to study newborn neuron development in adult mouse hippocampus,” STAR Protocols, 2(1). doi:10.1016/j.xpro.2021.100374.

194. Tarutani, A. et al. (2021) “Human tauopathy-derived tau strains determine the substrates recruited for templated amplification,” Brain, 144(8). doi:10.1093/brain/awab091.

195. Taşkiran-Sağ, A. and Yemişçi, M. (2020) “Neuroinflammation in alzheimer’s disease continuum,” Neurological Sciences and Neurophysiology, 37(4). doi:10.4103/nsn.nsn_190_20.

196. Taylor, Z. v. et al. (2021) “An optimized intracerebroventricular injection of CD4+ T cells into mice,” STAR Protocols, 2(3). doi:10.1016/j.xpro.2021.100725.

197. Tellechea, P. et al. (2018) “Early- and late-onset Alzheimer disease: Are they the same entity?,” Neurologia. doi:10.1016/j.nrl.2015.08.002.

198. Thinh, N.H., Hoang Tung, T. and Ha, L.V. (2020) “Depth-aware salient object segmentation,” VNU Journal of Science: Computer Science and Communication Engineering, 36(2). doi:10.25073/2588-1086/vnucsce.217.

199. Tiwari, S. et al. (2019) “Alzheimer’s disease: Pathogenesis, diagnostics, and therapeutics,” International Journal of Nanomedicine. doi:10.2147/IJN.S200490.

200. Tsatsanis, A. et al. (2021) “The acute phase protein lactoferrin is a key feature of Alzheimer’s disease and predictor of Aβ burden through induction of APP amyloidogenic processing,” Molecular Psychiatry [Preprint]. doi:10.1038/s41380-021-01248-1.

201. Tublin, J.M. et al. (2019) “Getting to the Heart of Alzheimer Disease,” Circulation Research. doi:10.1161/CIRCRESAHA.118.313563.

202. Uddin, M.S. et al. (2020) “Pharmacological approaches to mitigate neuroinflammation in Alzheimer’s disease,” International Immunopharmacology. doi:10.1016/j.intimp.2020.106479.

203. Upīte, J. et al. (2020) “Subchronic administration of auranofin reduced amyloid-β plaque pathology in a transgenic APPNL-G-F/NL-G-F mouse model,” Brain Research, 1746. doi:10.1016/j.brainres.2020.147022.

204. Upite, J. et al. (2021) “A New Tool for the Analysis of the Effect of Intracerebrally Injected Anti-Amyloid-β Compounds,” Journal of Alzheimer’s Disease, 84(4). doi:10.3233/JAD-215180.

205. Uslu, F. et al. (2020) “Image-analysis based readout method for biochip: Automated quantification of immunomagnetic beads, micropads and patient leukemia cell,” Micron, 133. doi:10.1016/j.micron.2020.102863.

206. Vally, M. and Kathrada, F. (2019) “Understanding alzheimer disease,” South African Family Practice, 61(2). doi:10.4102/safp.v61i2.4999.

207. van, T. et al. (2011) “Staining of Amyloid Beta (Abeta) Using (Immuno) Histochemical Techniques and Abeta42 Specific Peptides,” in Neuroimaging for Clinicians - Combining Research and Practice. doi:10.5772/24282.

208. Walsh, S. et al. (2021) “Aducanumab for Alzheimer’s disease?,” The BMJ. doi:10.1136/bmj.n1682.

209. Weil, M.T. et al. (2017) “Intracerebral injections and ultrastructural analysis of high-pressure frozen brain tissue,” Current Protocols in Neuroscience, 2017. doi:10.1002/cpns.22.

210. Weller, J. and Budson, A. (2018) “Current understanding of Alzheimer’s disease diagnosis and treatment,” F1000Research. doi:10.12688/f1000research.14506.1.

211. Wen, T.C. et al. (2018) “Plasticity in one hemisphere, control from two: Adaptation in descending motor pathways after unilateral corticospinal injury in neonatal rats,” Frontiers in Neural Circuits, 12. doi:10.3389/fncir.2018.00028.

212. Whelan, R., Hargaden, G.C. and Knox, A.J.S. (2021) “Modulating the blood–brain barrier: A comprehensive review,” Pharmaceutics. doi:10.3390/pharmaceutics13111980.

213. Whiley, L. et al. (2021) “Metabolic phenotyping reveals a reduction in the bioavailability of serotonin and kynurenine pathway metabolites in both the urine and

serum of individuals living with Alzheimer's disease," Alzheimer's Research and Therapy, 13(1). doi:10.1186/s13195-020-00741-z.

214. Willumsen, N. et al. (2021) "Variability in the type and layer distribution of cortical Aβ pathology in familial Alzheimer's disease," Brain Pathology [Preprint]. doi:10.1111/bpa.13009.

215. Xiao, J. et al. (2021) "Pesticides Exposure and Dopaminergic Neurodegeneration," Exposure and Health. doi:10.1007/s12403-021-00384-x.

216. Xie, J. et al. (2021) "Low-grade peripheral inflammation affects brain pathology in the App NL-G-Fmouse model of Alzheimer's disease," Acta Neuropathologica Communications, 9(1). doi:10.1186/s40478-021-01253-z.

217. Yamashita, M. (2021) "Auranofin: Past to Present, and repurposing," International Immunopharmacology. doi:10.1016/j.intimp.2021.108272.

218. Yang, J., Perrett, S. and Wu, S. (2021) "Single molecule characterization of amyloid oligomers," Molecules. doi:10.3390/molecules26040948.

219. Yang, P. et al. (2021) "Dopamine D1 + D3 receptor density may correlate with parkinson disease clinical features," Annals of Clinical and Translational Neurology, 8(1). doi:10.1002/acn3.51274.

220. Yasuno, F. et al. (2021) "An evaluation of the amyloid cascade model using in vivo positron emission tomographic imaging," Psychogeriatrics, 21(1). doi:10.1111/psyg.12589.

221. Yiannopoulou, K.G. and Papageorgiou, S.G. (2020) "Current and Future Treatments in Alzheimer Disease: An Update," Journal of Central Nervous System Disease, 12. doi:10.1177/1179573520907397.

222. Yu, H. and Wu, J. (2021) "Amyloid-β: A double agent in Alzheimer's disease?," Biomedicine and Pharmacotherapy. doi:10.1016/j.biopha.2021.111575.

223. Yu, T.W., Lane, H.Y. and Lin, C.H. (2021) "Novel therapeutic approaches for alzheimer's disease: An updated review," International Journal of Molecular Sciences. doi:10.3390/ijms22158208.

224. Yuede, C.M. et al. (2021) "Pimavanserin, a 5HT2A receptor inverse agonist, rapidly suppresses Aβ production and related pathology in a mouse model of Alzheimer's disease," Journal of Neurochemistry, 156(5). doi:10.1111/jnc.15260.

225. Zhang, W. et al. (2021) "The Role of the GABAergic System in Diseases of the Central Nervous System," Neuroscience. doi:10.1016/j.neuroscience.2021.06.037.

226. Zhang, X. et al. (2019) "Repurposing of auranofin: Thioredoxin reductase remains a primary target of the drug," Biochimie, 162. doi:10.1016/j.biochi.2019.03.015.

227. Zhang, X. et al. (2020) "Evidence for unique small RNA modifications in Alzheimer's disease," bioRxiv [Preprint]. doi:10.1101/2020.04.30.071100.

228. Zhao, J. et al. (2020) “Targeting Amyloidogenic Processing of APP in Alzheimer’s Disease,” Frontiers in Molecular Neuroscience. doi:10.3389/fnmol.2020.00137.

229. Zhou, L. and Li, Q. (2019) “Isolation of region-specific microglia from one adult mouse brain hemisphere for deep single-cell rna sequencing,” Journal of Visualized Experiments, 2019(154). doi:10.3791/60347.

8. SUPPLEMENTARY INFORMATION

8.1. Supplementary figure 1

(A, B) The round-shaped and uneven skull surface. (C, D) The surface of the cannula's pedestal is too big relative to the skull and has a flat surface which makes the fixation inappropriate without our silicone spacer. Panel (D) demonstrates the gap between the skull and the overhanging part of the cannula's pedestal with a scalpel placed underneath.

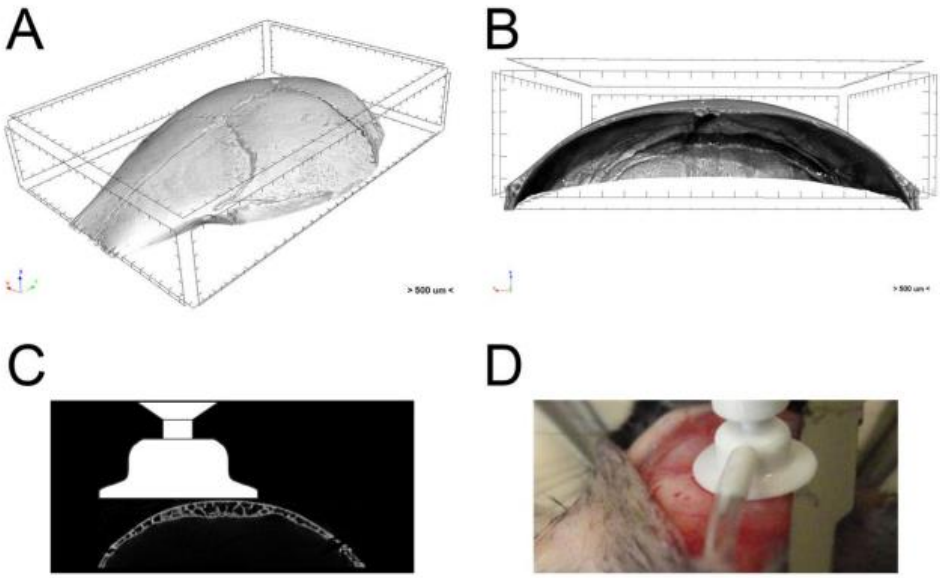

8.2. Supplementary material 1

Mathematical calculations

Slide calculations (worksheet "Slides")

In the following sections, we describe the equations and calculations behind the columns in the worksheet "Animals" (Supplementary Table 1).

Supplementary Table 1. **Equations and calculations behind the columns in the worksheet "Animals".**

Column	Value	Column	Value	Column	Value
X[H1]	x_1	X[I2]	x_{RP2}	b[SL(I1)]	b_{PSL1}
Y[H1]	y_1	Y[I2]	y_{RP2}	Side[I1]	
X[H2]	x_2	m[HSL]	m_{HSL}	X[SL(I2)]	x_{HSL2}
Y[H2]	y_2	b[HSL]	b_{HSL}	DeltaX[SL(I2)]	Δx
X[I1]	x_{RP1}	X[SL(I1)]	x_{HSL1}	b[SL(I2)]	b_{PSL2}
Y[I1]	y_{RP1}	DeltaX[SL(I1)]	Δx	Side[I2]	

Hemisphere straight line (HSL)

Using the general formula for a straight line

$$y = mx + b \tag{1}$$

where *m* is the slope and *b* the y-intercept of the line, and two given points on that line

$$P_1(x_1, y_1)$$

$$P_2(x_2, y_2)$$

defined previously in AxioVision (hemisphere border reference points), we can calculate *m* and *b* and thus, the equation of the hemisphere dividing straight line (HSL):

$$m_{HSL} = (y_2 - y_1)/(x_2 - x_1)$$

$$b_{HSL} = y_1 - (m_{HSL} \times x_1)$$

$$y = m_{HSL}x + b_{HSL}$$

Hemisphere determination

$P_{HSL}(x_{HSL}, y_{HSL})$ is the point on HSL that has the same y-value as the previously in AxioVision defined reference point $P_{RP}(x_{RP}, y_{RP})$. P_{RP} is either the ipsilateral injection point or the contralateral corresponding point. Then we can calculate x_{HSL} as follows:

$$x_{HSL} = (y_{RP} - b_{HSL})/m_{HSL}$$

To determine, in which hemisphere P_{RP} is located, we calculate the difference Δx:

$$\Delta x = x_{RP} - x_{HSL}$$

If Δx is negative, the reference point P_{RP} is in the left hemisphere, if Δx is positive, P_{RP} is in the right hemisphere. Together with the slide-specific information which side contains the injection channel (as given in the worksheet "Animals"), Δx is used to categorize each hemisphere as ipsi- or contralateral. Note: This calculation is performed twice, once for each reference point.

Parallel straight line (PSL)

The injection or reference channel is defined as the line parallel to the hemisphere border that goes through P_{RP} (injection or reference point, respectively). Thus, we can calculate b_{PSL} using m_{HSL} and P_{RP}

$$b_{PSL} = y_{RP} - (m_{HSL} \times x_{RP})$$

and use (1) to obtain the equation for the parallel straight line (PSL):

$$y = m_{PSL}x + b_{HSL}$$

Note: This calculation is performed twice, once for each reference point.

Plaque calculations (worksheet "Measured plaques")

In the worksheet "Measured plaques", we calculate for each plaque the distance from the reference point P_{RP}, the distance from the PSL, and to which size category (small, medium, or large, as defined in the worksheet "Main") they **belong (Supplementary Table 2).**

Supplementary Table 2. **Calculations behind the columns in the worksheet "Measured plaques".**

Column	Value
X[P]	x_Q
Y[P]	y_Q
X[HSL]	x_{HSLQ}
DeltaX	Δx
Side[P]	

d[RP]	d_{RP}
d[PSL]	d_{PSL}

Hemisphere determination

Let $Q(x_Q, y_Q)$ be a plaque and $P_{HSLQ}(x_{HSLQ}, y_Q)$ the point on HSL that has the same y-value as the plaque (similar to section 5.1.2). Then we can calculate x_{HSLQ} as follows:

$$x_{HSLQ} = (y_Q - b_{HSL})/m_{HSL}$$

To determine, in which hemisphere P_{RP} is located, we calculate the difference Δx:

$$\Delta x = x_Q - x_{HSLQ}$$

If Δx is negative, the plaque is in the left hemisphere, if Δx is positive, the plaque is in the right hemisphere. Together with the slide-specific information which side contains the injection channel (as given in the worksheet "Slides"), Δx is used to categorize each hemisphere as ipsi- or contralateral.

Distance from reference point

The distance d_{RP} of the plaque Q from the reference point P_{RP} is calculated using the Pythagorean theorem:

$$d_{RP} = \sqrt{(x_{RP} - x_Q)^2 + (y_{RP} - y_Q)^2}$$

Distance from PSL

The distance d_{PSL} is the distance of the plaque Q from the PSL (see section Parallel straight line (PSL)), a line that is parallel to the HSL and that goes through P_{RP}. d_{PSL} is calculated using the Hesse normal form to calculate the distance of a point from a line:

$$d_{PSL} = \frac{|m_{PSL} \times x_Q - y_Q + b_{HSL}|}{\sqrt{m_{HSL}^2 + 1}}$$

Distance categories

Depending on the values of d_{RP} and d_{PSL}, each plaque is categorized according to the five defined distance categories for RP and PSL. The user can change these categories.

8.3. Supplementary material 2

Presentation of calculated and measured values in diagrams performing statistical analysis

To demonstrate the possibilities of our analysis method, we analyzed data from eight PBS-injected APP Tg animals and quantified the number of plaques and other parameters in the ipsilateral compared to the contralateral hemisphere. The Excel template calculates the group means based on the number of blocks (i.e. animals, n=8) per group, while the value of each animal may be itself the mean of one or several slides (n=14 slides in total, 2 slides showed staining problems).

Number of plaques

We determined the number of Aβ plaques in the cortex comparing ipsi- and contralateral hemispheres. Similar data was obtained according to the two different distance category approaches: RP or PSL. No significant difference was observed in the total number of Aβ plaques in the cortex comparing contralateral versus ipsilateral hemispheres ($p = 0.6$; Suppl. Fig. 1A). Multiple comparisons showed that there was no significant difference between hemispheres in the Aβ plaque number by distance category (RP approach - 1st group: $p = 0.8$; 2nd group: $p = 0.9$; 3rd group: $p = 0.9$; 4th group: $p = 0.9$; 5th group: $p = 0.9$; Suppl. Fig. 1B; PSL approach - 1st group: $p = 0.9$; 2nd group: $p = 0.5$; 3rd group: $p = 0.9$; 4th group: $p = 0.9$; 5th group: $p = 0.9$; Suppl. Fig. 1C). If the pump is used to administer a potentially bioactive compound, this statistical comparison will provide information about the distribution of Aβ plaques around the injection site or channel. This information could be used to understand the distribution and efficiency of the experimental compound.

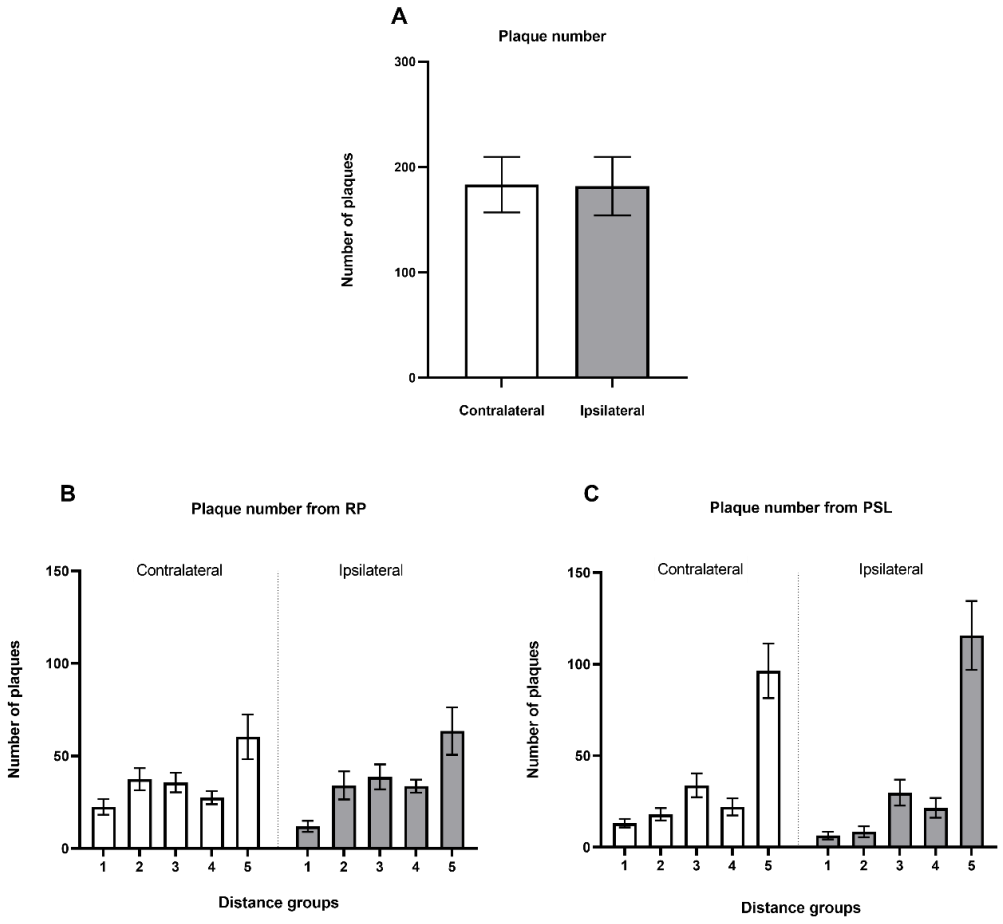

Suppl. Fig. 1. **Bar graphs show quantification according to the location of Aβ plaques (n = 8, control animals treated with PBS). Quantification of total plaque number (A), plaque number by distance category (RP approach) (B) and plaque number by distance category (PSL approach) (C) in the cortex area. Student's t-test (A), one-way analysis of variance (ANOVA) followed by Holm-Sidak's (B) and Kruskal-Wallis followed by Dunn's (C) multiple comparisons were used. The data are presented as the mean values ± standard errors of the means (S.E.M.). Statistical significance was set at P < 0.05.**

Cortex area covered by plaques

We determined the absolute area covered by Aβ plaques in the ipsilateral and contralateral hemisphere. We did not observe significant changes between the two hemispheres regarding the total plaque area (p = 0.7; Suppl. Fig. 2A). Similarly, there was no significant difference between hemispheres regarding the area covered by plaques when divided into groups according to the two different distance category approaches (RP approach - 1st group: p = 0.8; 2nd group: p = 0.9; 3rd group: p = 0.9; 4th group: p = 0.9; 5th group: p = 0.9; Suppl. Fig.

2B; PSL approach - 1st group: p = 0.9; 2nd group: p = 0.7; 3rd group: p = 0.9; 4th group: p = 0.9; 5th group: p = 0.9; Suppl. Fig. 2C).

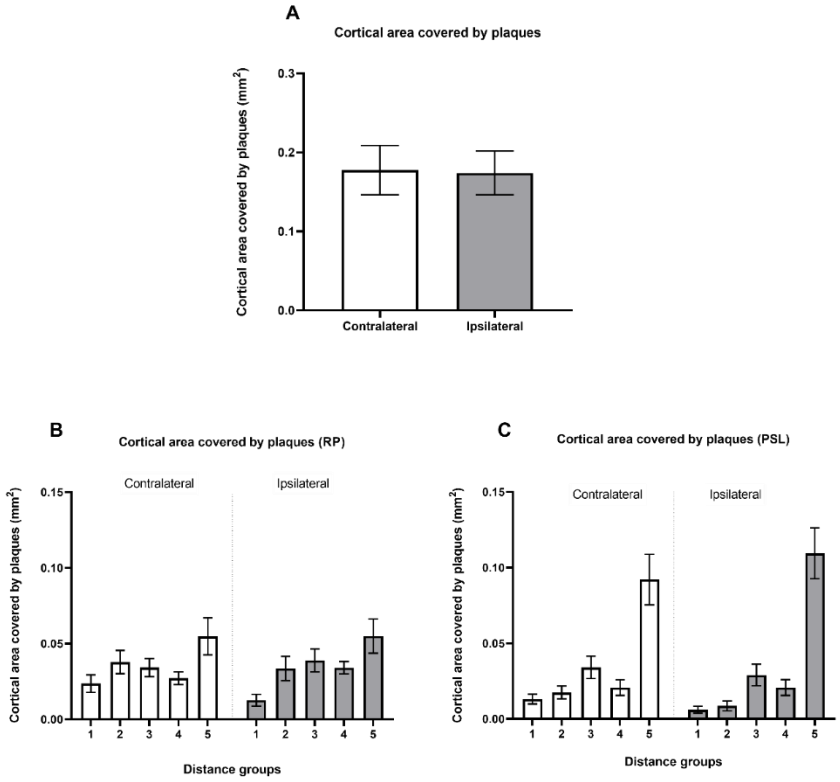

Suppl. Fig. 2. **Bar graphs show the absolute cortical area covered by Aβ plaques (n = 8, control animals treated with PBS). Quantification of cortical area covered by plaques (A), and cortical area covered by plaques according to distance category approaches RP (B) and PSL (C). Student's *t*-test (A) and one-way analysis of variance (ANOVA) Kruskal-Wallis followed by Dunn's (B, C) multiple comparisons were used. The data are presented as the mean values ± standard errors of the means (S.E.M.). Statistical significance was set at P < 0.05.**

Average plaque size

We further performed in-depth analysis of Aβ plaque size and size distribution in the cortex comparing ipsi- and contralateral hemispheres. Comparing the overall mean plaque size in each hemisphere, we did not find a significant difference (p = 0.6; Suppl. Fig. 3A). Additionally we compared the average Aβ plaque size between the two hemispheres by distance category and found no significant difference in any approach (RP approach - 1st group: p = 0.9; 2nd group: p = 0.9 ; 3rd group: p = 0.9 ; 4th group: p = 0.9; 5th group: p = 0.9; Suppl. Fig. 3B; PSL approach - 1st group: p = 0.9; 2nd group: p = 0.9; 3rd group: p = 0.9; 4th group: p

= 0.9; 5th group: p = 0.9; Suppl. Fig. 3C). This result suggests a homogenous distribution of differently sized Aβ plaques across each hemisphere.

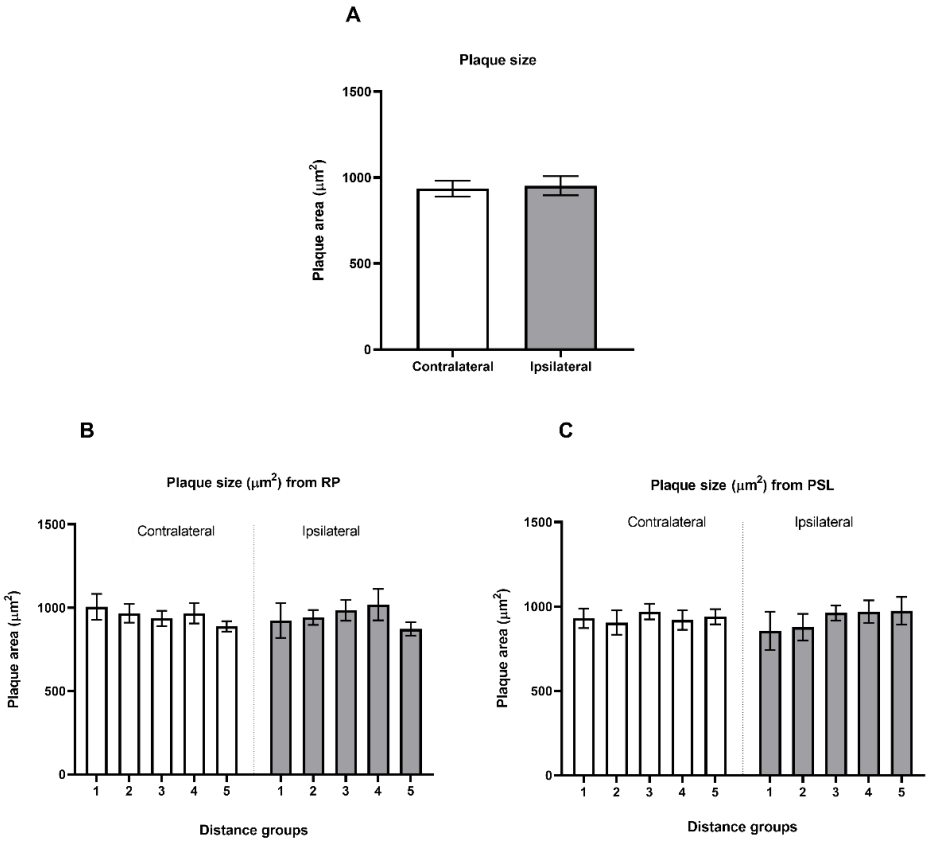

Suppl. Fig. 3. **Bar graphs show the mean number of Aβ plaques (n = 8, control animals treated with PBS). Quantification of plaque size (A), and plaque size according to distance category approaches RP (B) and PSL (C). Student's t-test (A), one-way analysis of variance (ANOVA) followed by Holm-Sidak's (B) and Kruskal-Wallis followed by Dunn's (C) multiple comparisons were used. The data are presented as the mean values ± standard errors of the means (S.E.M.).**

Number of plaques by size group

We determined the number of Aβ plaques by three size groups in the cortex comparing ipsi- and contralateral hemispheres. Plaques can be categorized into small (≤ 400 µm^2), medium (401 – 700 µm^2) and large (>700 µm^2) plaques. There was no statistically significant difference comparing the mean number of plaques by different sizes between contralateral and ipsilateral hemisphere (small: p = 0.9, medium: p = 0.9, large: p = 0.9; Suppl. Fig. 4A). Additionally, we compared the number of plaques by sizes small, medium and large divided into groups

according to the two different distance category approaches. We did not observe significant changes between the two hemispheres regarding the number of plaques by small size group (RP approach -1st group: p = 0.9; 2nd group: p = 0.9; 3rd group: p = 0.9; 4th group: p =0.9; 5th group: p = 0.9; Suppl. Fig. 4B; PSL approach - 1st group: p = 0.9; 2nd group: p = 0.7; 3rd group: p = 0.9; 4th group: p = 0.9; 5th group: p = 0.9; Suppl. Fig. 4C). Further we did not observed a statistical significance between the two hemispheres regarding the number of plaques by medium size group (RP approach - 1st group: p = 0.7; 2nd group: p = 0.9; 3rd group: p = 0.9; 4th group: p =0.9; 5th group: p = 0.6; Suppl. Fig. 4D; PSL approach - 1st group: p = 0.9; 2nd group: p = 0.5; 3rd group: p = 0.9; 4th group: p = 0.9; 5th group: p = 0.9; Suppl. Fig. 4E). Similarly, there was a no statistical significance observed between both hemispheres regarding the number of plaques by large size group (RP approach - 1st group: p = 0.8; 2nd group: p = 0.9; 3rd group: p = 0.9; 4th group: p = 0.9; 5th group: p = 0.9; Suppl. Fig. 4F; PSL approach - 1st group: p = 0.9; 2nd group: p = 0.3; 3rd group: p = 0.9; 4th group: p = 0.9; 5th group: p = 0.9; Suppl. Fig. 4G).

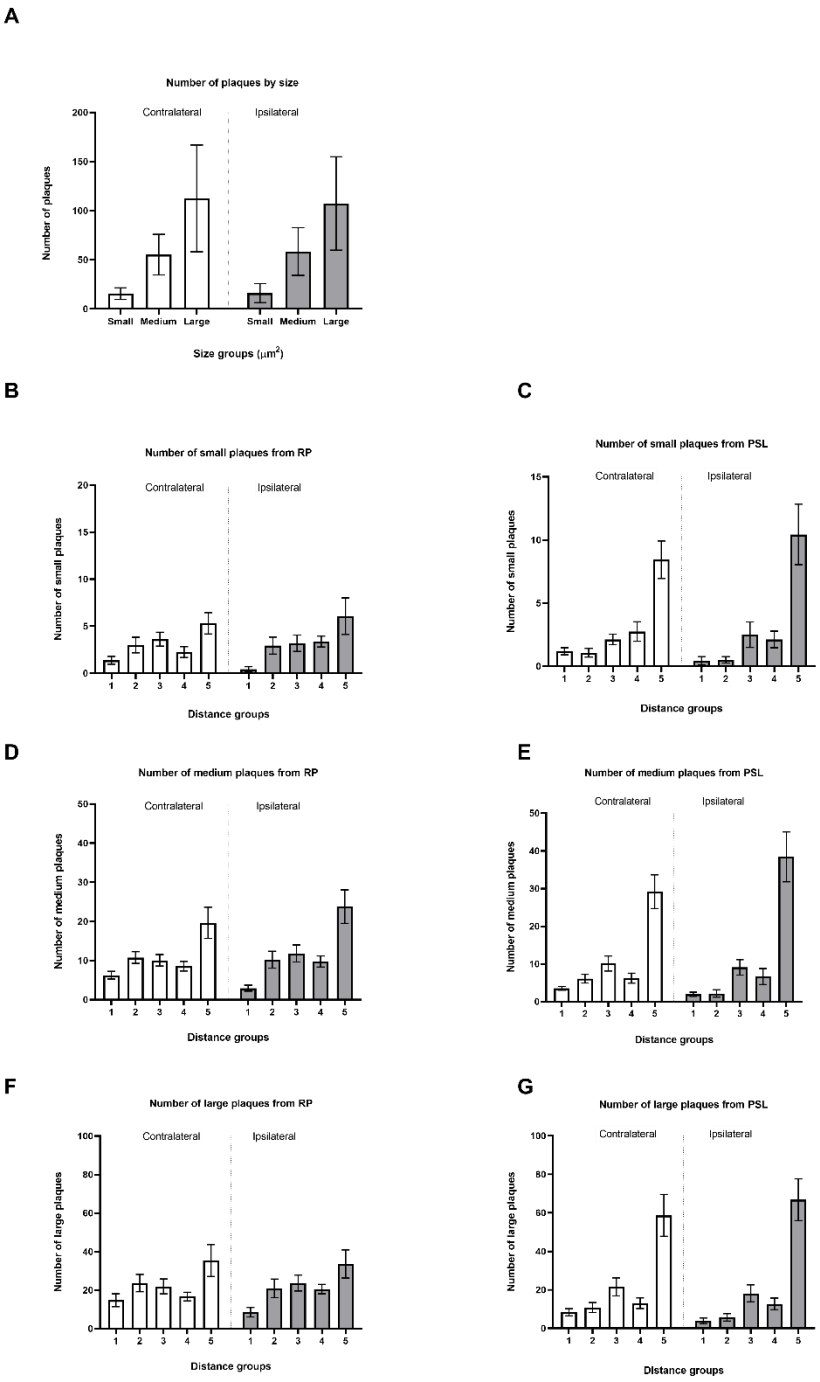

Suppl. Fig. 4. **Bar graphs show the mean number of Aβ plaques (n = 8, control animals treated with PBS). Quantification of number of plaques by size groups (A), number of small plaques according to distance category approaches RP (B) and PSL (C). Number of medium plaques according to distance category approaches RP (D) and PSL (E). Number of large plaques according two distance category approaches RP (F) and PSL (G). One-way analysis of variance (ANOVA) followed by Holm-Sidak's (A, D, F) and Kruskal-Wallis followed by Dunn's (B, C, E, G) multiple comparisons were used. The data are presented as the mean values ± standard errors of the means (S.E.M.)**